JPRS L/9929

24 August 1981

USSR Report

METEOROLOGY AND HYDROLOGY

No. 4, April 1981

FBIS FOREIGN BROADCAST INFORMATION SERVICE

NOTE

JPRS publications contain information primarily from foreign newspapers, periodicals and books, but also from news agency transmissions and broadcasts. Materials from foreign-language sources are translated; those from English-language sources are transcribed or reprinted, with the original phrasing and other characteristics retained.

Headlines, editorial reports, and material enclosed in brackets [] are supplied by JPRS. Processing indicators such as [Text] or [Excerpt] in the first line of each item, or following the last line of a brief, indicate how the original information was processed. Where no processing indicator is given, the information was summarized or extracted.

Unfamiliar names rendered phonetically or transliterated are enclosed in parentheses. Words or names preceded by a question mark and enclosed in parentheses were not clear in the original but have been supplied as appropriate in context. Other unattributed parenthetical notes within the body of an item originate with the source. Times within items are as given by source.

The contents of this publication in no way represent the policies, views or attitudes of the U.S. Government.

APPROVED FOR RELEASE: 2007/02/09: CIA-RDP82-00850R000400040041-8

JPRS L/9929

24 August 1981

USSR REPORT

METEOROLOGY AND HYDROLOGY

No. 4, April 1981

Translation of the Russian-language monthly journal METEOROLOGIYA I GIDROLOGIYA published in Moscow by Gidrometeoizdat.

CONTENTS

UDC 551.515.1

SOME FEATURES OF THE ENERGETICS OF TEMPERATE-LATITUDE CYCLONIC FORMATIONS

Moscow METEOROLOGIYA I GIDROLOGIYA in Russian No 4, Apr 81 pp 5-16

[Article by N. Z. Pinus, professor, and T. P. Kapitanova, candidate of physical and mathematical sciences, Central Aerological Observatory, manuscript received 30 Sep 80]

[Text]

Abstract: The article presents the results of investigations of the budgets of kinetic, potential and internal energy, as well as the energy of phase transformations, on the basis of the water vapor budget in different stages of evolution of temperate-latitude cyclones, making use of empirical material. Quantitative estimates of the energy capacity of the mechanisms forming the budgets are presented.

During recent years more and more attention has been devoted to study of the energetics of cyclonic formations in the temperate latitudes. These cyclones are an extremely important part of the general circulation of the atmosphere. Associated with these are atmospheric fronts and cloud systems, as well as precipitation fields determining the state of the weather over large areas and being extremely important for man's economic activity.

The budget of any type of energy, like the other characteristics of cyclonic formations (moisture cycle, etc.) can be studied in a moving coordinate system which moves along the trajectory of movement of cyclones or over a fixed area (polygon). The first research method makes it possible to study the features of energetics, taking into account different phases in the evolution of this synoptic formation. In a fixed polygon it is possible to trace the course of the atmospheric processes transpiring over it and compare the peculiarities of the budgets of different synoptic formations.

The nature and structure of the budgets of different types of energy in the atmosphere are dependent on the temporal and spatial scales of averaging; with an increase in these scales there is a smoothing of the values of the parameters making up the budget. In this connection a factor of great importance is the choice of the extent (area) of the polygon.

In our studies [1, 2, 4, 5, 7] we obtained preliminary evaluations of the role of different mechanisms forming the budgets of kinetic, potential and internal energy of different parts of a cyclonic formation and in different stages of its evolution, and also the role of the energy of phase transformations of water vapor. In particular, in the study of the energetics of a deep cyclone penetrating into the European USSR in November 1973 it was possible to detect and evaluate the role of horizontal advection through the lateral boundaries of a cyclonic formation (exchange with the external medium) and internal vertical redistributions of energy (and water vapor). It was established that local changes in kinetic, potential and internal energy are relatively small against the background of major energetic processes transpiring at different altitudes in cyclones; they constituted approximately 6-10% of the total changes of the corresponding budget. The law of compensation between the inflow (outflow) of kinetic energy and the outflow (inflow) of labile (the sum of internal and potential) energy is not operative within a cyclone. In a cyclone, in addition, especially in its central part, the contribution of the energy of phase transformations was substantial. It was important to check the degree of universality of the results on the basis of independent material and make a more precise evaluation of the energy capacity of temperate-latitude cyclonic formations.

In this article we examine the results of investigation of the energetics of individual cyclones moving in different zones of the European USSR in a moving coordinate system (Lagrangian budget), and also different parts of cyclonic formations observed over fixed polygons (Eulerian budget). Figure 1 shows the trajectories of the cyclones which we studied and the geographical position of three fixed polygons in which investigations were made of the atmospheric processes transpiring there. We investigated the energetics and moisture cycle of five cyclones observed in April (10-12) 1968, in October (22-25) 1973, in November (24-27) 1973, in February (18-21) 1978, in June (18-20) 1978, selected taking into account the nature and clarity of the trajectory of movement (surface center) and intensity of their evolution. The trajectories of these cyclones in general coincide well with the mean long-term paths of cyclones in the territory of the Soviet Union [3].

In the Balkhash polygon a study was made of the processes transpiring in May (13-27) 1972, in the Perm polygon in December (12-25) 1973, and in November-December [(11-18 November) and (29 November-9 December)] 1977, and in the Riga polygon in May (16-27) 1979.

The area of the moving and fixed polygons, equal to approximately $(2\text{-}4)\cdot 10^{11}$ m^2, in all cases was a hexagon based on the six nearest stations for temperature-wind sounding of the atmosphere with a seventh station at the center. Data from seven such stations served in all computations as the initial aerological information.

The equations describing the budgets in a quasistatic approximation (for a unit mass) are:
-- kinetic energy budget

$$\frac{\partial \overline{K}}{\partial t} = -\overline{\vec{\tau} \cdot K\vec{V}} - \frac{\partial \overline{\omega K}}{\partial p} - \overline{\vec{V} \cdot \vec{\nabla}\Phi} + \Delta_1; \qquad (1)$$

-- potential energy budget

$$\frac{\partial \overline{\Pi}}{\partial t} = -\overline{\vec{\nabla} \cdot \Pi \vec{V}} - \frac{\partial \overline{\omega \Pi}}{\partial p} + \overline{gW} + \Delta_2; \tag{2}$$

-- internal energy budget

$$\frac{\partial \overline{I}}{\partial t} = -\overline{\vec{\nabla} \cdot I \vec{V}} - \frac{\partial \overline{\omega I}}{\partial p} - \frac{\partial \overline{\Pi}}{\partial t} - \overline{\vec{\nabla} \cdot \Phi \vec{V}} - \frac{\partial \overline{\omega \Phi}}{\partial p} + \overline{\vec{V} \cdot \nabla \Phi} - \Delta_1 + \Delta_3; \tag{3}$$

-- water vapor budget

$$\frac{\partial \overline{q}}{\partial t} = -\overline{\vec{\nabla} \cdot q \vec{V}} - \frac{\partial \overline{\omega q}}{\partial p} + \Delta_4. \tag{4}$$

The following notations were used in these equations: K -- kinetic energy of mean motion, $\overline{\Pi}$ is potential energy, I is internal energy, q is specific humidity, p is pressure, Φ is geopotential, $\omega = \partial p / \partial t$ is the analogue of vertical velocity in a p coordinate system, W is the velocity of vertical movements, $\vec{V}$ is the wind vector,

$$\nabla = \frac{\partial}{\partial x} - \frac{\partial}{\partial y}.$$

The line at top denotes averaging for area.

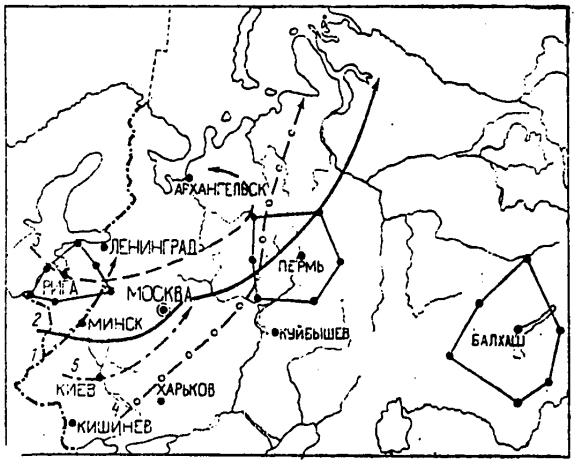

Fig. 1. Trajectories of cyclones and location of polygons. 1) October 1968; 2) October 1973; 3) November 1973; 4) February 1978; 5) June 1978.

In equations (1)-(4) the terms at the left describe local changes in the energy (moisture content), the first two terms at the right -- the changes due to horizontal inflows (outflows) through the lateral boundaries of a column of the atmosphere and the vertical redistribution, the third term in (1) at the right -- the generation of kinetic energy due to the operation of the force of the horizontal pressure gradient, the third term in (2) at the right -- the relative transformation of kinetic and potential energy, the third term in (3) at the right -- the

relative transformation of the internal and potential energy (through the change in kinetic energy in the ascending (descending) fluxes); the fourth and fifth terms in this equation describe the relative transformation of internal and kinetic energy (with broadening (compression) by pressure forces at the boundary of the volume), Δ_1 includes the dissipation of kinetic energy into heat, nonlinear interactions of movements of different scales, effects of errors of initial aerological information and computations on an electronic computer.

We note, as was demonstrated in [5, 7], that in the case of sufficiently great scales of spatial averaging the Δ_1 value has a negative sign and (with allowance for the errors in initial aerological information) describes the rate of dissipation of kinetic energy into heat. With a decrease in the averaging scale the effects of nonlinear interaction of disturbances of different scales and disturbances with a mean flux begin to exert an influence, as does the effect of thermal stratification of the atmosphere. In these cases Δ_1 can be either a positive or negative value and in addition, can attain large absolute values, Δ_2 are subgrid effects and the effects of errors of initial aerological information and computations on an electronic computer; $\Delta_3 = dQ/dt + \Delta'_3$ are the nonadiabatic inflows (outflows) of heat due to radiation heating (cooling), phase transformations of water vapor (condensation, evaporation), turbulent heat transfer, and also the effects (Δ'_3) of errors in initial aerological information and computations on an electronic computer;

$$\Delta_4 = -(q_{con} - q_{evap}) + D_q + \Delta_4,$$

where q_{con} is water vapor condensation, q_{evap} is the evaporation of cloud particles and precipitation particles, D_q is the turbulent transfer of water vapor, Δ'_4 are the effects of errors in initial aerological information and computations on an electronic computer. If it is assumed that D_q and Δ'_4 are small, the Δ_4 value is the total effect of condensation (sublimation) of water vapor and evaporation of cloud particles and precipitation particles in the considered volume. The Δ_4 value will be positive in the case of predominance of evaporation processes or negative in the case of a predominance of water vapor condensation (sublimation) processes.

All the terms in equations (1)-(4), except Δ_1, Δ_2, Δ_3 and Δ_4, were computed on an electronic computer using data from aerological observations. The Δ_1, Δ_2, Δ_3 and Δ_4 values were obtained as residual values on the basis of the balance of equations (1)-(4).

The method and procedures for computing energy and the moisture cycle were described in [1, 5]. These sources also give evaluations of the role of errors in initial aerological information. Numerical experiments indicated that although the errors in computations of energy and the moisture cycle due to the inaccuracy in aerological information are rather considerable, this applies, in particular, to an evaluation of the value of the residual terms in equations (1)-(4). They exert relatively little effect on the general patterns of spatial and temporal changes in energy and the moisture cycle and in addition, are numerically the smaller the greater the thickness of the considered layer of the atmosphere. Satisfactory results are

obtained with a thickness of the layers Δp = 200 gPa. On the average the error of the residual terms is 8-10%.

As indicated by investigations, cyclonic formations have enormous energy reserves: the kinetic energy in a column of the atmosphere is P_{surf} - 50 gPa, where P_{surf} is the surface pressure, on the average being $4 \cdot 10^6$ J/m^2, the potential energy is about $6 \cdot 10^8$ and the internal energy is about $1.7 \cdot 10^9$ J/m^2. The reserves of kinetic energy increase with altitude and in the vertical profile of the distribution have a maximum in the layer 400-200 gPa. The reserves of potential energy increase with altitude, whereas the reserves of internal energy decrease. In the layer 200-50 gPa the reserves of potential and internal energy are approximately identical; the difference does not exceed 5%.

The horizontal distribution of the reserves of kinetic energy even over the relatively small area of the polygon ($2 \cdot 10^{11}$ m^2) is characterized by a definite nonuniformity. The degree of the horizontal nonuniformity of reserves was evaluated by us as the standard deviation of the reserves in a column of the atmosphere over the area of each of the six triangles of the polygon from the total reserve over the area of the entire polygon, normalized to this total reserve. This ratio varied in the range from 10 to 60%. The degree of horizontal nonuniformity of the reserves of kinetic energy is different in different stages of cyclone evolution. In the generation period the degree of nonuniformity was relatively small and does not exceed 10%. With the deepening of the cyclone it increases to 40-60%.

An important parameter to a definite degree reflecting the dynamic activity of a cyclonic formation and weather-forming processes is the ratio of the kinetic energy value to the labile energy value. Whereas for the atmosphere in the northern hemisphere this ratio averages 0.01-0.07%, in temperate-latitude cyclones, as indicated by our computations, this ratio can attain 0.4-0.6%, and as an average was 0.18%. The vertical profile of this parameter has a maximum in the layer 400-200 gPa. This maximum is the more clearly expressed the greater are the energy reserves in the entire considered layer of the atmosphere (P_{surf} - 50 gPa).

The computations indicated that with respect to significance (contribution to budget) the kinetic energy budget is determined by:
-- the generation of kinetic energy (K_{gen}) due to the operation of the pressure gradient force transforming the potential energy into kinetic energy (internal energy source);
-- the inflows (outflows) of energy (K_{bound}) through the lateral boundaries of a column of the atmosphere (external source);
-- the vertical redistribution (K_{ver}) of energy (in a cyclone there is energy transfer from the lower half of the troposphere into the higher layers).

The budget of potential energy is determined by:
-- inflows (outflows) of energy (Π_{bound}) through the lateral boundaries of a column of the atmosphere;
-- the vertical redistribution of energy (Π_{ver});
-- the relative transformation of potential and internal energy.

The budget of internal energy is determined by:
-- the inflows (outflows) of energy (I_{bound}) through the lateral boundaries of a column of the atmosphere;
-- the vertical redistribution of energy (I_{ver});
-- the relative transformation of internal and potential energy;
-- the relative transformation of internal and kinetic energy;
-- the intensity of nonadiabatic processes (phase transformations of water vapor, radiation processes, etc.).

As an example, Figure 2 shows the structure of the budgets of kinetic and internal energy for the central part of the February (1978) cyclone in the stage of its maximum development. In computations of the structure the sum of the moduli of the parameters entering into equations (1) and (3) was assigned the value unity. The internal energy budget (Fig. 2b) gives data only on the contribution of I_t, I_{bound}, I_{ver}, $d\Pi/dt$ and Δ_3; the relative contribution of the remaining components of the budget totals less than 2%.

It can be seen that the contribution of the local changes of energy in both budgets is relatively small; in the P_{surf} - 800 gPa layer it is 6%, but at greater altitudes it is less than 3% in the budget of kinetic energy, whereas in the internal energy budget at all levels it is less than 2%.

The contribution of lateral effects and the vertical redistribution of energy is important. In the kinetic energy budget their total contribution for the atmospheric boundary layer (P_{surf} - 800 gPa) is about 25%, for the layer 800-600 gPa -- about 12%, for the layer 600-400 gPa -- about 25%, for the layer 400-200 gPa -- about 45%, and for the layer 200-50 gPa -- about 20%. In the internal energy budget these contributions are still more important and constitute 87, 33, 61, 59 and 28%.

The contribution of the generation of kinetic energy due to the operation of the pressure gradient force and subgrid effects (Δ_1) is decisive in the kinetic energy budget. In the internal energy budget a considerable contribution is from nonadiabatic factors, attaining almost 50% of the budget in the layer 600-400 gPa. The relative smallness of the contribution of nonadiabatic factors to the internal energy budget for the boundary layer (about 8%) is evidently attributable to the fact that in this atmospheric layer the changes in the energy of phase transformations of water vapor and changes due to radiation factors are opposite in sign and quantitatively to a considerable degree compensate one another. The contribution of the relative transformations of internal and potential energy at different levels attains 10-20%. It should be noted that although the relative contribution of the relative transformations of internal and kinetic energy to the budget is not great (less than 1%), the quantity of this energy is extremely great (see Tables 1 and 2).

The vertical redistribution of energy in cyclonic formations has the important characteristic that in them there is a transfer of energy from the layer P_{surf} = 400 gPa into the layer 400-50 gPa, most sharply expressed in the leading and central parts of a cyclone. On the periphery of an anticyclone, as demonstrated by investigations in fixed polygons, the transfer of energy occurs from the layer

50-400 gPa into the lower layers of the atmosphere. As an example, Fig. 3 shows the averaged profiles of the vertical redistribution of kinetic energy for the periphery of cyclones and the periphery of anticyclones, constructed on the basis of data for Riga polygon. This figure shows that at the cyclone periphery there was pumping of energy from the layer P_{surf}-400 gPa to the layer 400-50 gPa; the greatest outflow occurs at the layer 800-600 gPa (about 1 W/m^2), whereas the greatest inflow is in the layer 200-50 gPa (about 1 W/m^2). At the periphery of an anticyclone, on the other hand, there was a pumping of energy from the lower stratosphere and the upper troposphere into the lower layers; the greatest outflow was from the layer 50-200 gPa, whereas the greatest inflow was in the layer 400-600 gPa.

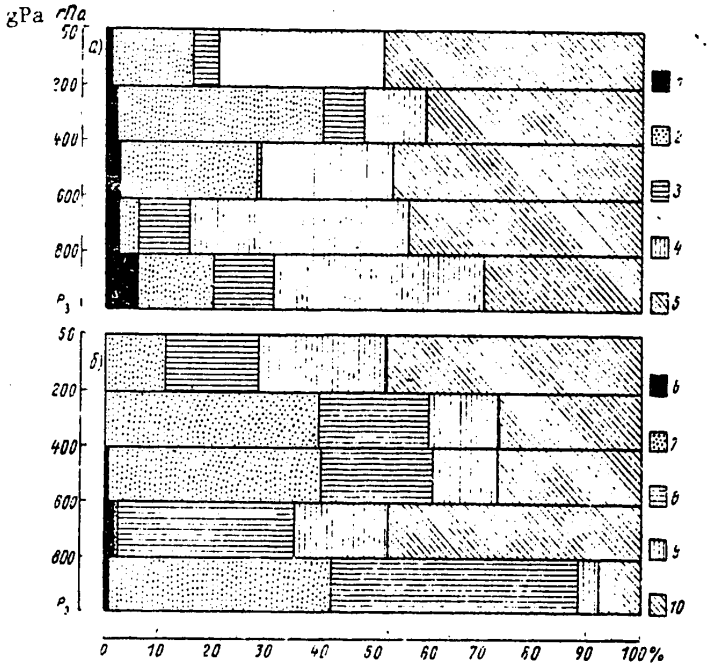

Fig. 3. Structure of budgets of kinetic (a) and internal (b) energy. 1) K_t, 2) K_{bound}, 3) K_{ver}; 4) K_{gen}, 5) Δ_1, 6) I_t, 7) I_{bound}, 8) I_{ver}, 9) $d\Pi/dt$, 10) Δ_3.

Similar patterns of the vertical redistribution of energy are also characteristic for processes in other polygons. A distinguishing characteristic of the Balkhash polygon is that the maximum pumping of energy in the mechanism of vertical redistribution occurs here at great altitudes (in the layer 600-400 gPa).

It should be noted that on the periphery of cyclones in the initial stage of their filling the pumping of energy upward from the layer P_{surf} - 600 gPa still continues, but at the same time there is pumping of energy downward from the

Table 1

Energy Capacity of Mechanisms Forming Budget, Billions of KW

Mechanism forming budget	Cyclonic formations			Periphery of anticyclone
	leading part	central part	southern periphery	
Kinetic energy:				
Generation	18.8	10.9	13.7	2.6
Lateral inflow (outflow)	10.1	8.3	4.9	1.8
Vertical redistribution	2.4	3.9	3.2	0.5
Potential energy:				
Lateral inflow (outflow)	860	760	430	400
Vertical redistribution	370	630	260	170
Internal energy:				
Lateral inflow (outflow)	1150	2830	980	700
Vertical redistribution	640	1570	640	540
Reciprocal transformation of internal and potential energy	120	700	970	540
Reciprocal transformation of internal and kinetic energy	110	80	200	500
Effective condensation of water vapor	40	43	16	8

Table 2

Energy Capacity of Mechanisms Forming Budget of Central Part of Cyclones in Dependence on the Stage of Evolution, Billions of KW

Mechanism forming budget	Stages in cyclone evolution			
	waves	deepening	maximum development	filling
Kinetic energy:				
Generation	4.6	24.1	19.4	11.2
Lateral inflow (outflow)	3.8	11.4	14.2	8.1
Vertical redistribution	0.9	4.9	2.4	1.2
Potential energy:				
Lateral inflow (outflow)	610	750	1680	510
Vertical redistribution	170	360	790	160
Internal energy:				
Lateral inflow (outflow)	1550	1100	2870	1260
Vertical redistribution	760	870	1590	550
Reciprocal transformation of internal and potential energy	110	280	1620	420
Reciprocal transformation of internal and kinetic energy	85	75	83	53
Effective condensation of water vapor	15	70	75	5

layer 50-200 gPa, as a result of which there is an increase in energy, especially in the layer 400-200 gPa. The patterns of vertical redistribution of potential and internal energy have the same character.

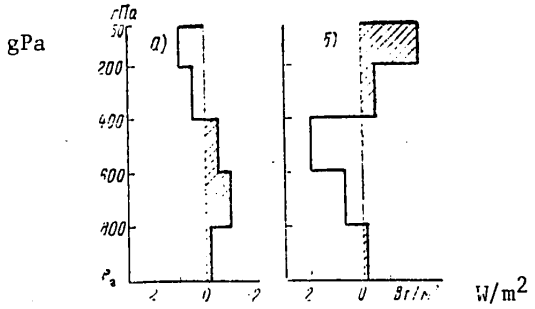

Fig. 3. Vertical redistribution of kinetic energy on periphery of cyclones (a) and periphery of anticyclones (b). Riga polygon.

Thus, although the vertical redistribution of energy in itself does not change the total energy reserves in the column of the atmosphere P_{surf}-50 gPa it exerts a strong effect on the structure of the budget of relatively thin layers of the atmosphere (Δp = 200 gPa) and determines the degree and character of the energy relationship between different layers.

The energy processes in temperate-latitude cyclonic formations have an enormous energy capacity. This is illustrated by the data given in Tables 1 and 2 for the column of the atmosphere P_{surf} - 50 gPa (ground-approximately 20 km) with an area of the base $2 \cdot 10^{11}$ m^2 ($\simeq$ 450 x 450 km). Table 1 gives averaged estimates of the energy capacity of the mechanisms forming the budget for different parts of cyclonic formations and the periphery of anticyclones and Table 2 gives similar data for the central part of cyclones in different phases of their evolution. The maximum values exceeded these means by a factor of 2-3.

Investigations confirmed that in the budget of both kinetic, potential and internal energy small local changes traced on the basis of data from scheduled aerological observations are formed against the background of extremely active processes of generation of kinetic energy, horizontal advection, vertical redistribution and also subgrid processes. This is attributable to the fact that active internal and external sources and losses of energy as a rule mutually compensate one another and are manifested together in the course of local energy changes.

Table 1 shows that lateral effects are expressed most strongly in the leading and central parts of cyclones in which the horizontal influx of kinetic energy averages 8-10 billion KW, with the corresponding figures for potential and internal energy being 760-860 and 1150-2830 billion KW. It should be noted that in the central part of a deep cyclone penetrating into the European USSR in November 1973, rare with respect to the intensity of processes and rate of movement [6], the contribution of horizontal advection to the kinetic energy budget exceeded by a factor of 1 1/2 the contribution from the generation of kinetic energy [5].

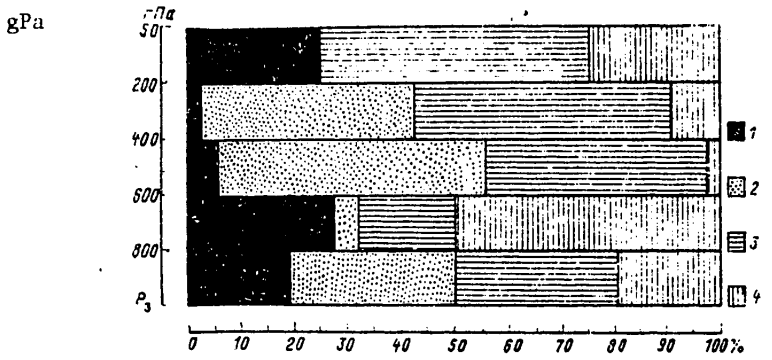

Fig. 4. Structure of water vapor budget.
1) q_t, 2) q_{bound}, 3) q_{ver}, 4) Δ_4.

Now we will turn to Table 2. The data in this table show that the role of the mechanisms forming the energy budget to a considerable degree is dependent on the stage of cyclone evolution. All the energy transformations transpire most actively in the maximum development stage.

Cyclones in general differ from one another both with respect to energy reserves and with respect to the activity of energy transformations, but the structure of the budgets of each of the types of energy for them in general is similar.

Table 3

Distribution of K_{ver}, Δ_4 and $\Delta T/\Delta t$ Parameters by Layers

p gPa	October 1973			November 1973		
	K_{ver} W/m^2	$\Delta_4 \cdot 10^2$ g/(m^2·sec)	$\frac{\Delta T}{\Delta t}$ K/hr	K_{ver} W/m^2	$\Delta_4 \cdot 10^2$ g/(m^2·sec)	$\frac{\Delta T}{\Delta t}$ K/hr
200—50	2,51	0,02	—	30,9	—0,22	—
400—200	6,21	—0,22	0,01	16,9	—1,49	0,072
600—400	—4,94	—1,68	0,08	—6,2	—6,80	0,306
800—600	—0,92	—4,03	0,18	—20,6	—11,36	0,512
P_3—800	—2,89	—2,89	0,13	—21,0	—6,34	0,285
p gPa	February 1978			June 1978		
	K_{ver} W/m^2	$\Delta_4 \cdot 10^2$ g/(m^2·sec)	$\frac{\Delta T}{\Delta t}$ K/hr	K_{ver} W/m^2	$\Delta_4 \cdot 10^2$ g/(m^2·sec)	$\frac{\Delta T}{\Delta t}$ K/hr
200—50	—1,80	0,03	—	2,70	—0,52	—
400—200	8,90	—0,09	0,004	7,19	—2,19	0,10
600—400	—3,60	0,12	—0,005	—7,07	—11,68	0,53
800—600	—0,80	—2,06	0,09	—0,43	—13,49	0,61
P_3—800	—2,70	—1,53	0,07	—2,39	—6,01	0,27

The moisture cycle and the energy of the phase transformations of water vapor associated with it occupies a special place in the energetics of cyclonic formations. As indicated in Tables 1 and 2, the energy of phase transformations in different parts of a cyclone is evaluated as an average of 20-40 billion KW; in the central part of cyclones in the stage of their deepening and maximum development it attains an average of 70-75 billion KW. With respect to its quantity this energy exceeds by several times the generation of energy due to the operation of the force of horizontal pressure gradients.

As indicated by computations, the water vapor reserves in the column of the atmosphere P_{surf} - 50 gPa with an area of the base $2 \cdot 10^{11}$ m^2 on the average are about 2 billion tons; about 80% of the moisture reserves are contained in the layer P_{surf} - 600 gPa. The degree of horizontal nonuniformity in the distribution of moisture reserves over the area of the polygon is dependent on the stage of cyclone evolution. In the generation of a cyclone it is about 20%; in the mature stage it is about 50%.

The water vapor budget is determined by:
-- the inflow (outflow) of water vapor (q_{bound}) through the lateral boundaries of a column of the atmosphere;
-- the vertical redistribution of water vapor (q_{ver});
-- the phase transformation of water vapor (Δ_4).

Table 4

Moisture Cycle in Cyclonic Formations, millions tons/hour

Mechanisms forming water vapor budget	Region (part) of cyclone			Stage in cyclone development			
	leading	central	southern periphery	waves	deepening	development maximum	filling
Lateral inflow	57	71	26	18	43	110	14
Vertical redistribution	25	41	27	15	33	55	25
Effective condensation	59	62	2	21	100	105	7

As an example, Fig. 4 shows the structure of the water vapor budget for the central part of the February (1978) cyclone in the stage of its maximum development. The local changes in the lower half of the troposphere are as follows: in the layer P_{surf} - 800 gPa their contribution was 19%, in the layer 800-600 gPa -- approximately 27, and at greater altitudes -- 5-2%. The horizontal inflow and the vertical redistribution were: in the layer P_{surf} - 800 gPa -- total 61%, in the layer 800-600 gPa -- about 22%, and in the layer 600-400 gPa -- even 92%. Whereas in the layer P_{surf} - 800 gPa the effective condensation contribution was approximately 20% of the budget, in the layer 800-600 gPa it was already 50%. At greater altitudes this contribution does not exceed several percent. It should be noted that in the layer 200-50 gPa the moisture budget is determined primarily by the vertical redistribution (inflow from the lower layers of the atmosphere), constituting 50% of the budget.

As indicated by an analysis of research data, there is a definite correlation between the profile of the vertical redistribution of kinetic energy and the profile of effective water vapor condensation due to the energy of phase transformations which is set free and atmospheric heating. Table 3 gives data on the vertical redistribution of kinetic energy (K_{ver}), the effective condensation of water vapor (Δ_4) and the rate of atmospheric heating ($\Delta T/\Delta t$) by the energy of phase transformations (assuming that all the energy of phase transformations is expended on the heating of air) for the central part of cyclones in the stage of their maximum development. This table shows that the maximum outflow of kinetic energy in the vertical redistribution is in the layer 600-400 gPa and the minimum outflow is in the layer 800-600 gPa. The maximum of the heating rate is in the layer 800-600 gPa, so that this atmospheric layer is heated to a greater degree than the layers P_{surf} - 800 and 600-400 gPa. Accordingly, the layer 600-400 gPa in time becomes thermally unstable and the pumping of energy into the higher layers is intensified in it.

In actuality, in the underlying layer relative to the layer with the maximum rate of heating the vertical temperature gradient decreases and with time this layer becomes thermally more stable, whereas in the above-lying layer, on the other hand, the vertical temperature gradient increases. This layer becomes thermally more unstable and convective movements can develop in it. These movements can be propagated upward and in turn favor the vertical transfer of water vapor. The rate of generation of buoyancy, equal to

$$g\alpha\frac{\Delta T}{\Delta t},$$

where g is the acceleration of free falling, and α is the coefficient of volumetric expansion of the air, can attain, as indicated by computations, 200-250 cm^2/sec^2 per hour.

Thus, the vertical movements of air, ensuring water vapor transfer, exert a significant influence on the structure of the water vapor budget and the effective condensation of water vapor, ensuring the release of the energy of phase transformations, in the feedback system exerts an influence on the intensity and vertical distribution of the vertical movements of air themselves. This phenomenon was manifested with particular clarity in the October (1973), February (1978) and June (1978) cyclones. In the November (1973) cyclone this phenomenon was masked by a strong horizontal inflow of kinetic energy in the layer P_{surf} -600 gPa, giving an intensification of the pumping of kinetic energy from the layer 800-600 gPa.

Quantitative evaluations of the role of each of the mechanisms enumerated above, forming the water vapor budget (for the column of the atmosphere P_{surf} - 50 gPa with an area of the base $2 \cdot 10^{11}$ m^2), are given in Table 4. The data in this table show that the moisture cycle is most intensive in the central part of a cyclone and in the stage of its maximum development. The effective condensation is maximum in the leading and central parts of cyclones (59 and 62 million tons/hour) and in the stage of deepening and maximum development (100 and 105 million tons/hour).

The data in Table 4 convincingly show that the water vapor budget is significantly related to the dynamics (energetics) of the atmosphere (intensity and nature of horizontal and vertical movements).

In conclusion we will examine some results of the investigation related to the moisture cycle and precipitation in cyclonic formations. Computations indicated that effective condensation (condensation minus evaporation) of water vapor in a cyclone in the wave stage, in the central part of a cyclone in the development (deepening) stage, in the leading part of a cyclone occurs 85-90% due to the lateral influxes of water vapor and only 15-10% due to the initial reserves. In the central part of the cyclone in the stage of its filling and on the southern periphery of a cyclone the effective condensation of water vapor occurs 70-100% due to the initial reserves.

Thus, the initial reserves of water vapor in a cyclone in the wave stage, in the central part of the cyclone in the development (deepening) stage and in the leading part of a cyclone are almost not entrained into the phase transformation processes and the formation of precipitation.

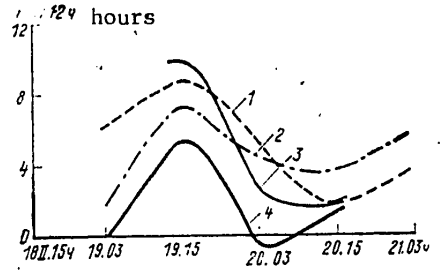

Fig. 5. Measured and computed quantity of precipitation during period 18-21 February 1978. In central part of cyclone: 1) measured, 4) computed; in leading part of cyclone, 2) measured, 3) computed.

Second, it must also be noted, as demonstrated by the comparisons in [1], that the effective condensation of water vapor satisfactorily reflects the presence and intensity of continuous precipitation (over an area) in cyclonic formations. This was also confirmed in subsequent investigations. As an example, Fig. 5 shows the quantity of precipitation measured in the precipitation-gage network and also the quantity of precipitation computed on the basis of the residual term for the leading and central parts of the February cyclone, from 18 through 21 February 1978. If one takes into account the present-day accuracy in measuring precipitation in the precipitation-gaging network, the density of this network and the accuracy of radiosonde measurements of air humidity, the agreement between the curves can be regarded as entirely satisfactory; the maximum quantity of precipitation was observed at 1500 hours on 19 February at the time of the maximum development of the February cyclone and it was confirmed by all the curves shown in Fig. 5.

BIBLIOGRAPHY

1. Kapitanova, T. P. and Pinus, N. Z., "Budget of Water Vapor and Precipitation in Temperate-Latitude Synoptic Formations," METEOROLOGIYA I GIDROLOGIYA (Meteorology and Hydrology), No 1, 1980.

2. Kogan, Z. N. and Pinus, N. Z., "Atmospheric Heat Balance in an Extratropical Cyclone and Over It," RADIATSIONNYYE PROTSESSY V ATMOSFERE I NA ZEMNOY POVERKHNOSTI (Radiation Processes in the Atmosphere and at the Earth's Surface), Leningrad, Gidrometeoizdat, 1979.

3. Kryzhanovskaya, A. P., "Mean Long-Term Paths and Frequency of Recurrence of Cyclones and Anticyclones Over the Northern Hemisphere," SINOPTICHESKIY BYULLETEN' GIDROMETTSENTRA SSSR I VNII GMI (Synoptic Bulletin of the USSR Hydrometeorological Center and the All-Union Scientific Research Institute of Hydrometeorological Information), 1977.

4. Pinus, N. Z. and Kapitanova, T. P., "Water Vapor Budget and Energy of Phase Transformations in a Temperate-Latitude Cyclone," METEOROLOGIYA I GIDROLOGIYA, No 10, 1978.

5. Pinus, N. Z. and Kogan, Z. N., "Budget of Kinetic Energy of Cyclonic Formations," METEOROLOGIYA I GIDROLOGIYA, No 9, 1976.

6. Chelyukanova, S. V., "Unusual Cyclone," METEOROLOGIYA I GIDROLOGIYA, No 3, 1974.

7. Kogan, Z. N. and Pinus, N. Z., "Some Aspects of Energy Budget in Middle Latitude Cyclones," SECOND SPECIAL ASSEMBLY, JAMAP, Seattle USA, 1977.

UDC 551.(571.34+583)

FORMATION OF MOISTENING OF THE LAND ACCOMPANYING CLIMATIC VARIATIONS

Moscow METEOROLOGIYA I GIDROLOGIYA in Russian No 4, Apr 81 pp 17-23

[Article by O. A. Drozdov, professor, State Hydrological Institute, manuscript received 17 Jun 80]

[Text]

Abstract: Since an increase in temperature increases the moisture content and vertical instability of air masses, but weakens westerly transfer and circulation in the temperate latitudes, in the modern epoch moistening in the temperate latitudes decreases during a warming. With a change in temperature by more than ±2°C relative to the modern level the correlation between temperature and precipitation becomes direct. Similar phenomena are observed in the annual variation of precipitation. The secular and intrasecular temperature variations over several centuries reveal an appreciable correlation with the objective characteristics of volcanism and reveal no correlation with Wolf numbers.

In preceding articles ([7] and others) studies were made of the correlation between the thermal regime and moistening. Although these correlations are complex and locally ambiguous, they are decisive in characterizing the precipitation of extensive territories in the temperate latitudes. The complexity of these correlations is attributable to a diversity of effects caused by temperature changes in the moistening regime. Direct correlations between the quantity of precipitation and an increase in temperature arise due to an increase in moisture content and instability of atmospheric stratification. They are clearly manifested with considerable changes in temperature: in the annual variation, in the variation of the quantity of precipitation with latitude and in a change in precipitation in warm and cold geological epochs.

On the other hand, since during warmings there is a decrease in the temperature difference between the poles and the equator, there is a weakening of westerly transfers in the temperate latitudes, which leads to a decrease in water vapor flows from the oceans into the interiors of the continents. The possibility of compensation of the role of westerly flows by meridional flows is noted only with a very

high temperature background (from the south -- in summer at the present time, from the northern seas -- in the geological past). A weakening of westerly transfers increases the intensity of the transfers along the meridians, which favors an increase in the temporal and spatial variability of temperature and precipitation. In addition, cyclonic activity attenuates over the continents and the temperature contrasts decrease within the cyclones themselves, which has a negative effect on the moistening of arid regions.

An analysis of the material shows that on the average for the temperate latitudes under modern conditions the moistening decreases with an increase in temperatures. Judging from the climatic variations in different parts of the spectrum in the Holocene and in the historical epoch this regularity persists at least with temperature changes from -1.7 to +1.3°C in comparison with the modern epoch. Cold epochs, including the "small glacial epoch," were relatively moist; the warm, including boreal and subboreal epochs, were dry. However, with an increase in the temperature level by 2°C the moistening was substantially increased (Atlantic epoch); during coolings greater than 2°C the quantity of precipitation evidently decreases (Fig. 1). A complex dependence of the quantity of precipitation on temperature is also obtained in the annual variation.

We examined the changes in precipitation in the annual variation with a change in temperature for 10 stations in Europe and Siberia situated to the north of the A. I. Voyeykov "great continental axis." Such a choice of stations ensured at them through the course of the year a predominance of winds with a westerly component, that is, relatively uniform conditions of atmospheric circulation. Among these stations six were on the plain, two on the western slope of the Ural Range, one to the east of the Sayan and one (Sverdlovsk) in the "saddle" of the Middle Urals, at the beginning of the leeward slope. The stations near the ranges differ somewhat from the others: the windward stations have relatively more and the leeward stations have relatively lesser winter precipitation and therefore this precipitation thereafter had to be excluded from consideration. At Sverdlovsk the annual variation of precipitation is similar to that observed at lowland stations.

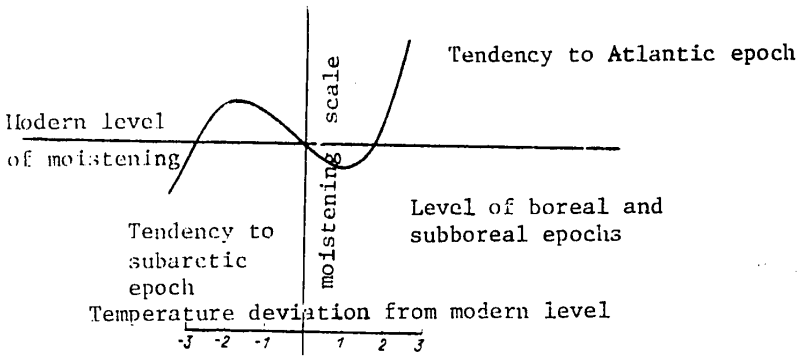

Fig. 1. Diagram of changes in mean annual precipitation in the temperate latitudes of the land with a change in temperature in comparison with the modern temperature.

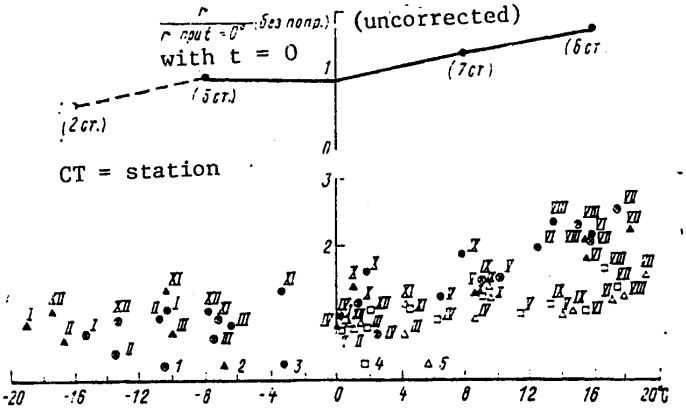

At bottom: monthly precipitation sums (without corrections) for stations, at top: mean of indicated stations. 1) Sverdlovsk; 2) Tomsk; 3) Kayani; 4) Copenhagen; 5) Berlin

Fig. 2. Change in monthly quantities of precipitation in annual variation relative to the precipitation falling at 0°C as a function of temperature in regions with small circulation-moisture differences in course of year.

The dependence of the actual quantity of precipitation, related to precipitation at 0°C, on temperature on the average indicated an increase in precipitation with an increase in temperature, being interrupted in the interval from -8 to 0°C. This interval evidently corresponds to a rapid change in interlatitudinal temperature differences due to degradation of the regime of snow-ice phenomena with an increase in temperatures.

In connection with the change in the temperature level from year to year there is also a change in the form of correlation with the quantity of precipitation [8]. In the warm season of the year the correlation between these parameters is negative (as in the Brickner cycles); in the cold season of the year it is positive. This circumstance in part is a consequence of the trivial fact that cyclonic activity, forming precipitation, decreases in summer, whereas in winter the temperature increases, but in part also reflects the regularities noted above.

In addition to the mentioned features of the correlation, during the cooling and warming in both the long-term and annual variation latitudinal shifts occur in the pressure-circulation zones (trajectories of cyclones, positioning of anticyclones, dislocations of atmospheric fronts, etc.). This circumstance has now already been noted by many Soviet and foreign authors [3, 4, 6, 17, 18 and others].

The superposing of this process on the dependences noted above creates an ambiguity in the changes in precipitation in dependence on the temperatures within large regions and a fundamental curvilinearity of the mentioned correlations for each point separately. The simultaneous effect of all the three above-mentioned correlation factors creates difficulties for an analysis of the regularities of the considered correlations.

In addition to the long-term climatic changes, in whose creation fluctuations in the elements of the earth's orbit, and possibly some other factors apparently participate, in the long-term variation of precipitation there is evidently a whole series

of relatively regular fluctuations in which it is possible to detect approximate-periodic components by correlation and spectral analysis methods. True, due to the nonstationary character of many of these fluctuations they are perceived by many as variants of "red noise" (for orders of the Markov process substantially higher than the first). The longest of these (about 1500-2000 years) are usually related to tidal phenomena [15], less frequently to solar activity. Neither such explanation fully agrees with the actual material. In solar activity fluctuations there is reliable determination only of rhythms not longer than 90 years and more prolonged rhythms are only postulated, frequently with an examination of the actual variation of climate (the tie-in between the variation in climate and shorter solar cycles, as will be demonstrated below, is also not ideal).

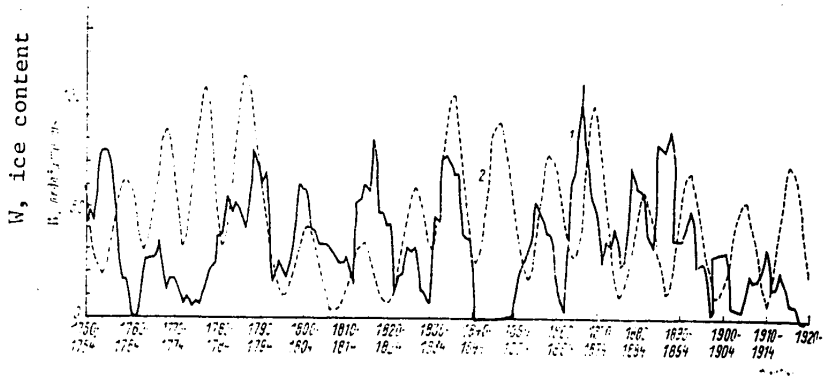

Fig. 3. Secular variation of ice content near Iceland (according to Koch) (1) in comparison with Wolf numbers W (five-year moving averages) (2).

The tie-in of long-term temperature and moisture fluctuations with an 1850-year tidal cycle, in addition to some unclarity in the physical scheme of its influence on climate, is also inadequately satisfactory. In analyzing the variation of these fluctuations from the present day into the past we find that already their first realizations in the historical past diverge from the tidal cycle up to two centuries (lagging or outpacing it in phase). Then into the depth of the past centuries the tie-in becomes still poorer. The temperature and moistening fluctuations themselves also in different parts of the hemisphere are not entirely synchronous; the phase differences can attain several centuries.

The tie-in of temperature and precipitation fluctuations is also not very rigorous. Evidently, even if the tidal phenomena are related to the considered fluctuations the synchronism of the effect is impaired by autooscillations in the atmosphere-ocean-polar ice system. According to the computations of V. Ya. and S. Ya. Sergin [13], the latter can vary in a considerable range of spectra.

The reasons for the shorter fluctuations (300-500 years [6], according to [16] 360 years; 200 years [14], according to [16] 180 years) are unclear. This was also true for secular cycles (60-120 years) [1, 7, 8] (dissimilar with respect to duration and phases in different parts of the hemisphere, and also varying with time)

and numerous shorter cycles (intrasecular, Brickner, and others). Many of these are traced on the basis of ice and isotopic indicators, and also on the basis of fluctuations of water bodies and deposits of silts in lakes over the course of several millenia [1, 7, 9, 10, 14, 16 and others]. Secular and more prolonged cycles since the time of their discovery have been manifested in different geophysical series more or less regularly.

Attempts at explaining intrasecular, secular and multiple (with respect to duration) fluctuations on the basis of the influence of solar activity meet with formal difficulties of a statistical nature. The spectra of secular fluctuations of different geophysical parameters are not identical to one another and do not coincide with the solar cycles (including for an average period up to 10 years or more [9]); in sufficiently long series the increasing difference in the phases of the fluctuations of helio- and geophysical factors becomes quite appreciable. Since for the time being no jumplike changes in phases in the fluctuations of geophysical parameters or time gaps have been discovered in their manifestations up to the time of restoration of the correspondence in phase with secular and other solar cycles, any phase difference can be accumulated between the fluctuations of geophysical parameters and the solar activity cycles.

Such, in particular, was found to be the case in a comparison of the Wolf cycles with the variation of the ice content of the sea near Iceland (according to the Koch index) (Fig. 3), although in both series there are fluctuations with a duration of 10-12 years.

A number of scientists (M. I. Budyko [2], H. H. Lamb [21, 22], H. Flohn [17, 18] and others) have attempted to establish a correlation between decreases in transparency caused by eruptions of groups of volcanoes (or, on the other hand, prolonged increases in transparency) with climatic fluctuations. As long as the effectiveness of eruptions was determined on the basis of indirect criteria, including on the basis of temperature anomalies in the northern hemisphere, it was possible to doubt the objectivity of such comparisons, at least during the time prior to the development of actinometric observations. Even in recent studies with the use of information on eruptions substantially refining and prolonging 2000 years backward the statistics cited by Lamb [19], the correlation between volcanic activity and climate left much to be desired. However, the precipitation of soluble products of eruption onto the glaciers of Greenland (H_2SO_4, $(NH_4)_2SO_4$), some of which make a substantial contribution to the formation of turbidity, created change in the conductivity of ice persisting for many hundreds of years and detected in cores during drilling.

For the time being these data have been obtained only on the basis of drilling in Greenland for a period of 350 years; it is desirable that such refinements be obtained for other regions of the earth. And nevertheless the results of drillings make it possible to conclude that short climatic fluctuations are tied into volcanic-induced atmospheric turbidity considerably better than could be demonstrated before. For example, the last three secular warmings, which were separated by intervals of about 100 years (1930-1940, 1840-1860, 1730-1740), confirmed by the paleotemperatures of Greenland, a decrease in the volume of ice near Iceland and an increase in the growth of wood at the northern boundary of the forest in the Taz River basin, were accompanied by a sharp decrease in the conductivity of the cores.

Similar warmings in 1650-1660 and 1530-1540 can be established only on the basis of the indirect data mentioned above and the virtually zero values of the dust curtain index, according to Lamb, in the years 1514-1550, 1552-1564, 1573, 1588, 1590-1661. Most of the years with increased transparency either precede or occupy the years of warming maxima.

Thus, the hypothesis for the first time expressed by M. I. Budyko [2] concerning the reasons for the secular warmings is confirmed, although for the time being on the basis of limited material. With respect to climatic fluctuations of higher frequencies, they are relatively well dated on the basis of increases in ice volume near Iceland (by a value greater than 20 Koch units [20]). These coolings also agree satisfactorily with the temperature of long-series stations in Western Europe [22], European USSR [12] and the growth of wood at the northern boundary of the forest in Western Siberia [14]. More than 75% of these fluctuations during the period of adequately complete information (from the second half of the 18th century) correlate with the group eruptions of volcanoes. In one case (the eruption of Armagora in 1846) Lamb exaggerated the volcanic component of temperature variation. (Because of the year preceding the eruption, characterized by an anomalously high temperature for some undetermined reason. This initial level should not be taken into account and the subsequent cooling must be reckoned from the mean level of temperatures for the group of preceding years).

After correction of this variation in accordance with data on conductivity, the agreement with the variation of temperature indicators is restored. In three cases (1865-1869, 1885-1892, 1938-1942) the coolings were unrelated to volcanism and according to the information available for the two latter cases the coolings had either a local character (1938-1942) or were noted in the American sector of the Arctic with a relatively high temperature in the Eurasian sector, which in Eurasia formed winter colds of a monsoonal character.

Earlier we made the assumption that such coolings, usually local, are associated with circulation conditions forming in the Arctic and in all probability caused by the distribution of polar ice in periods when its volume was relatively small. This increases meridional transfers, at definite longitudes creating advection from the Arctic, and at others -- either advection of heat, or at the longitudes of sectors with a small quantity of ice, an intensification of monsoonal phenomena on the temperate-latitude continents in winter. For the considered cases this is in general confirmed.

Thus, secular and intrasecular fluctuations of climate are frequently, although not always, associated with the variation of decreases in atmospheric transparency; in the remaining cases the development of meridional intrusions of cold or anticyclones is favorable for them. With respect to more prolonged coolings in the supersecular cycles, according to the data in [18], bursts of active volcanism longer than 1 1/2 centuries apparently do not occur. Accordingly, the problem of the origin of fluctuations of 1500-2000 years for the time being remains open.

BIBLIOGRAPHY

1. Adamenko, V. N., "Variability of Moistening Over a Period of the Last 5000 Years on the Basis of an Analysis of Indirect Indices," DOKLADY AN SSSR (Reports of the USSR Academy of Sciences), Vol 228, 1978.

2. Budyko, M. I., IZMENENIYA KLIMATA (Climatic Changes), Leningrad, Gidrometeoizdat, 1974.

3. Budyko, M. I., Vinnikov, K. Ya., Drozdov, O. A. and Yefimova, N. A., "Impending Climatic Changes," IZV. AN SSSR: SERIYA GEOGRAFICH. (News of the USSR Academy of Sciences. Geographical Series), No 6, 1978.

4. Vitel's, L. A., SINOPTICHESKAYA METEOROLOGIYA I GELIOGEOFIZIKA. IZBRANNYYE TRUDY (Synoptic Meteorology and Heliogeophysics. Selected Works), Leningrad, Gidrometeoizdat, 1977.

5. Gordiyenko, F. G., "Investigation of Dust in Glacial Covers and Its Use in Determining the Age of Ice," MATERIALY GLYATSIOLOGICHESKIKH ISSLEDOVANIY. KHRONIKA, OBSUZHDENIYA (Materials of Glaciological Investigations. News, Discussions), Moscow, USSR Academy of Sciences, No 36, 1979.

6. Drozdov, O. A., "Influence of Man's Economic Activity on the Moisture Cycle," TRUDY GGO (Transactions of the Main Geophysical Observatory), No 316, 1974.

7. Drozdov, O. A., "Investigations of Moistening Variations," METEOROLOGIYA I GIDROLOGIYA (Meteorology and Hydrology), No 4, 1978.

8. Drozdov, O. A. and Grigor'yeva, A. S., VLAGOOBOROT V ATMOSFERE (Moisture Cycle in the Atmosphere), Leningrad, Gidrometeoizdat, 1963.

9. Drozdov, O. A. and Malkova, I. V., "On the Problem of the Use of Autocorrelation Functions for an Analysis of Very Long Dendrochronological Series," DENDROKLIMATOKHRONOLOGIYA I RADIOUGLEROD (Dendroclimatochronology and Radiocarbon. Materials of the Second All-Union Conference on Dendrochronology and Dendroclimatology), Kaunas, 1972.

10. Maksimov, I. V., GEOFIZICHESKIYE SILY I VODY OKEANA (Geophysical Forces and Ocean Waters), Leningrad, Gidrometeoizdat, 1970.

11. Monin, A. S. and Shishkov, Yu. A., ISTORIYA KLIMATA (History of Climate), Leningrad, Gidrometeoizdat, 1979.

12. Rubinshteyn, Ye. S. and Polozova, L. G., SOVREMENNYYE IZMENENIYA KLIMATA (Modern Climatic Changes), Leningrad, Gidrometeoizdat, 1966.

13. Sergin, V. Ya. and Sergin, S. Ya., SISTEMNYY ANALIZ PROBLEMY BOL'SHIKH KOLEBANIY KLIMATA I OLEDENENIYA ZEMLI (Systems Analysis of the Problem of Large Fluctuations of Climate and the Earth's Glaciation), Leningrad, Gidrometeoizdat, 1978.

14. Shiyatov, S. G., "Dendrological Study of Siberian Spruce in the Lower Reaches of the Taz River," DENDROKLIMATOKHRONOLOGIYA I RADIOUGLEROD. MATERIALY VTOROGO VSESOYUZNOGO SOVESHCHANIYA PO DENDROKHRONOLOGII I DENDROKLIMATOLOGII, Kaunas, 1978.

15. Shnitnikov, A. V., "Multisecular Rhythm of Development of Landscapes," KHRONOLOGIYA PLEYSTOTSENA I KLIMATICHESKAYA STRATIGRAFIYA (Chronology of the Pleistocene and Climatic Stratigraphy), Leningrad, Geograficheskoye Obshchestvo SSSR, 1978.

16. Dansgaard, W., Johnson, S. J., Clausen, H. B. and Langway, C. C., Jr., "Climatic Record Revealed by the Camp Century Ice Core," LATE CENOZOIC GLACIAL AGES, edited by K. K. Turkian, Yale University Press, Chapter 3.

17. Flohn, H., "Summary Review and Some Thoughts on Future Climatic Evolutions," EVOL. ATMOS. PLANET ET CLIMATOL. TERRE. COLLOQ. INTERN., Nice, 1978, Toulouse, 1979. R. Zh. (Referativnyy Zhurnal), 09/07b, METEOROLOGIYA I KLIMATOLOGIYA (Meteorology and Climatology), No 1, 1980.

18. Flohn, H., "A Scenario of Possible Future Climates -- Natural and Man-Made," World Colloq., Intern., Nice 1978, Toulouse, 1979, R. Zh. 09/o7b, No 4, 1980.

19. Hirschboeck, K. K., "A New World-Wide Chronology of Volcanic Eruptions (With a Summary of Historical Ash-Producing Activity and Some Implications for Climatic Trends of the Last One Hundred Years)," PALAEOGEOGR., PALAEOCLIM., PALAEOECOL., 29 (1979/1980), No 3-4.

20. Koch, L., "The East Greenland Ice," MEDDELELSER ON GRONLAND, Kobenhavn, Bd 130, No 3, 1945.

21. Lamb, H. H., "Volcanic Dust in the Atmosphere; With a Chronology and Assessment of its Meteorological Significance," PHIL. TRANS. OF THE R. S. OF LONDON. A MATHEMATICAL AND PHYS. SER., Vol 266, No 1178, 2 July 1970.

22. Lamb, H. H., "Volcanic Activity and Climate," PALAEOGEOGR., PALAEOCLIM. AND PALAEOECOL., Vol 10, 1971.

23. Lauter, E. A., "Long-Term Temperature Variations in Middle and West Europe and the Influence of Solar Cycle Variations," ZEITSCH. f. METEOR., Bd 29, H 6, 1979.

UDC 551.(510.4+583)

EFFECT OF CO_2 ON THE THERMAL REGIME OF THE EARTH'S CLIMATIC SYSTEM

Moscow METEOROLOGIYA I GIDROLOGIYA in Russian No 4, Apr 81 pp 24-34

[Article by I. I. Mokhov, candidate of physical and mathematical sciences, Institute of Atmospheric Physics, USSR Academy of Sciences, manuscript received 25 Jun 80]

[Text]

Abstract: A study was made of the influence exerted on the temperature regime of the earth's climatic system by the parameters to which it is most sensitive with a change in atmospheric CO_2 content. It is shown that the results of different climatic models can be analyzed usefully and conveniently using the effective response parameter χ characterizing the derivative of the mean hemispherical surface temperature relative to atmospheric CO_2 concentration. The reasons for the differences in the model results set forth in the article are validated quantitatively. With the use of empirical data it was found that $\chi = 3.5$ K. Allowance for the lag of the annual variation of the mean hemispherical albedo relative to the variation of the mean hemispherical temperature leads to a decrease and even a virtual absence of the influence of a dependence of albedo on mean temperature for the year; in this case χ is close to 2 K. The conclusion is drawn that χ is considerably influenced by the type of cloud cover and stratospheric parameterizations. It was found that the χ parameter for a zonally averaged model is greater than for a hemispherically averaged model.

At the present time the most preferred estimate of the global increase in surface temperature with a doubling of the atmospheric CO_2 content is usually assumed to be 3 K [3, 15], although there is a quite great scatter in the estimates from a half-degree to four or more degrees, that is, differing by an order of magnitude [4, 7-9, 12, 14, 21, 25, 26, 29, 31, 32]. Qualitatively the reasons for such differences for some climatic models are discussed, for example, in a review by

S. Schneider [31]. The purpose of this study was to obtain quantitative estimates of the influence of the parameters of the earth's climatic system to which it is most sensitive with a change in atmospheric CO_2 content. This is done in a simple but quite general formulation suitable for different models and for a comparison with experimental data.

We will examine the energy balance equation for the earth's climatic system, averaged for the northern hemisphere

$$F_{\downarrow}(T, n) - F_{\uparrow}(T, n, q) = 0. \tag{1}$$

Here $F_{\downarrow}$ is the solar radiation absorbed in the system and $F_{\uparrow}$ is the outgoing thermal radiation. These are represented by the functions T -- surface temperature and n -- extent of cloud cover, but $F_{\uparrow}$ is also a function of q -- atmospheric CO_2 content. The solar radiation absorbed in the system can be written in the form

$$F_{\downarrow} = Q(1-\alpha), \tag{2}$$

where 4Q is the solar constant (1360 W/m^2) and albedo α is represented by the formula

$$\alpha = \alpha_0 n + \alpha_n (1-n). \tag{3}$$

[π = cf = cloud free]

The albedo of the cloud system α_0 with the extent of cloud cover n and the albedo of the cloudless system α_{cf} are assumed to be functions of temperature.

It follows from (1) on the assumption of a dependence of the extent of cloud cover n on temperature T that

$$\frac{\partial F_{\downarrow}}{\partial T} dT - \frac{\partial F_{\uparrow}}{\partial T} dT - \frac{\partial F_{\uparrow}}{\partial q} dq = 0. \tag{4}$$

Now we will determine an expression for the differential parameter of response of the temperature regime of the hemisphere to the relative change in atmospheric CO_2 content q:

$$\varkappa = q \frac{dT}{dq} = q \frac{\frac{\partial F_{\uparrow}}{\partial q}}{\frac{\partial F_{\downarrow}}{\partial T} - \frac{\partial F_{\uparrow}}{\partial T}}. \tag{5}$$

Most of the model computations are made for determining an integral characteristic -- the temperature change ΔT of the climatic system with a doubling of the atmospheric CO_2 content. The introduced $\varkappa$ parameter is convenient for a comparison of the ΔT evaluations made in different models with use of the mean value $\Delta F_{\uparrow} = \int_{q_0}^{2q_0} \frac{\partial F_{\uparrow}}{\partial \ln q} d\ln q$ in the numerator of expression (5) with a doubling of q_0,

$$\Delta T = \int_{q_0}^{2q_0} \varkappa \, d\ln q = \int_{q_0}^{2q_0} \frac{\frac{\partial F_{\uparrow}}{\partial \ln q} d\ln q}{\frac{\partial (F_{\downarrow} - F_{\uparrow})}{\partial T}} = \frac{\Delta F_{\uparrow}}{\frac{\partial (F_{\downarrow} - F_{\uparrow})}{\partial T}(q_c)} \approx \tag{5a}$$

$$\approx \frac{\Delta F_{\uparrow}}{\frac{\partial (F_{\uparrow} - F_{\downarrow})}{\partial T}(q_0)} = \varkappa_{эфф} \qquad (5a)$$

[эфф = eff]

where $q_0 < q_c < 2\,q_0$, q_0 is the present-day q value. [Similarly it is possible to estimate the change in T for different changes in q, making use of the approximate expression

According to [29], $\frac{\partial F_{\uparrow}}{\partial \ln q} = -5.9$ W/m^2.] It is important that $\Delta F_{\uparrow}$ varies little from model to model and is about -4 W/m^2 [4, 5, 8, 13, 15, 29]. However, the derivatives of such an effective response parameter $\varkappa$ differ substantially in different models, and as is especially important, they can be evaluated on the basis of experimental data.

In expression (5) it is possible to take into account all the feedbacks and evaluate the influence of all possible climatic variables and parameters: the extent of cloud cover, albedo of the cloud system, relative humidity, vertical temperature gradient, altitude and temperature of clouds, quantity of precipitation, parameters of the stratosphere, biosphere, etc. For example, discriminating the influence of cloud cover extent on the temperature regime, we obtain

$$\varkappa = q \frac{\frac{\partial F_{\uparrow}}{\partial q}}{\frac{\partial F_{\uparrow}}{\partial T} + \frac{\partial F_{\uparrow}}{\partial n}\frac{dn}{dT} - \frac{\partial F_{\downarrow}}{\partial T} - \frac{\partial F_{\downarrow}}{\partial n}\frac{dn}{dT}}. \qquad (6)$$

It is also possible to evaluate the stratospheric influence on $\varkappa$, the importance of an allowance for which is mentioned in [31]. The influence of the stratosphere can be attributed, first of all, to the fact that with a greater atmospheric CO_2 content there is an increase in stratospheric cooling (which decreases stratospheric temperature) and a decrease in stratospheric transparency in the warm range. Second, the increased absorption of solar radiation by both CO_2 and water vapor observed in such cases leads to an increase in temperature [9, 31]. It is simplest to evaluate the stratospheric influence by representing outgoing thermal radiation $F_{\uparrow}$ in the form [10]

$$F_{\uparrow} = F_{\uparrow tr} D_{st} + B_{st}(1 - D_{st}). \qquad (7)$$

Here $F_{\uparrow tr}$ is the outgoing thermal radiation of the troposphere; D_{st} is the integral transmission function for the stratosphere for thermal radiation; $B_{st} = \sigma T_{st}^4$, where σ is the Stefan-Boltzmann constant, T_{st} is the temperature of the isothermic layer of the stratosphere.

Then in place of (5) we obtain

$$\varkappa = q \frac{\frac{\partial F_{\uparrow tr}}{\partial q} D_{st} + \frac{\partial D_{st}}{\partial q}(F_{\uparrow tr} - B_{st}) - \frac{\partial F_{\downarrow st}}{\partial q}}{\frac{\partial F_{\downarrow}}{\partial T} - \frac{\partial F_{\uparrow tr}}{\partial T} D_{st} - \frac{\partial B_{st}}{\partial T}(1 - D_{st})}. \qquad (8)$$

In (8) $F_{\downarrow st} = F_{\downarrow st}(q)$ is the absorption of solar radiation in the stratosphere as a function of q. Using (7), from the energy balance it is possible to obtain the condition for cooling of the stratosphere with an increase in q (with $F_{\downarrow st} = 0$):

$$\frac{\partial B_{st}}{\partial T}(1-D_{st})\,dT - B_{st}\frac{\partial D_{st}}{\partial q}\,dq > 0. \tag{9}$$

Or otherwise

$$\frac{\partial D_{st}}{\partial q} < \frac{4}{T_{st}}\frac{\partial T_{st}}{\partial T}(1-D_{st})\frac{dT}{dq} < 0. \tag{10}$$

with $dT/dq > 0$ and $\partial T_{st}/\partial T < 0$. For example, in [31] there is an estimate of the value $\partial T_{st}/\partial T = -4$, in order to obtain which it is necessary to take into account the absorption of solar radiation in the stratosphere. We note that the stratosphere with D_{st} close to 1 considerably increases dT/dq.

Table 1

Comparison of ΔT and $\varkappa$ Parameters for Different Models

Climatic models		T K	K
Energy balance	[12]	0.5	0.5
	[33]	0.7	0.7
	[9]	1.1	1.1
		3.0	3.1
	[29]	3.2	3.6
Radiation-convective	[14]	2.0	1.9
		3.2	3.0
General circulation	[24]	2.9	2.7

We estimated the values of the effective parameter $\varkappa$ using formula (5) with (5a) taken into account for different models. Table 1 gives an evaluation of $\varkappa$ for some models with appreciably differing changes in mean surface temperature ΔT with a doubling of the atmospheric CO_2 content: for the general circulation model [24], for the radiation-convective model [14], for energy balance models [9, 12, 29, 33]. For model [24] the values of the temperature radiation influx derivatives were taken from [18]. Table 1 shows that the $\varkappa$ parameter reflects well the properties of the models, that is, a knowledge of the derivative radiation influxes with respect to different variables makes possible a quite precise evaluation of the change in the temperature regime of the climatic system with a change in the atmospheric CO_2 content.

On the basis of the model comparisons made the conclusion can be drawn that there is an appreciable sensitivity of $\varkappa$ to the parameterization of cloud cover: the dependence of albedo and the quantity of clouds on temperature. The substantial influence of cloud cover on the sensitivity of the climatic system can also be seen when using data from satellite measurements in [27]. In particular, the positive dependence of cloud system albedo on temperature in models [12, 33] also determines lower temperature changes with a doubling of atmospheric CO_2 content. For example, if the positive dependence of cloud albedo on temperature in the model proposed in [8] is excluded, the value of the temperature increment more than triples -- from 0.5 to 1.7 K without allowance for influence of the stratosphere.

An important reason for the difference in the results in the models [9, 14, 29] is the difference in the derivatives of outgoing thermal radiation for temperature $\partial F_\uparrow / \partial T$. The difference in the results in the different variants of the radiation-convective model [14] is associated, for example, with the difference in $\partial F_\uparrow / \partial T$ in cases of a constant temperature or altitude of the upper cloud level. The variants of model [9] differ in the dependence of albedo on temperature, and not only due to the influence of the snow and ice cover, but also due to the influence of a change in the biosphere on albedo.

In comparing the model evaluations of change in the temperature regime with evaluations based on real data for the northern hemisphere we will use a number of equations and dependences obtained using the corresponding regressions based on empirical zonally and hemispherically averaged data in the annual variation and for the mean annual regime. Data for surface temperature were taken from [19]. For outgoing thermal radiation in the annual variation, according to mean monthly data [20], averaged for the hemisphere, using the linear regression

$$F_\uparrow = A + B\,(T - T_0), \tag{11}$$

where T_0 = 273 K, we determine A = 204 W/m^2 and B = 2.0 W/(m^2·K) with a correlation coefficient r = 0.83. We note that in the regression using mean annual zonally averaged data, the coefficients coincide with those determined within the limits of 2% accuracy. All the latitude zones in the regression based on mean annual data were represented with an equal weight.

The dependence of albedo of the hemisphere α ($\alpha = \int_0^1 \alpha(x)\, S(x)\, dx$, $x = \sin\varphi$, φ is latitude, S(x) is the insolation distribution function, satisfying the condition

$$\int_0^1 S(x)\, dx = 1$$

on the mean surface temperature of the hemisphere

$$\left(T = \int_0^1 T(x)\, dx\right)$$

on the basis of mean monthly data for $\alpha(x)$ in the annual variation [20], was determined using the linear regression

$$\alpha = \alpha_0 + \alpha_1\,(T - T_0). \tag{12}$$

In (12) an allowance was made for the time lag in the annual variation of albedo, for example, due to the inertia of the cryosphere, relative to the temperature variation. The maximum correlation coefficient (0.9) for (12) was obtained with a lag time Δt equal to approximately 3 months. With Δt = 3 months we determined $\alpha_1 = d\alpha/dT = -0.0024\ K^{-1}$ and $\alpha_0 = 0.340$.

On the basis of the empirically determined expressions (11) and (12) for the northern hemisphere in the annual variation we determine (specifically with $\Delta F_\uparrow = -4.1$ W/m^2 [29]) in accordance with (5) the value of the effective parameter χ -- 3.5 K.

The determined value confirms the conclusions [3, 15] that the most preferable estimate is 3°K for the change in the mean global surface temperature with a doubling of atmospheric CO_2 content.

Allowance for a lag of a quarter period (3 months) in the annual variation of mean hemispheric albedo relative to the variation of mean hemispheric temperature leads to a decrease and even a virtual absence of the influence of the dependence of albedo on temperature as an average for the year. [We will demonstrate the influence of a lag in the annual variation of mean hemispheric albedo α relative to the annual variation of mean hemispheric temperature T in an example. As a simplification we will represent the annual variation of T and α in the following form:

$$T=\overline{T}+\Delta T\sin\omega t,$$

$$\alpha=\overline{\alpha}-\Delta\alpha\sin\omega(t-\Delta t).$$

Here ω is the angular frequency of the earth's revolution; $\Delta t=\frac{\frac{\pi}{2}-\delta}{\omega}$, where δ determines the difference from a quarter of the lag period α relative to T; $\overline{T}$ and $\overline{\alpha}$ are the mean annual values, and ΔT and $\Delta\alpha$ are the amplitudes of the annual variation of the mean hemispheric temperature and albedo respectively. Using the expressions for T and α, we obtain the formula $\frac{d\alpha}{dT}=\frac{d\alpha}{dT}\frac{dt}{dt}=-\frac{\Delta\alpha}{\Delta T}(\cos\delta\operatorname{tg}\omega t-\sin\delta)$.

With averaging for a year $(2\pi/\omega)$ we obtain $\overline{d\alpha}/dT = \sin\delta$, since $\int_0^{2\pi/\omega}\operatorname{tg}\omega t\,dt=0$.

However, if the lag is equal to a quarter period (3 months), that is $\delta = 0$, then $d\alpha/dT = 0$ and as an average for the year there appears to be no dependence of α on T.] In the absence of a dependence of planetary albedo on temperature the $\varkappa$ value is close to 2°K. This estimate coincides with the results of computations by S. Manabe and R. Stouffer using a general circulation model with an annual variation for an increase of mean global temperature with a doubling of atmospheric CO_2 content [25]. We note that for long-term changes of the climatic system the influence of the dependence of planetary albedo on temperature must not be precluded. It is possible to evaluate the influence of the stratosphere on the $\varkappa$ parameter. For example, with $\Delta F_\uparrow$ for the tropospheric model from [10] we estimate $\varkappa = 2$°K, indicating the importance of stratospheric influence on the $\varkappa$ parameter.

One of the most important problems in climate theory is that of the influence of cloud cover on the thermal regime of the earth's climatic system. This problem has not yet been solved due to the shortage of experimental data on cloud cover. It is all the more important to evaluate the criticality of the results of computations for a possible uncertainty in cloud cover parameterization [6, 11]. In this case we evaluate the influence of cloud cover on the $\varkappa$ parameter. It follows from a representation of hemispheric albedo α in the form (3) that

[п = hemi(sphere)] $$\frac{d\alpha}{dT}=\frac{d\alpha_0}{dT}n+\frac{d\alpha_n}{dT}(1-n)+\frac{dn}{dT}(\alpha_0-\alpha_n). \qquad (13)$$

The dependence of the extent of cloud cover on temperature in (13) can be determined from the nonstationary equation

$$\tau_n\frac{dn}{dt}=-(n-\overline{n})+c(T-\overline{T}) \qquad (14)$$

for the extent of cloud cover, averaged for the hemisphere, in the annual variation according according to data in [2]. Here n and T are the stationary mean annual cloud cover and temperature, τ_n is the characteristic inertia time for cloud cover extent. In (14), by the least squares method, for the regression

$$y=a_1z_1+a_2z_2 \qquad (15)$$

with $z_1 = T - \overline{T}$, $y = n - \overline{n}$, $z_2 = dn/dt$, $a_1 = c$, $a_2 = -\tau_n$ we determine the values $\tau_n = 0.05$ month and $c = 0.004\ K^{-1}$ with a correlation coefficient $r = 0.93$ (14). It is important to note that according to [1] with an increase in the extent of cloud cover without the falling of precipitation the temperature at the surface is reduced. However, the temperature increase due to an increase in the quantity of heat released during the condensation of water vapor is greater than the decrease in temperature due solely to the increase in cloud cover and the total effect is expressed in a temperature increase. However, with the use of mean annual data for different latitudes the correlation coefficient for the extent of cloud cover and temperature is negative [16]. Accordingly, it must be noted that the change in the extent of cloud cover with latitude is associated not only with the temperature distribution with latitude and generally speaking, it is impossible to determine their correlation from the latitudinal variation of the parameters. In order to describe the correlation between the extent of cloud cover and temperature, for example, it is necessary to investigate changes in cloud cover and temperature with time over the stipulated area.

In order to determine the dependence of the albedo of a cloud-free system use was made of the nonstationary dependence of the area of the snow-ice cover x_s on the mean surface temperature T of the hemisphere. In a linear approximation for small deviations of x_s and T from their stationary mean annual values $\overline{x}_s$ and $\overline{T}$ the sought-for equation assumes the form

$$\tau_s \frac{dx_s}{dt} = -(x_s - \overline{x}_s) + d(T - \overline{T}). \tag{16}$$

Here $x_s = \sin \varphi_s$; φ_s is the latitude of the continuous snow and ice cover, determined from the mean monthly data from [30] on the fraction of sea ice and snow in different latitude zones in the course of the year; τ_s is the characteristic inertia time for sea ice and the snow cover of the land.

On the basis of equation (16), by the least squares method for a regression in the form (15) with $y = x_s - \overline{x}_s$, $z_1 = T - \overline{T}$, $z_2 = dx_s/dt$, $a_1 = d$, $a_2 = -\tau_s$ we find that with $\tau_s = 0.44$ month, $\varphi_s = 60°N$, the correlation coefficient for the latitude of the snow-ice boundary with the temperature $d = 0.0144\ K^{-1}$ is 0.99. In this case $z_2 = dx_s/dt$ in the computations were determined as the central differences of the x_s values for adjacent months. By determining the coefficient dx_s/dT it is possible to find $d\alpha_{cf}/dT$ from the expression

$$d\alpha_{cf}/dT = -(\alpha_{ice} - \alpha_{if})\frac{dx_s}{dT}, \tag{17}$$

where α_{ice} and α_{if} are the albedo of the system over ice and over ice-free surfaces respectively

We will determine the mean hemispherical albedo values α_{ice}, α_{if} and α_0, using the data in [20] for the mean annual distribution of albedo α with the latitude ($x = \sin \varphi$), on the basis of the following equations:

[п = cf; л = ice]

$$\alpha_n = \alpha_n \int_{\overline{x}_s}^{1} S(x)\,dx + \alpha_0 \int_{0}^{\overline{x}_s} S(x)\,dx, \tag{18}$$

$$\alpha_n(1 - n) + \alpha_0 n = \int_{\overline{x}_s}^{1} S(x)\,\alpha(x)\,dx \Big/ \int_{\overline{x}_s}^{1} S(x)\,dx,$$

$$\alpha_6 (1 - n) + \alpha_0 n = \int_0^{\overline{x_s}} S(x)\ \alpha(x)\ \alpha x \Big/ \int_0^{\overline{x_s}} S(x)\ dx.$$

Here S(x) is the function of distribution of insolation with latitude. In order to evaluate the mean hemispherical albedo values α_{ice}, α_{if} and α_0 in (18) we use $n = 0.5$ and $\alpha_{cf} = 0.18$, as in [16], on the basis of the data in [20]. With $\varphi_s = 60°N$ ($x_s = \sin \varphi_s$) we obtain $\alpha_{if} = 0.15$, $\alpha_{ice} = 0.56$, $\alpha_0 = 0.43$. With the determined albedo values $d\alpha_{cf}/dT = -0.0059\ K^{-1}$ and using the value $d\alpha/dT = -0.0024\ K^{-1}$ obtained above, from equation (13) for $dn/dT = 0.004\ K^{-1}$ we determine $d\alpha_0/dT = -0.001\ K^{-1}$. We will evaluate the reliability of the resulting value $d\alpha_0/dT$. If it is assumed that the extent of cloud cover is not dependent on temperature, then from (13) it follows that $d\alpha_0/dT = 0.001\ K^{-1}$. Thus, the uncertainty in the dependence of the extent of cloud cover on temperature leads to an uncertainty in the sign of the dependence of cloud system albedo on temperature.

The response of outgoing thermal radiation $F_\uparrow$ to a change in temperature and the extent of cloud cover is determined using a representation in the form [4]

$$F_\uparrow = a + b\ (T - T_0) - [a_1 + b_1\ (T - T_0)]\, n. \tag{19}$$

Due to the already mentioned uncertainty in the parameterization of cloud cover there are considerable differences in the coefficients of expression (19). In particular, the $\partial F_\uparrow / \partial n$ value in the studies of different authors varies in the range from 34 to 91 W/m^2 [17]. Such an uncertainty exerts a considerable effect when finding the relative influence of cloud cover on the response of the climatic system in this case to a change in atmospheric CO_2 content.

In order to evaluate the influence of cloud cover on the $\varkappa$ parameter we will use parameterization of outgoing thermal radiation from [10], for which the $\partial F_\uparrow / \partial n$ value falls in the middle of the above-mentioned range. In [10], on the basis of the proposed model, analytical expressions were obtained for the coefficients in (19) and their values were determined:

$$F_\uparrow = 230 + 2.4\ (T - T_0) - [54 + 0.6\ (T - T_0)]\, n. \quad [W/m^2] \tag{20}$$

(The coefficients in (20) differ somewhat from those cited in [10], since in [10] the outgoing thermal radiation was parameterized through the extent of cloud cover in the thermal wavelength range). It follows from (20) that

$$\frac{dF_\uparrow}{dT} = 2{,}1 - 63\frac{dn}{dT} \quad [W/(m^2 \cdot K)] \tag{21}$$

with values n = 0.5 and T = 288 K for present-day mean hemispherical cloud cover extent and surface temperature.

We note that for a coincidence of the $dF_\uparrow/dT$ values from (11) and (21) it is necessary that $dn/dT = 0.002\ K^{-1}$. It follows from (13) that $d\alpha_0/dT = 0$. On the basis of these parameterizations it is possible to represent the effective parameter $\varkappa$ as a function of the cloud cover characteristics dn/dT and $d\alpha_0/dT$:

$$\varkappa = \frac{\Delta F_\uparrow}{f_1 + f_2 \frac{d\alpha_0}{dT} + f_3 \frac{dn}{dT}}, \tag{22}$$

where $f_1 = b + Q(1 - n)d\sigma_{cf}/dT$, $f_2 = Qn$, $f_3 = Q(\alpha_0 - \alpha_{cf}) - (a_1 + b_1 T)$.

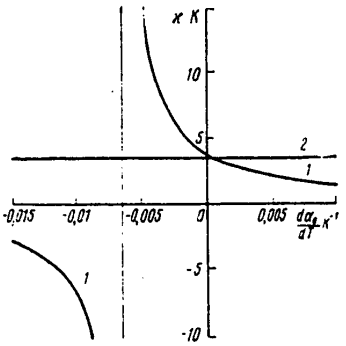

Fig. 1. Dependence of the χ parameter on $d\alpha_0/dT$ with $dn/dT = 0$ (hyperbola 1). The straight line 2 corresponds to $\chi = 3.5°K$.

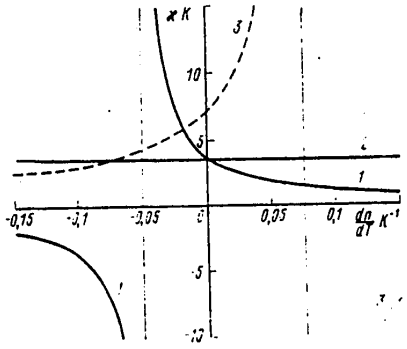

Fig. 2. Dependence of χ parameter on dn/dt with $d\alpha_0/dT = 0$. For the parameterization of outgoing thermal radiation $F_\uparrow$ from [10] -- hyperbola 1, for the parameterization of $F_\uparrow$ from [16] -- hyperbola 3. The straight line 2 corresponds to $\chi = 3.5°K$.

For an evaluation of the response of χ to the $d\alpha_0/dT$ and dn/dT values Figures 1 and 2 give curves (hyperbola 1) of the dependence of the χ parameter on $d\alpha_0/dT$ with $dn/dT = 0$ and on dn/dT with $d\alpha_0/dT = 0$ in accordance with (22). Table 2 gives the corresponding computed χ values with the $d\alpha_0/dT$ and dn/dT values used in different models. Evaluations of χ without allowance for influence of the stratosphere with $\Delta F_\uparrow$ from [10] are given in parentheses. It follows from the cited evaluations that the different model parameterizations of cloud cover can substantially change the value of the χ parameter. However, we note that the dependence of the extent of cloud cover on temperature $dn/dT = 0.004\ K^{-1}$ found in this study for the northern hemisphere on the basis of empirical data in the annual variation exerts little influence on the χ parameter. The stratosphere exerts a considerable influence on χ.

It is interesting to note that with a sufficiently strong negative dependence of albedo and cloud cover extent on temperature an increase in atmospheric CO_2 content can lead to a temperature decrease. (However, this regime is evidently unstable.) It can also be seen that the χ parameter is sensitive to a change in $d\alpha_0/dT$ and dn/dT and with an increase of their negative values in absolute terms increases with $\chi > 0$. In this connection it is necessary to note the inadequate accuracy and completeness of present-day data on cloud cover on a global scale for drawing final conclusions concerning its influence. For example, the $\partial F_\uparrow / \partial n$

values near the upper boundary of the range of uncertainty correspond to a weaker (and even opposite in sign) dependence of the χ parameter on the dn/dT value characterizing the correlation between the extent of cloud cover and temperature. In particular, the hyperbola 3 in Fig. 2 was computed for the upper boundary of the $\partial F_\uparrow / \partial n$ value for the uncertainty range [16]. As a comparison, Figures 1 and 2 show the straight lines 2 corresponding to the value of the parameter $\chi = 3.5°K$, evaluated on the basis of experimental data.

Table 2

Evaluation of χ Parameter in Dependence on $d\alpha_0/dT$ with dn/dT = 0 and on dn/dT with $d\alpha_0/dT = 0$

$\chi\left(\frac{d\alpha_0}{dT}\right)$	$\frac{d\alpha_0}{dT}$ K^{-1}	$\chi\left(\frac{dn}{dT}\right)$	$\frac{dn}{dT}$ K^{-1}
1,1 (0,6)	0.015 [12]	2,5 (1,4)	0,026 [28]
3,2 (1,8)	0,001	3,5 (1,9)	0,004 [11]
3,7 (2,1)	0	3,7 (2,1)	0
4,1 (2,3)	—0.0005 [22]	4,1 (2,3)	—0,004 [11]
4,4 (2,5)	—0,001	4,7 (2,6)	—0,01 [16]
<0	<—0,0065	<0	<—0,05

All the cited computations were made for a climatic system averaged for the hemisphere. With conversion to a zonally averaged energy balance system there is a meridional transfer of energy $F_{\leftrightarrow}$ and a dependence of temperature on latitude φ(x = sin φ). The initial energy balance equation (1) for a system averaged for the hemisphere can be written in the form:

$$\langle F_\downarrow \rangle = \langle F_\uparrow \rangle, \tag{1a}$$

where $\langle F_\downarrow \rangle = Q(1 - \langle \alpha \rangle)$, $\langle \alpha \rangle = \int_0^1 \alpha(x) S(x)\, dx$,

$$\langle F_\uparrow \rangle = \int_0^1 F_\uparrow(x)\, dx.$$

In the case of a zonally averaged system the energy balance equation has the form

$$F_\downarrow(x) - F_\uparrow(x) = F_{\leftrightarrow}(x). \tag{23}$$

Here $F_\downarrow(x) = QS(x)[1 - \alpha(x)]$, $\alpha = \alpha[x, T(x)]$, $F_\uparrow = F_\uparrow[T(x)]$, $n = n(x)$.

If we assume a meridional transfer of the temperature function at a particular latitude T(x) and a mean hemispherical temperature

$$\langle T\rangle = \int_0^1 T(x)\,dx,$$

for example, as in the model [4]

$$F_{\leftrightarrow} = F_{\leftrightarrow}[T(x),\ \langle T\rangle], \tag{24}$$

then the response parameter $\varkappa$ assumes the form

$$\varkappa_1 = \frac{-\frac{\partial\langle F_\uparrow\rangle}{\partial q}}{\frac{\partial\langle F_\uparrow\rangle}{\partial\langle T\rangle} - \frac{\partial\langle F_\downarrow\rangle}{\partial\langle I\rangle}} = \frac{-\frac{\partial\langle F_\uparrow\rangle}{\partial q}}{\frac{\partial\langle F_\uparrow\rangle}{\partial\langle T\rangle} + Q\int_0^1 \frac{-\frac{\partial F_{\leftrightarrow}}{\partial\langle T\rangle}\frac{\partial\alpha}{\partial T}S(x)\,dx}{\left[QS(x)\frac{\partial\alpha}{\partial T} + \frac{\partial F_\downarrow}{\partial T} + \frac{\partial F_{\leftrightarrow}}{\partial T}\right]}}. \tag{25}$$

In particular, in model [4] the meridional transfer is expressed in the form

$$F_{\leftrightarrow} = \gamma\,(T - \langle T\rangle), \tag{26}$$

then

$$\varkappa_1 = \frac{-\frac{\partial\langle F_\uparrow\rangle}{\partial q}}{\frac{\partial\langle F_\uparrow\rangle}{\partial T} + Q\int_0^1 \frac{\frac{\partial\alpha}{\partial T}S(x)\,dx}{1 + \frac{1}{\gamma}\left[QS(x)\frac{\partial\alpha}{\partial T} + \frac{\partial F_\downarrow}{\partial T}\right]}}. \tag{27}$$

We note that the dependence of system albedo on temperature is determined for the most part by the high and middle latitudes due to the high albedo of snow and ice [22].

On the basis of the data used in this study it is possible to determine that the $\varkappa_1$ parameter is greater than the $\varkappa_0$ parameter for a hemispherically averaged model and approaches $\varkappa_0$

$$\varkappa_1 \underset{\gamma\to\infty}{\to} \varkappa_0 \tag{28}$$

in the case of intensive meridional transfer with $\gamma\to\infty$. (In accordance with [9] the real value of the γ parameter in the computations was assumed equal to 3.75 W/(m^2·K)). The computations in [23, 24, 32, 33] confirm that the response of the models to a change in atmospheric CO_2 content increases with an increase in the dimensionality of the model, for example, with conversion from mean hemispherical to zonally averaged models. As is well known, in zonally averaged models there is a great change in temperature in the high latitudes with an increase in atmospheric CO_2 content.

In conclusion the author expresses appreciation to G. S. Golitsyn and also to A. S. Ginzburg, V. K. Petukhov and R. D. Sess for useful discussion.

BIBLIOGRAPHY

1. Adem, Yu., "Use of Thermodynamics in the Study of Climatic Changes," FIZICHESKAYA I DINAMICHESKAYA KLIMATOLOGIYA. TRUDY SIMPOZIUMA PO FIZICHESKOY I DINAMICHESKOY KLIMATOLOGII (Physical and Dynamic Climatology. Transactions of the Symposium on Physical and Dynamic Climatology), Leningrad, Gidrometeoizdat, 1974.

2. Berlyand, T. G., Strokina, L. A. and Greshnikova, L. Ye., "Zonal Distribution of the Quantity of Clouds Over the Earth," METEOROLOGIYA I GIDROLOGIYA (Meteorology and Hydrology), No 3, 1980.

3. Budyko, M. I., "The Problem of the Anthropogenic Change in Climate," Report at the All-Union Conference on the Problem of Anthropogenic Change in Climate, Leningrad, 1980.

4. Budyko, M. I., IZMENENIYA KLIMATA (Climatic Changes), Leningrad, Gidrometeoizdat, 1974.

5. Ginzburg, A. S., Communication at the All-Union Conference on the Problem of Anthropogenic Change in Climate, Leningrad, 1980.

6. Golitsyn, G. S. and Mokhov, I. I., "Evaluations of the Response and Role of Cloud Cover in Simple Models of Climate," IZV. AN SSSR: FIZIKA ATMOSFERY I OKEANA (News of the USSR Academy of Sciences: Physics of the Atmosphere and Ocean), No 8, 1978.

7. Dymnikov, V. P., Galin, V. Ya. and Perov, V. L., "Numerical Experiments for Computing the Influence of Change in the Concentration of Carbon Dioxide on Climate," Report at the All-Union Conference on the Problem of Anthropogenic Change in Climate, Leningrad, 1980.

8. Mokhov, I. I. and Petukhov, V. K., "On the Problem of Modeling of the Influence of an Increase in the Concentration of Carbon Dioxide on the Thermal Regime," Report at the All-Union Conference on the Problem of Anthropogenic Change in Climate, Leningrad, 1980.

9. Mokhov, I. I., CHUVSTVITEL'NOST' I USTOYCHIVOST' ZONAL'NYKH TERMODINAMICHESKIKH MODELEY KLIMATA (Response and Stability of Zonal Thermodynamic Models of Climate), Dissertation for the Award of the Academic Degree of Candidate of Physical and Mathematical Sciences, Moscow, 1979.

10. Mokhov, I. I. and Petukhov, V. K., PARAMETERIZATSIYA UKHODYASHCHEY DLINOVOLNOVOY RADIATSII DLYA KLIMATICHESKIKH MODELEY (Parameterization of Outgoing Long-Wave Radiation for Climatic Models), Preprint IFA AN SSSR, 1978.

11. Mokhov, I. I., "Reaction of a Simple Energy Balance Model of Climate to the Change in Its Parameters," IZV. AN SSSR: FIZIKA ATMOSFERY I OKEANA (News of the USSR Academy of Sciences: Physics of the Atmosphere and Ocean), No 4, 1979.

12. Petukhov, V. K., Feygel'son, Ye. M. and Manuylova, N. I., "Regulating Role of Cloud Cover and Thermal Effects of Anthropogenic Aerosol and Carbon Dioxide," IZV. AN SSSR: FIZIKA ATMOSFERY I OKEANA, No 8, 1975.

13. Ackerman, T. P., "On the Effect of CO_2 on Atmospheric Heating Rates," TELLUS, Vol 31, No 2, 1979.

14. Augustsson, T. and Ramanathan, V., "A Radiative-Convective Model Study of the CO_2 Climate Problem," J. ATMOS. SCI., Vol 34, No 3, 1977.

15. CARBON DIOXIDE AND CLIMATE: A SCIENTIFIC ASSESSMENT REPORT OF AN AD HOC STUDY GROUP ON CARBON DIOXIDE AND CLIMATE, Woods Hole, Massachusetts, July 23-27, 1979. National Academy of Sciences, Washington, D. C., 1979.

16. Cess, R. D., "Climate Change: An Appraisal of Atmospheric Feedback Mechanisms Employing Zonal Climatology," J. ATMOS. SCI., Vol 33, No 10, 1976.

17. Cess, R. D. and Ramanathan, V., "Averaging of Infrared Cloud Opacities for Climate Modeling," J. ATMOS. SCI., Vol 35, No 5, 1978.

18. Coakley, J. A., Jr. and Wielicki, B. A., "Testing Energy Balance Climate Models," J. ATMOS. SCI., Vol 36, No 11, 1979.

19. Crutcher, H. L. and Meserve, J. M., "Selected-Level Heights, Temperatures and Dew Point Temperatures for the Northern Hemisphere," NAVAIR 50-IC-52, Washington, D. C., 1970.

20. Ellis, J. and Vonder Haar, T. H., "Zonal Average Earth Radiation Budget Measurements From Satellites for Climatic Studies," ATMOS. SCI. PAPERS, Vol 240, Colorado State Univ., 1976.

21. Lee, S. P. and Snell, F. M., "An Annual Zonally Averaged Global Climate Model With Diffuse Cloudiness Feedback," J. ATMOS. SCI., Vol 34, No 6, 1977.

22. Lian, M. S. and Cess, R. D., "Energy-Balance Climate Models: A Reappraisal of Ice-Albedo Feedback," J. ATMOS. SCI., Vol 34, No 7, 1977.

23. Manabe, S. and Wetherald, R. T., "Thermal Equilibrium of the Atmosphere With a Given Distribution of Relative Humidity," J. ATMOS. SCI., Vol 24, No 3, 1967.

24. Manabe, S. and Wetherald, R. T., "The Effects of Doubling the CO_2 Concentration on the Climate of a General Circulation Model," J. ATMOS. SCI., Vol 32, No 1, 1975.

25. Manabe, S. and Stouffer, R. J., "A CO_2 Climate Sensitivity Study With a Mathematical Model of the Global Climate," NATURE, Vol 282, 1979.

26. Ohring, G. and Adler, S., "Some Experiments With a Zonally Averaged Climate Model," J. ATMOS. SCI., Vol 35, No 2, 1978.

27. Ohring, G., Clapp, P., Heddinghaus, T. R. and Krueger, A. F., "The Sensitivity of the Earth's Radiation Budget to Changes in Cloudiness," COSPAR. TWENTY-THIRD PLENARY MEETING, Budapest, Hungary, 2-14 June 1980. Abstracts.

28. Paltridge, G. W., "Global Cloud Cover and Earth Surface Temperature," J. ATMOS. SCI., Vol 31, No 6, 1974.

29. Ramanathan, V., Lian, M. S. and Cess, R. D., "Increased Atmospheric CO_2: Zonal and Seasonal Estimates of the Effect on the Radiation Energy Balance and Surface Temperature," JGR, Vol 84, No C8, 1979.

30. Robock, A., "The Seasonal Cycle of Snow Cover, Sea Ice and Surface Albedo," MON. WEATHER REV., Vol 108, No 3, 1980.

31. Schneider, S. H., "On the Carbon Dioxide-Climate Confusion," J. ATMOS. SCI., Vol 32, No 11, 1975.

32. Temkin, B. L. and Snell, F. M., "An Annual Zonally Averaged Hemispherical Climatic Model With Diffuse Cloudiness Feedback," J. ATMOS. SCI., Vol 33, No 9, 1976.

33. Weare, B. C. and Snell, F. M., "A Diffuse Thin Cloud Atmospheric Structure as a Feedback Mechanism in Global Climatic Modeling," J. ATMOS. SCI., Vol 31, No 7, 1974.

UDC 551.510.(522+575+576)

NUMERICAL MODELING OF THE DIURNAL EVOLUTION OF THE ATMOSPHERIC BOUNDARY LAYER IN THE PRESENCE OF CLOUDS AND FOGS

Moscow METEOROLOGIYA I GIDROLOGIYA in Russian No 4, Apr 81 pp 35-44

[Article by M. V. Buykov, doctor of physical and mathematical sciences, and V. I. Khvorost'yanov, candidate of physical and mathematical sciences, Ukrainian Regional Scientific Research Institute, manuscript received 30 Jun 80]

[Text]

Abstract: The article describes a numerical model of low clouds and fogs which takes into account the processes of transfer of heat, moisture and turbulent energy, long-wave and solar radiation, and growth and evaporation of droplets in a turbulent medium. The authors carried out modeling of the diurnal variation of the atmospheric boundary layer (ABL) during the formation of stratiform clouds over snow and the process of dispersal of a fog by the sun. It is shown that allowance for solar radiation leads to greater turbulence and thickening of the ABL, more rapid development of a cloud, lowering of its lower boundary and the enlargement of droplets. The opposite effects are observed during the nighttime hours. It was established that during the dispersal of a fog by the sun the main role is played by the heating of the underlying surface and the turbulent transfer of heat upward; direct absorption of solar radiation by droplets is less important. In the case of small solar altitudes (in autumn, spring) a fog can be transformed into cloud cover.

Increasing requirements on the quality of weather forecasting and the development of work on artificial modification have stimulated the appearance of a whole series of studies in the Soviet and foreign literature during the last 15 years which have been devoted to the mathematical modeling of low cloud cover and fogs in the atmospheric boundary layer. These models, differing with respect to the methods for computing the turbulence characteristics, radiation and condensation processes (for a review and comparison of models, see [1]), made it possible to describe the principal regularities in the formation and evolution of low cloud cover and fog.

However many models either do not take radiation processes into account or take into account only long-wave radiation, that is, relate to nighttime conditions. In [13] the authors included the processes of transfer of solar radiation, but arctic stratiform clouds are modeled during the time of the polar day, the solar altitude is fixed and there is no diurnal variation.

The inclusion of solar radiation transfer processes also makes it possible to model the diurnal variation of low clouds and fogs and can help in better understanding of the mechanisms of their formation and evolution, reciprocal transformations and energetics. In this communication the model of low clouds and fogs formulated earlier [2, 11] is generalized for the case of presence of solar radiation. The modeling of two situations was accomplished: formation and evolution of cloud cover over a snow-covered underlying surface and the process of the dispersal of a fog at sunrise. In this model, in contrast to the others, use is made of a microphysical approach: the spectrum of droplets is computed in each time interval by the solution of a kinetic equation. This made possible a more orderly relating of radiation and microphysical characteristics and as a result -- investigation of the influence of solar radiation on the cloud microstructure, and also allowance for the fact that radiation characteristics of the droplet phase (coefficients of scattering, absorption, etc.) vary greatly with time together with the droplet spectrum.

Block Diagram of Model

The system of equations for the model is given in [2, 11]. Here only a block diagram of the model (Fig. 1) is given. Each group of processes in the ABL is described by its own system of equations. The method of component-by-component splitting is used in the numerical solution.

The blocks in the diagram correspond to the splitting of the model into special problems; the arrows correspond to the sequence of the computations, and the symbols over them correspond to the exchange of information between blocks.

The equations for describing all the processes, other than the transfer of solar radiation, and also the algorithms for their solution, were set forth in [2, 11]. For computing the effective solar flux $F_S = F_S^{\uparrow} - F_S^{\downarrow}$ and the influx $(\partial T/\partial t)_S$ we used the method developed by R. Goody and G. Herman [13], based on a solution of the transfer equations in a two-flux approximation. As was demonstrated in [9], in a comparison of the method of distribution of photons by paths with a two-flux approximation, the latter has an adequate accuracy, but is simpler in its numerical realization. For F_S we solved the equation

$$\frac{d^2 F_{S\lambda}}{d\tau_\lambda^2} = \gamma_\lambda^2 F_{S\lambda}; \quad \gamma_\lambda^2 = 3\frac{1-\omega_\lambda \cos\theta}{1-\omega_\lambda}. \tag{1}$$

Here ω_λ is single-particle albedo,

[B = air]

$$\omega_\lambda = \frac{\sigma_{\lambda L} q \rho_B}{\sigma_{\lambda L} q \rho_B + \sigma_{\lambda V} q \rho_V + \sigma_{\lambda L} q \rho_B}, \tag{2}$$

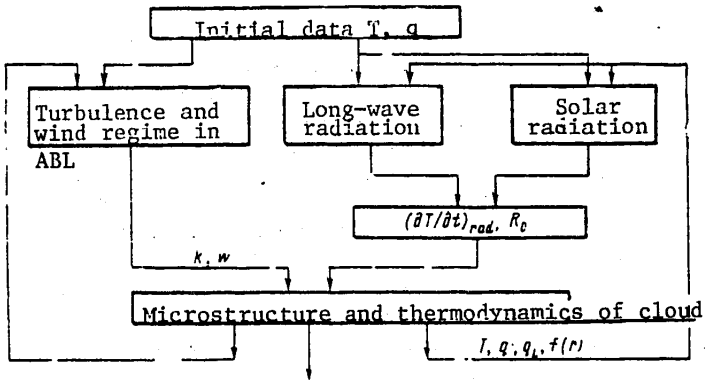

Output information in each time interval

Horizontal u, v and vertical w components of wind velocity, turbulence coefficient k, turbulent energy and components of its balance, spectral and integral long-wave and solar receipts and losses; spectral coefficients of scattering and absorption, rate of radiation change of temperature $(\partial T/\partial t)_{rad}$, radiation balance R_0, temperature T, humidity q, supersaturation Δ, droplet spectrum f(r) and its moments, liquid-water content q_L, droplet concentration N, mean radius $\bar{r}$, visibility range χ.

Fig. 1. Block diagram of model.

where $\sigma_{\lambda L}$ is the spectral mass coefficient of scattering of droplet water, $\alpha_{\lambda L}$ and $\alpha_{\lambda V}$ are the spectral mass coefficients of water and vapor absorption, q_L, q and ρ_{air} are liquid-water content, humidity and air density, $<\cos\theta>$ is the scattering asymmetry factor, τ_λ is spectral optical thickness,

[B = air]
$$\tau_\lambda(z) = \int_0^\infty (\alpha_{\lambda V} q \rho_V + \alpha_{\lambda L} q_L \rho_B)\, dz. \qquad (3)$$

As the boundary condition for $F_{S\lambda}$ at the underlying surface we used the reflection condition, at the upper boundary (10 km) -- the equality of the descending flux to the value $I_\lambda \cos\mu$, where I_λ is the solar constant, $\cos\mu$ is the solar zenith angle, which was computed as a function of latitude, season of the year and time of day.

In [13] the spectrum of absorption of solar radiation by vapor was broken down into two sectors with large and small vapor absorption coefficients. The coefficients of absorption and scattering of droplet water were not dependent on time. In this communication spectral computations were made for 32 wavelengths, taking into account the eight principal absorption bands in the interval 0.4-4 μm (see Table 1). For the coefficients of scattering $\sigma_{\lambda L}$ and absorption $\alpha_{\lambda L}$ we used analytical expressions obtained in [12] for the spectra of droplets in the form of gamma distributions. For this purpose the computed droplet spectra in each time interval were approximated by gamma distributions whose significant parameters were then substituted into the formulas from [12]. The intensity and profile of the effective fluxes of solar radiation, computed by this method, were close to those observed under cloudy conditions with corresponding solar altitudes [5, 6, 8].

As in [2], the initial relative humidity in the boundary layer was considered constant and temperature was considered as decreasing linearly with altitude; droplet water was absent. If at some altitude humidity for the first time attains saturation, N_m of condensation nuclei is activated and the droplet phase is formed.

Evolution of Clouds Over Snow

In modeling the albedo of snow was considered equal to 80%; solar altitude was computed for the latitude of Kiev for 21 March and 21 December. Qualitatively both cases are similar; in the first of them the amplitude of the diurnal variations is greater. The initial conditions are as follows: geostrophic wind 10 m/sec, relative humidity in the boundary layer constant and equal to 90%, surface temperature 5°C and decreases with altitude with a gradient 6°C/km. Humidity at the surface was equal to the saturating humidity over ice. Calculations begin at 0350 hours. The evolution of the ABL is illustrated in Fig. 2. Due to long-wave radiation cooling the surface temperature decreases by 6°C at 0400 hours, the turbulence coefficient k decreases (maximum value -- from 9 to 4 m^2/sec) and relative humidity increases. At 0810 hours at an altitude of 300 m a cloud is generated and the long-wave radiation balance at the surface decreases sharply. At 0820 hours (here and in the text which follows the time is astronomical) the sun rises, but the total radiation balance R_0 remains negative for a period of a half-hour (cooling continues). At 0855 R_0 changes sign, the surface temperature rises, the thickness of the ABL and turbulent exchange increase, the k maximum at 1200-1400 hours is at an altitude 200 m and increases by a factor of almost 10, attaining 35 m^2/sec.

The increase in the solar and total radiation balances continues to midday; the temperature increase continues to 1400 hours. This is followed by onset of surface cooling, although R_0 is still positive. The reason is that now the soil surface, covered with snow, is warmer than the deeper soil layers. Such a temperature gradient arises in the soil that with these solar altitudes the radiation balance no longer can compensate for the flux of heat from the surface into the depths of the soil. Beginning at this moment turbulent exchange again begins to decrease.

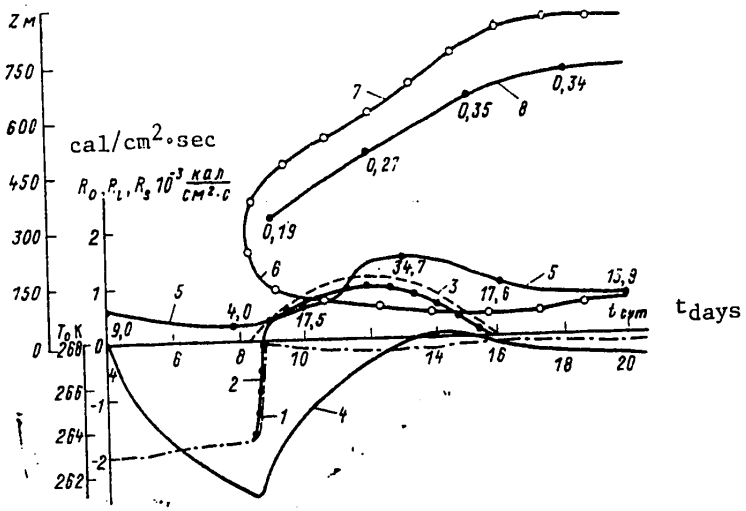

Fig. 2. Evolution of meteorological parameters in ABL. Computations for latitude of Kiev, 21 December. 1) long-wave balance R_L; 2) short-wave balance R_S: 3) total balance R_0; 4) surface temperature T_0; 5) altitude of maximum of turbulence coefficient, the figures are its values in m^2/sec; 6 and 7) altitudes of the lower and upper cloud boundaries; 8) altitude of maximum liquid-water content, the figures represent its value in g/kg.

An increase in cloud thickness occurs during the course of the entire day, for the most part due to upward increase. The liquid-water maximum is in the upper part of the cloud, which is caused by radiation cooling. Beginning with 1700-1800 hours there is a stabilization of the ABL and clouds. This quasistationary state is associated with the blocking effect of the inversion over the upper boundary and the fact that the total heat balance at the surface is close to zero.

The effect of heating and additional turbulence of the ABL in winter over the snow is observed only in the presence of a cloud. With the modeling of cloud dissipation by descending vertical movements [4] under these same conditions it was discovered

that after the disappearance of a cloud even at the midday hours the negative long-wave balance is greater than the solar balance so that the total radiation balance is negative (high albedo and low sun), a temperature inversion develops and turbulence decreases.

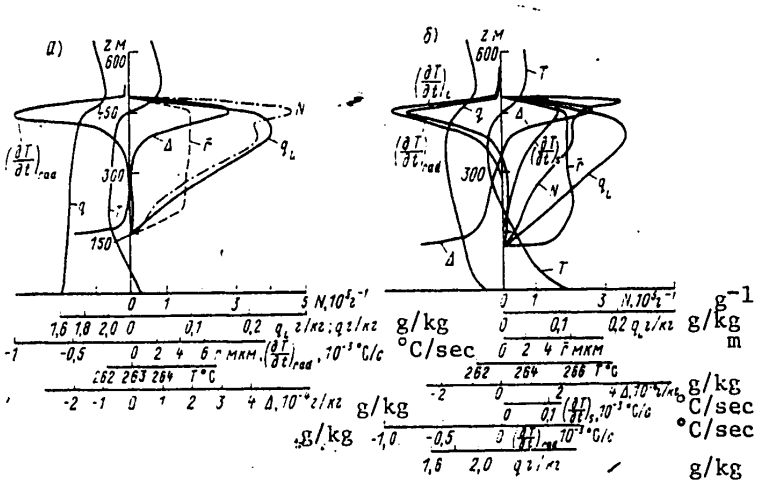

Fig. 3. Vertical sections of cloud after two hours of development. a) without allowance for solar radiation; b) with allowance for solar radiation (latitude of Kiev, 21 March), T is temperature; q is humidity; q_L is liquid-water content; N and $\overline{r}$ are the concentration and mean radius of the droplets; Δ is supersaturation;

$$(\partial T/\partial t)_L,\ (\partial T/\partial t)_S,\ (\partial T/\partial T)_{rad}$$

are the rates of long-wave, solar and total radiation changes of temperature.

Thus, under winter conditions cloud cover exerts a warming effect (greenhouse effect), screening long-wave radiation and transmitting solar radiation.

The influence of solar radiation on cloud development is illustrated in Fig. 3. The extremal values of the long-wave and solar influxes are attained almost at the same altitude, 50 m below the upper cloud boundary, but the second of them is much less. A positive solar influx partially compensates radiation cooling in the upper part of the cloud; here there is a decrease in the condensation rate, liquid-water content maximum and total influx. Solar radiation exerts the most important influence on the lower part of the cloud. As a result of a temperature increase and a decrease in undersaturation at the snow surface the lower boundary of the cloud drops down. Radiation heating in the lower part of the cloud, caused by the total effect of long- and short-wave radiation, is now twice as great; its maximum is close to 0.2 degree/hour and is attained at an altitude of 120 m over the lower cloud boundary. The lower two-thirds of the cloud exist in an undersaturation state because

greater heating causes more intensive evaporation in the lower part of the cloud. Since small droplets evaporate more rapidly, this leads to an increase in the mean size of droplets by 20-30%. Whereas in the absence of the sun the mean radius of the droplets has a tendency to an increase with altitude (Fig. 3a), in the presence of solar radiation the mean radius has a distinct maximum in the lower part of the cloud (Fig. 3b), caused by more intense evaporation. Due to turbulent mixing, in the upper part of the cloud the size of the droplets increases by 10-15% and their concentration decreases.

Thus, solar radiation intensifies the pattern of existence of a cloud in a state of dynamic equilibrium: in its upper third condensation transpires, whereas evaporation transpires in the lower two-thirds. The close correlation between radiation and microphysical characteristics leads to the following: in the presence of solar radiation a cloud over snow is somewhat "drawn" downward; the liquid-water content in it decreases and it is redistributed from small to larger droplets.

Such a change in the microstructure of a cloud causes a change in its radiation characteristics. Table 1 gives the spectral coefficients of scattering and absorption obtained using the formulas from [12] using the spectra of droplets computed at an altitude of 300 m at two moments in time.

The decrease (almost by a factor of 2) in the scattering coefficients in the entire spectral region and the absorption coefficients in the bands X and 3.2 was caused by an increase in the mean radius of the droplets at this altitude from 4.4 to 9.8μm and emphasizes the need for joint computation of the radiation and microphysical characteristics. The constancy of $\alpha_{\lambda L}$ in the case of weak absorption is attributable to their nondependence on the spectrum of droplets [2, 12].

An interesting problem is that of the contribution of the radiation factor to the energetics of a cloud, especially in connection with the recently arising discussion of the role of radiation in the dynamics of cloud formation [7, 10]. Table 2 represents the temporal variation of the rates of temperature change due to the heat influxes: long-wave $(\partial T/\partial t)_{\ell}$, solar $(\partial T/\partial t)_S$, phase $(\partial T/\partial t)_{cond}$, turbulent $(\partial T/\partial t)_{ed}$ and total velocity $(\partial T/\partial t)_{tot}$ at the altitude z, where radiation cooling is maximum (under the upper boundary). In the morning hours long-wave cooling and the negative turbulent influx caused by a temperature inversion are compensated by only 20% by the heat of condensation so that the total rate of cooling is greater than 3°C/hour. By midday the heating of the surface and the restructuring of temperature stratification lead to a change in the sign of the turbulent influx, which together with the phase and increasing solar influx to a considerable degree compensates long-wave cooling. At 1400 hours the total rate of cooling is less than 0.4°C/hour, that is, an order of magnitude less than the long-wave cooling. Table 2 is also an answer to the question raised in [10] concerning the mechanisms of smoothing of the powerful "thermal well" formed by a cloud relative to long-wave radiation. With a decrease in solar altitude and surface temperature the turbulent heating decreases and the total rate of cooling increases We note that in the modeled situation the role of solar radiation is reduced for the most part to an increase in the radiation balance at the surface; the direct absorption of solar radiation in a cloud is small in comparison with other types of influx.

Table 1

Coefficients of Scattering (Numerator) and Absorption (Denominator) of Solar Radiation by Droplets in cm^2/g

t	Band							
	a	0,8 μ	ρσ:	Φ	Ψ	Ω	X	3,2
0850 hrs	2362 / 0,018	2364 / 0,045	2364 / 0,22	2367 / 0,87	2353 / 18,9	2314 / 69	1281 / 1149	1184 / 1180
1250 hrs	1401 / 0,018	1401 / 0,018	1401 / 0,22	1402 / 0,87	1389 / 18,8	1336 / 68	711 / 700	701 / 700

Table 2

Temporal Variation of Different Heat Influxes (°C/hour) at Level of Maximum Radiation Cooling

	t day hrs				
	8.5	10	12	14	18
z м	300	450	540	630	840
$(\partial T/\partial t)_l$	−3,96	−3,56	−3,04	−3,93	−3,19
$(\partial T/\partial t)_s$	0,08	0,34	0,45	0,36	—
$(\partial T/\partial t)_{cond}$	1,21	1,01	0,68	1,15	0,88
$(\partial T/\partial t)_{ed}$	−0,44	−0,23	0,61	2.04	1,23
$(\partial T/\partial t)_{tot}$	−3,11	−2.44	−1,30	−0,38	−1,08

Table 3

Temporal Variation of Temperature (°C) and Its Rate of Change (°C/hour) at Lower Cloud Boundary

	t day hours						
	8,5	10	12	14	15	16	18
$T_{low\ bound}$ °C	−10,38	−10,03	−7,28	−6,07	−5.91	6,06	−6,41
$(\partial T/\partial t)_{tot}$	−0,96	1,12	0.952	0.312	−0.024	−0.264	−0.114

We note that the maximum value of the solar influx in a cloud of 0.45°C/hour (Table 2) for the variant of 21 December with a solar altitude h_S = 15.5° and a maximum value 0.74°C/hour, obtained in the variant for 21 March with h_S = 30°, agree fairly well with the measured values 0.63°C/hour with h_S = 40° from [5] and 0.8-1°C/hour with h_S = 26° from [8]. This agreement is evidence of a satisfactory accuracy of the method used for computing solar radiation.

Changes in the temperature of the lower cloud boundary are determined for the most part by variations of the radiation balance at the surface. This is illustrated by Table 3. In the morning hours $T_{low\ bound}$ drops down, which is associated with a a temperature inversion in the layer below the clouds. An increase in $T_{low\ bound}$ begins with heating of the surface at the time of sunrise. According to our computations, the total rate of heating due to long- and short-wave radiation (which is attained at 50-70 m above the lower boundary) does not exceed 0.15°C/hour, that is, the increase in temperature at the lower boundary is almost completely attributable to the turbulent heat influx from the surface.

Table 3 shows that it is maximum at 1000 hours when the temperature gradients in the surface layer are maximum and decreases with an evening-out of temperature in the layer below the clouds. After 1500 hours, up to the next sunrise, $T_{low\ bound}$ drops down.

In [7], on the basis of data from aircraft sounding, it was demonstrated that the correlation of temperature change after 12 hours at the upper ΔT_{up} and lower $\Delta T_{low\ bound}$ boundaries of St-Sc is positive, although it is known [8] that the radiation changes of temperature near the upper and lower boundaries have different signs and the conclusion was drawn that radiation plays a small role in comparison with advection and vertical currents.

In our case, as can be seen from a comparison of Table 2 and 3, the signs on $\partial T_{up}/\partial t$ and $\partial T_{low\ bound}/\partial t$ in the first hour after cloud generation are identical, before 1500 hours are different and after 1500 hours are again identical. As follows from what was stated above, the different signs on $\Delta T_{low\ bound}$ and ΔT_{up} at the near-midday hours are related to the turbulent influx of heat near the lower boundary from the underlying surface, and not to an increase in radiation heating caused by solar radiation.

Thus, different signs apply to ΔT_{up} and ΔT only in the course of 20% of the day and therefore with the use of sounding data each 12 hours, as in [7], the probability of positive correlations of $\Delta T_{low\ bound}$ and ΔT_{up} is greater than the probability of negative correlations.

In addition, some time after the formation of a cloud there will be relative stabilization of the ABL and the diurnal variations of temperature caused by short- and long-wave radiation are relatively small, as is indicated by the surface temperature curve in Fig. 2, after 1100-1200 hours, i.e., after 3-4 hours of cloud development when the ABL has been transformed from cloudless conditions to cloudy conditions. Table 3 shows that from 1200 to 1500 hours $\Delta T_{low\ bound}$ is less than 1.4°C, and from 1500 to 1800 hours $\Delta T_{low\ bound} = -0.5$°C. The temperature difference after 12 hours can be still less since the signs on $\Delta T_{low\ bound}$ to the time of attaining the maximum $T_{low\ bound}$ (1400-1500 hours) and thereafter are opposite. Accordingly, the changes of $T_{low\ bound}$, identical in sign with the changes T_{up} and caused by advection and ascending vertical movements, as was noted correctly in [7], can be greater than the changes caused by diurnal variation.

These computations show that at least in the absence of vertical movements the existence of a positive correlation between ΔT_{up} and $\Delta T_{low\ bound}$ by no means is evidence of a negligible role of radiation in the formation and energetics of stratified clouds (Table 2).

We note further that the role of radiation in the formation of a temperature inversion over lower-level clouds is entirely comparable with the role of vertical movements. An inversion is formed due to radiation and in the absence of vertical movements (Fig. 3). The modeling of the evolution of clouds with allowance for radiation and vertical movements [11] indicated that in the absence of vertical velocities the intensity of the inversion is $\Delta T = 2.5°C$ when there are descending movements (-1 cm/sec) $\Delta T = 5.5°C$. Ascending movements in the absence of radiation should lead to complete disappearance of the inversion, but with allowance for radiation the inversion persists (Fig. 2 in [11]).

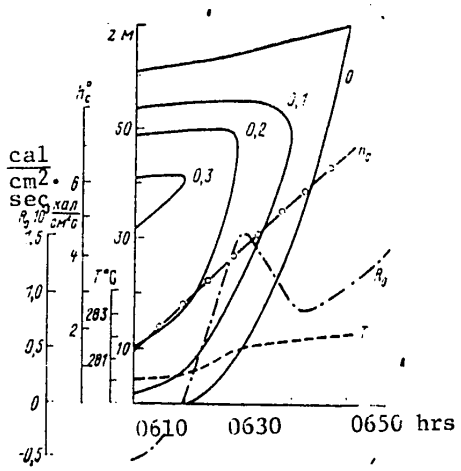

Fig. 4. Dispersal of fog over dry soil after sunrise (latitude of Kiev, 21 September). Solid curves -- isolines of liquid-water content, the figures near them represent the liquid-water content in g/kg; T is soil temperature; R_0 is the radiation balance at the surface; h_S is solar altitude.

Table 4

Rates of Temperature Change (°C/hour) -- Radiation (Numerator), Total (Denominator) at Altitudes 10 and 50 m

z м		t day				
		0600 hrs	0610 hrs	0620 hrs	0630 hrs	0640 hrs
10	$\frac{(\partial T/\partial t)_{rad}}{(\partial T/\partial t)_{tot}}$	$\frac{-1,51}{-0,05}$	$\frac{-1,43}{0,41}$	$\frac{-1,08}{2,06}$	$\frac{0,22}{3,85}$	$\frac{0,10}{3,92}$
50	$\frac{(\partial T/\partial t)_{rad}}{(\partial T/\partial t)_{tot}}$	$\frac{-2,82}{-1,74}$	$\frac{-3,22}{-0,95}$	$\frac{-3,40}{0,27}$	$\frac{-2,81}{1,83}$	$\frac{-1,42}{2,99}$

It follows from everything stated above that the radiation factor exerts a very significant influence on the dynamics of at least lower-level clouds and that it must be taken into account in numerical models together with other factors involved in cloud formation, the importance of which is mentioned in [7]: turbulent exchange and vertical currents.

Dispersal of Radiation Fog at Sunrise

The computations were made when there was a geostrophic wind of 3 m/sec, an initial humidity of 90%, over dry soil (albedo 25%) for a solar altitude at the latitude of Kiev on 21 September. The calculations began at a time corresponding to 0300 hours. Under these conditions the formation of a fog begins an hour after the onset of the calculations and after three hours of calculations its thickness is 60 m. The sun rises at this time, corresponding to 0600 hours. Evolution of the fog is illustrated in Fig. 4. The dispersal begins from below; the detachment of the lower boundary (isoline "0") from the earth occurs after 20 minutes, the fog is transformed into a cloud, which thins out, both its boundaries move upward and after 30 minutes come together at an altitude of 75 m, that is, full dispersal occurs 50 minutes after sunrise when the altitude is 7°. In this process there is a predominance of evaporation from below, whereas for some time cooling and condensation continue near the upper boundary and therefore in the process prior to fog dispersal it rises by 15 m. The solar influx in the fog layer is extremely small and constitutes less than 7% of the long-wave influx.

An interesting effect is observed in the behavior of the radiation balance (Fig. 4). Its increase, caused by sunrise, when t = 0630 hours, is replaced by a dropoff. The reason for this is that by this moment there is a great decrease in the optical thickness of the fog and an increase in the negative long-wave balance. Then, when the sun rises above the horizon, the short-wave balance increases more rapidly than the long-wave balance and the total balance again increases.

The contribution of the radiation factor to the energetics of fog dispersal is illustrated in Table 4. It follows from this that at an altitude of 10 m after 10 minutes and at an altitude of 50 m 20 minutes after sunrise heating will begin, that is, the positive turbulent heat influx from the surface will be greater than the sum of radiation cooling and the expenditures of heat on evaporation.

Thus, in the dispersal of a fog by the sun the main role is played by an increase in the radiation balance, heating of the soil and turbulent transfer of heat upward and the direct absorption of solar radiation by droplets plays a secondary role. This circumstance is confirmed by observational data [14].

The authors of [3] made computations of the evolution of a fog under a thermal influence, which was modeled by adding to the heat balance equation a term similar to the short-wave balance and close to it in value. In this case the pattern of fog evolution is qualitatively similar to the evolution of a fog at sunrise. Its principal stages are the same as in Fig. 4: transformation of a fog into a cloud, its rising, thinning and evaporation.

For dispersal the minimum value of the additional (short-wave) balance should exceed the value of the long-wave balance by a factor of 3-4; otherwise there will be a restructuring of the fog without dispersal [3]. This condition can be used in predicting the fact of fog dispersal after sunrise when there are measurement data for the long- and short-wave balances. If the initial thickness of the fog is sufficiently great (>100 m) and the short-wave balance is small, after its transformation into a cloud the rising of the lower cloud boundary, caused by solar heating, and the rising of the upper boundary, caused by long-wave cooling, occur with an identical rate [3]. Thus, the appearance of the sun in the morning hours in autumn or spring may not lead to fog dispersal, but its transformation into low stratiform cloud cover, as agrees with observational data.

BIBLIOGRAPHY

1. Buykov, M. V., CHISLENNOYE MODELIROVANIYE OBLAKOV SLOISTYKH FORM (Numerical Modeling of Stratiform Clouds), Obninsk, 1978.

2. Buykov, M. V. and Khvorost'yanov, V. I., "Formation and Evolution of a Radiation Fog and Stratiform Cloud Cover in the Atmospheric Boundary Layer," IZV. AN SSSR: FIZIKA ATMOSFERY I OKEANA (News of the USSR Academy of Sciences: Physics of the Atmosphere and Ocean), Vol 13, No 4, 1977.

3. Buykov, M. V. and Khvorost'yanov, V. I., "Modeling of Fog Modification by a Thermal Method," TRUDY UkrNIGMI (Transactions of the Ukrainian Scientific Research Hydrometeorological Institute), No 161, 1978.

4. Buykov, M. V. and Khvorost'yanov, V. I., "Modeling of the Process of Restoration of Stratiform Clouds After Artificial Dispersal," TRUDY UkrNIGMI (Transactions of the Ukrainian Scientific Research Hydrometeorological Institute), No 185, 1981.

5. Goysa, N. I. and Shoshin, V. M., "Experimental Model of the Radiation Regime of an 'Average' Stratiform Cloud," TRUDY UkrNIGMI, No 82, 1969.

6. Kondrat'yev, K. Ya., Gayevskaya, G. N. and Nikol'skiy, G. A., "Influence of Cloud Cover on Short-Wave Radiation Fluxes in the Troposphere and Stratosphere," RADIATSIONNYYE PROTSESSY V ATMOSFERE I NA ZEMNOY POVERKHNOSTI. MATERIALY X VSESOYUZNOGO SOVESHCHANIYA PO AKTINOMETRII (Radiation Processes in the Atmosphere and at the Earth's Surface. Materials of the Tenth All-Union Conference on Actinometry), Leningrad, Gidrometeoizdat, 1979.

7. Matveyev, L. T., "Reasons for the Formation of Clouds," METEOROLOGIYA I GIDROLOGIYA (Meteorology and Hydrology), No 8, 1978.

8. POLNYY RADIATSIONNYY EKSPERIMENT (Full Radiation Experiment), Leningrad, Gidrometeoizdat, 1976.

9. Feygel'son, Ye. M. and Krasnokutskaya, L. D., POTOKI SOLNECHNOGO IZLUCHENIYA I OBLAKA (Solar Radiation Fluxes and Clouds), Leningrad, Gidrometeoizdat, 1978.

10. Feygel'son, Ye. M., "Role of Radiation in the Formation of Stratiform Clouds," METEOROLOGIYA I GIDROLOGIYA, No 8, 1979.

11. Khvorost'yanov, V. I., "Feedbacks Between Turbulence, Vertical Currents and Cloud Cover in the Atmospheric Boundary Layer," IZV. AN SSSR: FIZIKA ATMOSFERY I OKEANA, Vol 15, No 8, 1979.

12. Khvorost'yanov, V. I., "Approximate Computations of the Scattering and Absorption Coefficients for Short-Wave Radiation by Clouds," RADIATSIYA V OBLACHNOY ATMOSFERE (Radiation in the Cloudy Atmosphere), Leningrad, Gidrometeoizdat, 1981.

13. Herman, G. and Goody, R., "Formation and Persistence of Summertime Arctic Stratus Clouds," J. ATMOS. SCI., Vol 33, No 4, 1976.

14. Jiusto, J. E. and Garland, L. G., "Thermodynamics of Radiation Fog Formation and Dissipation," J. RECH. ATMOS., Vol 13, No 4, 1979.

UDC 551.(510.534+507.362)

MODELING OF AN A PRIORI ENSEMBLE OF SOLUTIONS OF THE INVERSE PROBLEM AND STABILITY OF OPTIMUM PLANS FOR AN OZONE SATELLITE EXPERIMENT

Moscow METEOROLOGIYA I GIDROLOGIYA in Russian No 4, Apr 81 pp 45-51

[Article by M. S. Biryulina, Leningrad State University, manuscript received 8 Jul 80]

[Text] Abstract: The article gives computations of the optimum plans for an ozone satellite experiment for different latitudes and seasons for the purpose of checking their stability. The basis for the computations was model a priori covariation matrices of the ozone profiles, the method for whose construction is described and substantiated. It is shown that optimum two- and three-channel schemes for an ozone satellite experiment must not have appreciable seasonal and latitudinal variations.

Satellite methods for obtaining information on the atmospheric content of ozone have become especially timely during recent years, in particular, in connection with possible variations of the ozone layer as a result of natural and anthropogenic changes in atmospheric composition [8, 11]. The need for obtaining global information on the characteristics of the ozonosphere associated with this has stimulated the development of special satellite methods for determining ozone content based on the interpolation of data on outgoing atmospheric radiation in different spectral ranges.

In earlier studies [6, 7] we evaluated the theoretical possibilities of indirect methods for restoring the vertical profile and total content of ozone for different satellite schemes: IR method (band 9.6μm), UV method (backscattering), joint use of the IR method with the heterodyne or UV method. These very same studies gave recommendations for creating the corresponding specialized satellite instruments based on optimization of the scheme for measurements in the IR spectral range by the V. P. Kozlov method [2, 3]. Computations of the designs of these instruments were made using a priori statistics for ozone profiles for the conditions prevailing in Berlin [10]. However, it is known [4, 5] that the optimum conditions for satellite measurements for other meteorological parameters, computed by the Kozlov method, are dependent on the statistics used. In this connection it seems important to clarify the applicability and effectiveness of the proposed optimum schemes of an ozone experiment for other sounding conditions -- other latitudes and seasons. This article is devoted to this subject.

The lack of a sufficient quantity of information on the statistical characteristics of ozone distribution in the atmosphere for different regions of the earth makes solution of the formulated problem difficult. Under these conditions a solution was obtained by using model a priori covariation matrices of the ozone profiles K_{qq}.

One of the well-known methods for modeling covariation matrices is constructing elements of the matrix using a formula from [1]

$$\tilde{K}^{ij}_{qq} = \sigma_i(q)\,\sigma_j(q)\,\exp\left(-\frac{|z_i - z_j|}{r}\right), \tag{1}$$

where $\tilde{K}^{ij}_{qq}$ is an element of the matrix with the superscripts i, j; $\sigma_i(q)$ and $\sigma_j(q)$ are the standard variations of ozone content at the i-th and j-th levels in the atmosphere; z_i and z_j are the altitudes of the i-th and j-th levels; r is a parameter of the model.

It can be shown rigorously that the use of a priori covariation matrices of such a type in the algorithm for the statistical regularization method is equivalent to application of the first-order Tikhonov regularization method to solution of the inverse problem. Thus, the proposed method for modeling the K_{qq} matrices is to an adequate degree theoretically substantiated.

We selected the following criterion for a correct evaluation of the r parameter: dispersion of the total ozone content ensured by a model matrix in accordance with the formula

$$\sigma_U^2 = \int_0^{z_0}\int_0^{z_0} \tilde{K}_{qq}(z_i, z_j)\,dz_i\,dz_j \tag{2}$$

(σ_U^2 is the dispersion of the total ozone content; $\tilde{K}_{qq}(z_i, z_j) \equiv \tilde{K}^{ij}_{qq}$) coincides with the real dispersion of the total content at a given point on the earth for a particular season.

The modeling method which we selected (formula (1) plus the criterion of evaluation of the r parameter) was checked for the conditions prevailing in Berlin, for which, as we have already mentioned, we had natural covariation matrices for ozone. In this case equation (2) for evaluating the r parameter assumes the form

$$\int_0^{z_0}\int_0^{z_0} K_{qq}(z_i, z_j)\,dz_i\,dz_j = \int_0^{z_0}\int_0^{z_0} \tilde{K}_{qq}(z_i, z_j)\,dz_i\,dz_j, \tag{2a}$$

where K_{qq} is the real covariation matrix of ozone and $\tilde{K}_{qq}$ is the model covariation matrix of ozone.

As an evaluation of experimental accuracy, as usual [6, 7], we used the value

$$\varphi_q(p) = \left(1 - \frac{\hat{\sigma}_q(p)}{\sigma_q(p)}\right)\cdot 100\%, \tag{3}$$

where $\sigma_q(p)$ is the natural standard variation of ozone concentration at the level p (corresponding to the a priori matrix K_{qq}), $\hat{\sigma}_q(p)$ is the mean square error of restoration at this same level (corresponding to the residual covariation matrix $\hat{K}_{qq}$).

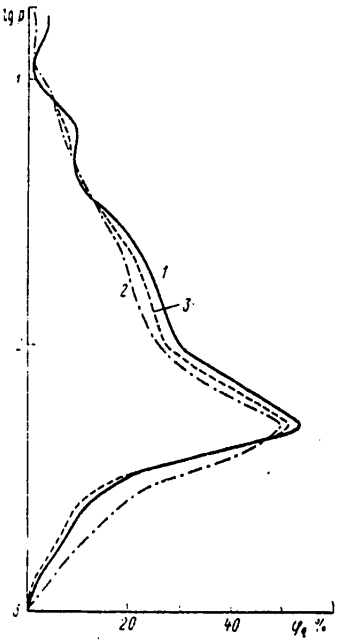

Fig. 1. Vertical variation of parameter $\varphi_q(p)$ (p in millibars) for summer conditions in Berlin region.

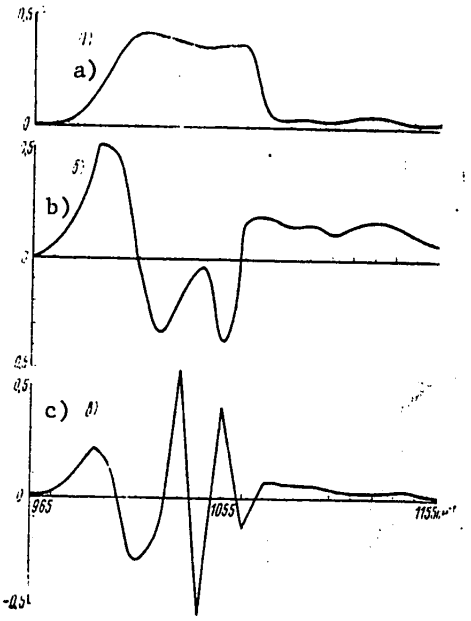

Fig. 2. First (a), second (b) and third (c) eigenvectors of Kozlov informational operator for summer in the Berlin region (real a priori statistics).

In the case of use of so-called "extraneous" statistics (in our case -- the model statistics $\tilde{K}_{qq}$) a formula is known [6, 7] for the residual covariation matrix which is transformed to the form

$$\hat{K}_{qq} = \tilde{K}_{qq} - \tilde{K}_{qq} A^{T} (A\tilde{K}_{qq} A^{T} + \Sigma)^{-1} A\tilde{K}_{qq} + \Delta\hat{K}_{qq}, \tag{4}$$

where

$$\Delta K_{qq} = (I - RA)^{T} \Delta K_{qq} (I - RA). \tag{4a}$$

Here A is an operator of the direct problem; R is a decision operator of the problem; $\sum$ is the covariation matrix of measurement errors; I is a unit operator; ΔK_{qq} is the deviation of the used a priori statistics from the true statistics

$$(\Delta K_{qq} = K_{qq} - \tilde{K}_{qq});$$

$\Delta\tilde{K}_{qq}$ is the correction to the residual covariation matrix caused by inadequacy of the a priori statistics; T is the transposition symbol.

Figure 1 shows the vertical variation of $\varphi_q(p)$ for three cases: 1) the true a priori statistics; 2) model a priori covariation matrix; 3) same as (2), but without allowance for the correction $\Delta\hat{K}_{qq}$ for the inadequacy of the a priori statistics. The curves are shown for a level of mean square measurement error σ_I erg/cm^2·sec·sr·cm^{-1}).

The closeness of all three curves in the figure indicates that a model covariation matrix of the type (1) quite well represents the real a priori statistical ensemble of ozone profiles (the 4a correction is small) and can be used with a good degree of accuracy without taking this correction into account.

Now we will discuss the informational content of the experiment. In the V. P. Kozlov method it is determined by the information volume, which characterizes the number of states of the object distinguishable in the experiment:

$$V = \left(\prod_{i=1}^{k} \lambda_i \right)^{1/2}, \tag{5}$$

where λ_i are the eigenvalues of the Kozlov informational operator $C = \sum^{-1} AK_{qq}A^T$ and are greater than unity (k is the number of the last of such eigenvalues). The computations indicated that for all schemes of the IR experiment ("full" experiment, optimum two- or three-channel instrument -- see [6]) the V value (for any $\sum$) persists well when using in the informational operator C the model matrix $\tilde{K}_{qq}$. Moreover, as indicated by Table 1, the eigenvalues λ_i themselves, and not only their product, persist with a good accuracy. At the same time, the eigenvectors of the C operator, on the basis of which the optimum plan of the experiment is computed by the Kozlov method [3], also virtually do not change. Figure 2 shows the first three eigenvectors of the C operator for summer conditions in Berlin with the use of a real covariation matrix. The corresponding vectors for the model matrix within the limits of accuracy of the figure do not differ from those shown. The optimum plans, computed on the basis of these vectors, completely coincide. Their configuration is illustrated in [6].

Table 1

Comparison of Eigenvalues of C Operator (σ_I = 1) erg/(cm^2·sec·sr·cm^{-1})) and Values of Information Volume for Real and Model A Priori Statistics for Berlin, Summer, m is the Number of Sounding Channels

m	Statistics	λ_1	λ_2	λ_3	V σ_I=1 erg: (cm^2·sec·sr·cm^{-1})	V σ_I=0.1 erg: (cm^2·sec·sr·cm^{-1})
20	K_{qq}	41,35	0,3694	$0.3161 \cdot 10^{-2}$	6	391
	$\tilde{K}_{qq}$	42.46	0,4103	$0.3211 \cdot 10^{-2}$	6	417
3	K_{qq}	1945	10,53	$0.2913 \cdot 10^{-1}$	143	24430
	$\tilde{K}_{qq}$	1975	11,75	$0,2603 \cdot 10^{-1}$	152	24580

We limited ourselves to a discussion only of the first three eigenvectors of the Kozlov informational operator on the basis that the optimum scheme for an ozone satellite experiment in the IR spectral range with the modern level of measurement errors includes not more than three registry channels [6]. If one continues the comparison of the eigenvectors and the numbers of the C operator for real and

model a priori statistics, it is possible to confirm their close coincidence to the sixth number inclusive (we did not examine eigenvectors and numbers at higher levels). This fact once again confirms the representativeness of the model covariation matrix (1) and the reliability of the optimum plans for an ozone satellite experiment determined on its basis.

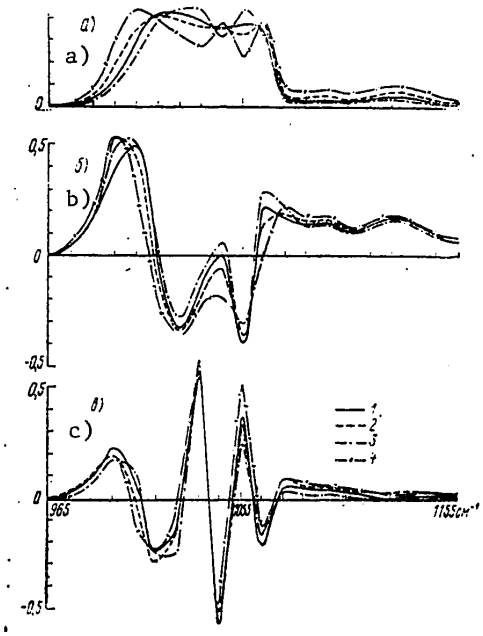

Fig. 3. First (a), second (b) and third (c) eigenvectors of Kozlov informational operator for northern part of western hemisphere. 1) φ= 50°, summer; 2) φ = 50°, winter; 3) φ = 20°, summer; 4) φ= 80°, winter.

Similar computations made for other seasons in the Berlin region gave similar results.

The results of study of the possibility of modeling of the covariation matrices of ozone on the basis of formula (1) for the conditions prevailing at Berlin made it possible to proceed to modeling of the a priori statistics for other regions of the earth for the purpose of checking the stability of optimum schemes for an ozone satellite experiment.

For this purpose we used data in [12], which gives the latitudinal variation (with a 10° interval) of the mean seasonal vertical ozone profiles for the northern part of the western hemisphere with the corresponding standard variations. On the basis of these data, and also data on the total ozone content taken from [9] (by means of statistical processing of a sample of values of the total content it was possible to ascertain the σ_U value), using the scheme described above we computed the eigenvalues and eigenvectors of the operator $C = \sum^{-1} AK_{qq} A^T$ for φ= 20°N, (summer), 50°N (summer and winter) and 80°N (winter) (in our opinion, the most representative situations). Figure 3 shows the first three eigenvectors of the C

operator for the mentioned conditions. The figure shows that they are extremely close with respect to the nature of the change and the vectors for the middle latitudes (summer) virtually do not differ from the corresponding Berlin vectors (see Fig. 2). The optimum plans, computed for all four considered situations, coincide with one another and with the optimum plans obtained earlier for the conditions prevailing in Berlin [6]. [The author expresses appreciation to V. P. Kozlov, who undertook these computations.]

Table 2

Values of Informational Volume of Ozone Satellite Experiment for Different Latitudes and Seasons for Two Levels of Measurement Errors (Three-Channel Optimum Instruments)

North latitude, season	$V\sigma_I$ = 1 erg/(cm^2·sec·sr·cm^{-1})	$V\sigma_I$ = 0.1 erg/(cm^2·sec·sr·cm^{-1})
20°, summer	92	30910
50°, summer	177	28110
50°, winter	240	30860
80°, winter	133	26400

Table 2 gives the values of the corresponding informational volumes of the satellite experiment for two levels of measurement error with the use of an optimum three-channel instrument. The table shows that the informational content of the experiment has an insignificant latitudinal and seasonal variation (which is dependent on the measurement error); the values of the informational volumes for the middle latitudes of the northern part of the western hemisphere (summer) are close to the corresponding values for Berlin (see Table 1).

The observed latitudinal and seasonal stability of the optimum plans for an ozone satellite experiment (at least for the considered conditions) is directly related to the circumstance that, as already mentioned, with the present-day level of measurement error in the IR spectral range the optimum scheme for an ozone experiment contains not more than three registry channels (the method makes it possible to determine not more than two or three independent parameters of the ozone profile). Already the fourth vector of the C operator has insignificant seasonal but well-expressed latitudinal variations. However, the eigenvalue corresponding to this vector has a value of about 10^{-4}-10^{-5} with a measurement error σ_I = 1 erg/(cm^2·sec·sr·cm^{-1}). Thus, the inclusion of a fourth channel in the optimum scheme is reasonable, according to the Kozlov criterion, with a measurement error level not worse than 10^{-2}-10^{-3} erg/(cm^2·sec·sr·cm^{-1}), which in the spectral region 8-12μm cannot be realized at the present time. It follows from this that a three-channel optimum scheme is some limiting case of an optimum scheme for the registry of radiation in an ozone experiment, with respect to which one can hope for its seasonal and latitudinal stability. With respect to a two-channel scheme, it is known that it should not have significant seasonal and latitudinal variations.

Now we will concisely formulate the conclusions from the results of this study:
1) The method for modeling of a priori covariation matrices of ozone proposed in this study is theoretically substantiated;

2) Model covariation matrices of the proposed type with a good accuracy describe the a priori statistical ensemble of ozone profiles;
3) The known positive determinancy, symmetry and good conditionality of these matrices and the small number of parameters by which they are described make it possible to use them in the operational processing of satellite information;
4) Computations of the optimum plans for an ozone satellite experiment, carried out on the basis of such matrices for different latitudes and seasons, indicated that the optimum two- and three-channel schemes for an ozone experiment obtained in [6] should not have significant seasonal and latitudinal variations.

In conclusion the author expresses appreciation to Yu. M. Timofeyev for consultations and attention to the work.

BIBLIOGRAPHY

1. Gandin, L. S., STATISTICHESKIYE METODY INTERPRETATSII METEOROLOGICHESKIKH DANNYKH (Statistical Methods for the Interpretation of Meteorological Data), Leningrad, Gidrometeoizdat, 1976.

2. Kozlov, V. P., "Numerical Restoration of the Vertical Temperature Profile From the Spectrum of Outgoing Radiation and Optimization of the Measurement Method," IZV. AN SSSR: FIZIKA ATMOSFERY I OKEANA (News of the USSR Academy of Sciences: Physics of the Atmosphere and Ocean), Vol 2, No 12, 1966.

3. Kozlov, V. P., "One Problem in the Optimum Planning of a Statistical Experiment," TEORIYA VEROYATNOSTEY I YEYE PRIMENENIYE (Theory of Probabilities and its Application), Vol 19, No 1, 1974.

4. Koslov, V. P., Timofeyev, Yu. M. and Kuznetsov, A. D., "Optimization of Conditions for the Measurement of Outgoing Radiation in the Problem of Indirect Restoration of the Vertical Water Vapor Profile," IZV. AN SSSR: FIZIKA ATMOSFERY I OKEANA, Vol 12, No 5, 1976.

5. Kozlov, V. P. and Timofeyev, Yu. M., "Optimum Conditions for Measuring Outgoing Radiation in the CO_2 Absorption Bands and the Accuracy of the Method of Thermal Sounding of the Atmosphere," IZV. AN SSSR: FIZIKA ATMOSFERY I OKEANA, Vol 15, No 12, 1979.

6. Timofeyev, Yu. M., Biryulina, M. S. and Kozlov, V. P., "Accuracy in Determining the Atmospheric Ozone Content Using Data From Measurements of Outgoing Radiation," METEOROLOGIYA I GIDROLOGIYA (Meteorology and Hydrology), No 3, 1980.

7. Timofeyev, Yu. M. and Biryulina, M. S., "Joint Use of Measurements of Outgoing UV and IR Radiation for Restoring the Vertical Profile and Total Content of Ozone," IZV. AN SSSR: FIZIKA ATMOSFERY I OKEANA (in press).

8. Hidalgo, H. and Crutzen, P. J., "The Tropospheric and Stratospheric Composition Perturbed by NO Emission of High-Altitude Aircraft," JGR, Vol 82, No 37, 1977.

9. OZONE DATA FOR THE WORLD, Fish and Environ., Canada.

10. Spankuch, D. and Dohler, W., "Statistische Charakteristika der Vertikalprofile von Temperature und Ozon and Ihre Kreuzkorrelation uber Berlin," GEOD. GEOPHY. VEROFF., R II, H 19, 1975.

11. Vupputuri, R. K., "Seasonal and Latitudinal Variations of CF_XCL_y (Freons) and Cl (Cl, ClO, HCl) in the Stratosphere and Their Impact on Stratospheric Ozone and Temperature," Downsview, Atmos. Environ. Service Contr., 1976.

12. Wilcox, R. W. and Belmont, A. D., "Ozone Concentration by Latitude, Altitude and Month Near 80°W," Contr. Data Corp. Res. Division, Rept. No FAA-AEQ-77-13, Aug 1977.

UDC 551.510.522

EVALUATION OF ACCURACY IN DETERMINING TURBULENT FLUXES USING STANDARD HYDROMETEOROLOGICAL MEASUREMENTS OVER THE SEA

Moscow METEOROLOGIYA I GIDROLOGIYA in Russian No 4, Apr 81 pp 52-59

[Article by A. S. Gavrilov, candidate of physical and mathematical sciences, and Yu. S. Petrov, Leningrad Hydrometeorological Institute, manuscript received 21 Jul 80]

[Text]

Abstract: A quite simple model is proposed for computing the turbulent fluxes of heat, water vapor and momentum on the basis of data from standard shipboard hydrometeorological measurements. It is based on the use of experimental dependences for the universal functions of similarity theory in the near-water layer. On the basis of this model a quantitative analysis is made of the relative errors in determining turbulent fluxes. Three principal sources of errors are considered: errors in standard measurements, inaccuracy in stipulation of universal functions and incorrectness in the parameterization of heat and moisture exchange in the immediate neighborhood of the water surface. Analytical expressions are derived for the corresponding weighting coefficients and computations are given for some mean conditions.

The use of data from standard shipboard hydrometeorological measurements for computing the turbulent fluxes of momentum, heat and water vapor in the near-water layer is of great importance for the solution of many problems in climatology and weather forecasting, since only these data are available in a volume adequate for statistical analysis. The successful use of mass material from standard measurements requires a clear understanding of the accuracy with which at the present stage information can be extracted from these data on the values of the mentioned turbulent fluxes. One of the possible approaches to solution of this problem is developed in this investigation.

The basis for modern methods for computing turbulent fluxes of momentum, heat and water vapor on the basis of measurements of wind velocity (u), potential temperature (T) and specific humidity (q) at two levels in the near-ground (near-water) layer is the Monin-Obukhov similarity theory [2], asserting that the dimensionless gradients of wind velocity, temperature and humidity

$$\varphi_u = \frac{\varkappa z}{U_*}\frac{\partial u}{\partial z}, \quad \varphi_T = \frac{\varkappa z}{T_*}\frac{\partial T}{\partial z}, \quad \varphi_q = \frac{\varkappa z}{Q_*}\frac{\partial q}{\partial z} \tag{1}$$

are universal functions of only one dimensionless variable

$$\zeta = \frac{\varkappa z \beta T_* M}{U_*^2}. \tag{2}$$

Here $\varkappa = 0.4$ is the Karman constant, U_* is dynamic velocity, $T_* = -H_0/U_*$ is the temperature scale, $Q_* = -E_0/U_*$ is the humidity scale (H_0 and E_0 are the vertical kinematic turbulent fluxes of heat and specific humidity), $\beta = g/T$ is the buoyancy parameter, $M = 1 + 0.07/B_0$ is a factor taking into account the influence of humidity stratification on the stability of the near-water layer, $B_0 = c_p H_0/(\hat{L} E_0)$ is the Bowen number (c_p and L are the specific heat capacity of the air at a constant pressure and the specific heat of vaporization respectively).

The universal functions φ_u, φ_T, φ_q (ζ) have been repeatedly determined from experimental data (for example, see the reviews in [3, 4]). The general scatters of experimental values obtained by different authors under the most diverse conditions approximately correspond to the discriminated regions in Fig. 1. The reason for this scatter is not only possible measurement errors, the peculiarities of the employed instrumentation and the methods employed in carrying out the experiment, but also, as is more important, the deviations from the main postulates of Monin-Obukhov similarity theory, always existing under real conditions, caused by the joint effect of the most different mechanisms, such as the nonstationary character of the situation, radiation heat exchange, horizontal inhomogeneity and some others. It goes without saying that in principle it is possible to formulate a similarity theory for the surface layer taking into account at least the most important of the enumerated factors by means of the introduction of some set of new dimensionless parameters, but for all practical purposes for the use of such a theory there must be additional extensive information exceeding the framework of data from standard measurements. Along these lines it is natural to examine this sort of deviation as random and to assume that the universal functions of similarity theory φ_u, φ_T and φ_q are stipulated with some error.

For the universal functions we will use simple expressions adequately well approximating the experimental data,

$$\varphi_u(\zeta) = \begin{cases} (1 - \alpha_1^{(1)}\zeta)^{-1/3}, & \zeta < 0 \\ 1 + \alpha_1^{(2)}\zeta, & \zeta \geqslant 0; \end{cases} \tag{3}$$

$$\varphi_q(\zeta) = \varphi_T(\zeta) = \begin{cases} \alpha_3(1 - \alpha_2^{(1)}\zeta)^{-1/3} + \frac{\alpha_4}{1 + \alpha_5\zeta^2}, & \zeta < 0, \\ \alpha_3 + \alpha_4 + \alpha_2^{(2)}\zeta, & \zeta \geqslant 0. \end{cases} \tag{4}$$

The equality of the universal functions φ_q and φ_T follows from the usually surmised similarity of the temperature and humidity profiles in the near-water layer, as is confirmed in general by measurement data [3].

The cited approximations for φ_u, φ_T and φ_q, in the case of free convection ($\zeta \to -\infty$) satisfy the "-1/3" law, following from Monin-Obukhov similarity theory. In this sense they differ from the frequently used power-law expressions obtained by different authors [3,4] on the basis of formal considerations.

The integration of (3) and (4) leads to quite simple expressions for the dimensionless functions of wind velocity and temperature:

$$U_n \begin{cases} \ln \frac{x-1}{\sqrt{x^2+x+1}} + \sqrt{3}\,\mathrm{arctg}\,\frac{2x+1}{\sqrt{3}} + C_1, & \zeta < 0 \\ \ln \zeta + \alpha_1^{(2)}\zeta + C_2, & \zeta \geq 0; \end{cases} \tag{5}$$

$$T_n = \begin{cases} \alpha_3 \left[\ln \frac{y-1}{\sqrt{y^2+y+1}} + \sqrt{3}\,\mathrm{arctg}\,\frac{2y+1}{\sqrt{3}} \right] + \alpha_4 \ln \frac{|\zeta|}{\sqrt{1+\alpha_5\zeta^2}} + \\ + C_3, \quad \zeta < 0 \\ (\alpha_3 + \alpha_4) \ln \zeta + \alpha_2^{(2)}\zeta + C_4, \quad \zeta \geq 0, \end{cases} \tag{6}$$

where C_1, C_2, C_3, C_4 are integration constants,

$$x = (1 - \alpha_1^{(1)}\zeta)^{1/3}, \quad y = (1 - \alpha_2^{(1)}\zeta)^{1/3}.$$

The determination of dynamic velocity, the turbulent fluxes of heat and humidity requires data on wind velocity u_a, potential temperature T_a and specific humidity q_a at some altitude z_a (the level of standard measurements). As the second measurement level it is possible to use the water surface at which the temperature T_w is stipulated and humidity is considered saturating. The procedure for determining the fluxes is reduced to solution of the following equations which together with (5) and (6) form a closed system:

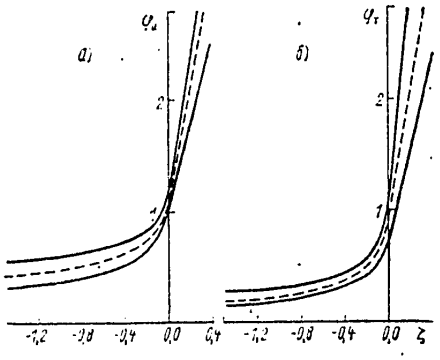

Fig. 1. Universal functions in similarity theory for surface layer. The solid curves approximately limit the region of scatter of experimental values using data from [3,4]. The dashed curves are for computations of the universal functions using (3) and (4).

$$U_* = \frac{\varkappa u_a}{\Delta U_n}, \tag{7}$$

$$T_* = \frac{\varkappa \Delta T}{\Delta T_n}, \tag{8}$$

$$Q_* = \frac{\varkappa \Delta q}{\Delta T_n}, \tag{9}$$

$$B_0 = \frac{c_p \Delta T}{\hat{L} \Delta q}, \tag{10}$$

$$\Delta T = T_a - T_w, \tag{11}$$

$$\Delta q = q_a - q_{\text{нас}}\,(T_w), \tag{12}$$

$$\Delta T_n = T_n\,(\zeta_a) - T_n\,(\zeta_0^T), \tag{13}$$

$$\Delta U_n = U_n\,(\zeta_a) - U_n\,(\zeta_0), \tag{14}$$

$$\zeta_a = z_a/L, \quad \zeta_0 = z_0/L, \quad \zeta_0^T = \zeta_0/a_T, \tag{15}$$

$$L = \frac{U_*^2}{\varkappa\beta T_* M}, \quad M = 1 + \frac{0{,}07}{B_0}, \tag{16}$$

[Нас = sat]

$$z_0 = m \frac{U_*^2}{g}. \tag{17}$$

Here the $q_{sat}(T_w)$ value is saturating specific humidity when $T = T_w$ and is computed using one of the psychrometric formulas; the roughness level of the sea surface z_0 is determined using the well-known Charnok formula (17) [1], a_T is some correction factor, equal to the ratio of the roughness level for wind velocity to the level at which the air temperature coincides with the temperature of the water surface and humidity is saturating. The a_T value can be regarded as a universal constant only with a certain degree of approximation. It is possible to achieve a greater accuracy in the description of the processes of heat and moisture exchange near the water surface by using finer methods for the parameterization of transfer processes in this region, but for the purposes of this study the employed approach is entirely acceptable.

Proceeding on the basis of the general formulation of the problem, it is possible to discriminate three principal sources of errors arising in the computation of turbulent fluxes in the near-water layer. First, these are ordinary errors in determining u_a, T_a, q_a and T_w in the process of carrying out standard shipboard observations, second, the inaccuracy in stipulating the universal functions φ_u, φ_T, and third, the incorrectness of parameterization of the processes of heat and moisture exchange directly at the water surface.

Assuming that the latter two types of errors to a definite degree can characterize the errors in stipulating the universal constants of the employed model, we will write the following expressions for the relative variations of the sought-for turbulence characteristics:

$$\frac{\delta U_*}{U_*} = F_1^u + F_2^u + F_3^u, \tag{18}$$

$$\frac{\delta H_0}{H_0} = F_1^T + F_2^T + F_3^T, \tag{19}$$

$$\frac{\delta E_0}{E_0} = F_1^q + F_2^q + F_3^q, \tag{20}$$

where for $\mu = u, T, q$:

$$F_1^\mu = A_1^\mu \frac{\delta u}{u} + A_2^\mu \frac{\delta T}{\Delta T} + A_3^\mu \frac{\delta q}{\Delta q} + A_4^\mu \frac{\delta M}{M},$$

$$F_2^\mu = \sum_{i=1}^{5} B_i^\mu \frac{\delta z_i}{z_i}, \quad F_3^\mu = D_1^\mu \frac{\delta m}{m} + D_2^\mu \frac{\delta a_T}{a_T}.$$

Here as a simplification it was assumed that

$$\delta T = \frac{1}{2} \delta (\Delta T), \quad \delta q = \frac{1}{2} \delta (\Delta q).$$

The F_1^μ functions correspond to the first group of errors, F_2^μ -- to the second, and F_3^μ -- to the third. The determination of the weighting coefficients A_i^μ, B_i^μ and D_i^μ, on the basis of whose value it is possible to judge concerning the relative contribution of different measurement errors and errors of the model to the total error of the computed turbulent flux, is the principal goal of the reasonings which follow.

These coefficients, as functions of the stability parameter ζ_a and the ζ_0 and ζ_0^T parameters can be determined as a result of solution of a system of linear algebraic equations derived by varying all the variables in the initial equations of the model (5)-(17), including the parameters u_a, ΔT, Δq, M, α_i (i = 1,...,5) m and a_T. After some transformations it is thus possible to obtain:

$$A_1^u = \frac{K}{\Delta T_n}(\varphi_u - \varphi_T^{\circ} + \Delta T_n), \quad A_2^u = \frac{2K}{\Delta U_n}(1 - \varphi_u),$$

$$A_3^u = 0, \quad A_4^u = \frac{1}{2} A_2^u, \quad B_1^u = -A_1^u X_1,$$

$$B_i^u = -A_4^u X_i \quad (i = 2, \ldots, 5),$$

$$D_1^u = \frac{K}{\Delta T_n \Delta U_n}(\varphi_T - \varphi_u + \varphi_T^{\circ} + \Delta T_n), \quad D_2^u = -A_4^u \frac{\varphi_T^{\circ}}{\Delta T_n},$$

$$K = \left[1 + \frac{\varphi_T - \varphi_T^{\circ}}{\Delta T_n} - \frac{2}{\Delta U_n}\left(\varphi_u + \frac{\varphi_T - \varphi_T^{\circ}\varphi_u}{\Delta T_n}\right)\right]^{-1}.$$

Here the following notations were used:

$$\varphi_T^{\circ} = \varphi_T(0) = \alpha_3 + \alpha_4,$$

$$X_1 = \frac{1}{\Delta T_n}\int_{\zeta_0}^{\zeta_a}\left[\frac{\partial \varphi_u}{\partial \alpha_1^{(i)}}\alpha_1^{(i)}\right]\frac{d\gamma_i}{\gamma_i},$$

$$X_j = \frac{1}{\Delta T_n}\int_{\zeta_0^T}^{\zeta_a}\left[\frac{\partial \varphi_T}{\partial \alpha_j^{(i)}}\alpha_j^{(i)}\right]\frac{d\gamma_i}{\gamma_i} \quad (j = 2, \ldots, 5),$$

where i = 1 corresponds to unstable stratification, i = 2 corresponds to stable stratification. The functions φ_u, φ_T, ΔU_n and ΔT_n entering into the expressions cited above are computed using formulas (3)-(6), (13) and (14). Quite simple analytical expressions can be obtained for the X_j parameters.

Similarly it is possible to obtain the coefficients in expressions (19) and (20):

$$A_1^q = A_1^T = \frac{K}{\Delta T_n}(3\varphi_T - \varphi_T^{\circ} + \Delta T_n), \quad A_2^q = A_2^T - 2,$$

$$A_2^T = \frac{2K}{\Delta U_n}(1 + \Delta U_n - 3\varphi_u), \quad A_3^T = 0, \quad A_3^q = 2,$$

$$A_4^q = A_4^T = K\left[\frac{1 - \varphi_u}{\Delta U_n} + \frac{\varphi_T^{\circ} - \varphi_T}{\Delta T_n} + \frac{2}{\Delta U_n \Delta T_n}(\varphi_T - \varphi_T^{\circ}\varphi_u)\right],$$

$$B_1^q = B_1^T = -A_1^T X_1,$$

$$B_i^q = B_i^T = -\frac{A_2^T}{2} X_i \quad (i = 2, \ldots, 5),$$

$$D_1^q = D_1^T = \frac{K}{\Delta T_n \Delta U_n} [\Delta T_n + \varphi_T^\circ \Delta U_n + 3 (\varphi_T - \varphi_T^\circ \varphi_u)],$$

$$D_2^q = D_2^T = -\frac{A_2^T \varphi_T^\circ}{2}.$$

The weighting coefficients are evaluated using some optimum values of the constants α_i, determined on the basis of the experimental data cited in Fig. 1. These values, together with their relative errors following from an analysis of Fig. 1, are given in Table 1. This table also gives the mean value of the m constant recommended in [1] and its relative error.

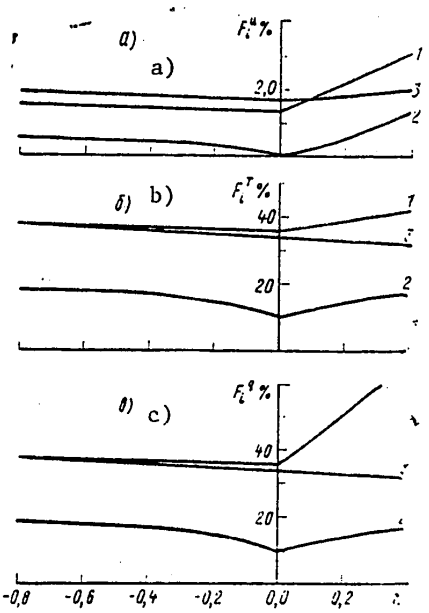

Fig. 2. Contribution of different mechanisms of generation of errors to total relative error in computing the parameters u_* (a), H_0 (b) and E_0 (c) as function of stability parameter ζ . 1) contribution of errors in standard measurements, 2) contribution of errors in determination of universal functions, 3) errors as a result of incorrectness in description of the processes of heat and moisture exchange directly at water surface.

Table 2

Weighting Coefficients for Different Values of Stability Parameter

	σ															
	−0,8		−0,6		−0,4		−0,2		0		0,2		0,4			
	u	T	u	T	u	T	u	T	u	T	u	T	u	T		
A_1^1	1,18	1,24	1,19	1,26	1,21	1,30	1,24	1,36	1,34	1,54	1,74	2,36	2,13	3,15		
A_2^1	0,18	2,31	0,16	2,28	0,13	2,24	0,09	2,17	0,00	2,00	−0,39	1,22	−0,77	0,46		
A_3^1	0,00	0,00	0,00	0,00	0,00	0,00	0,00	0,00	0,00	0,00	0,00	0,00	0,00	0,00		
A_4^1	0,09	0,16	0,08	0,14	0,07	0,12	0,05	0,09	0,00	0,00	−0,20	−0,40	−0,39	−0,77		
B_1^1	0,08	0,09	0,07	0,08	0,06	0,07	0,05	0,05	0,00	0,00	−0,22	−0,30	−0,48	−0,71		
B_2^1	0,00	0,05	0,00	0,05	0,00	0,04	0,00	0,03	0,00	0,00	0,03	−0,09	0,09	−0,06		
B_3^1	−0,07	−0,85	−0,06	−0,84	−0,05	−0,83	0,00	−0,80	0,01	−0,73	0,13	−0,39	0,22	−0,13		
B_4^1	−0,02	−0,30	−0,02	−0,30	−0,02	−0,29	−0,03	−0,28	0,00	−0,24	0,04	−0,13	0,07	−0,04		
B_5^1	0,00	0,01	0,00	0,01	0,00	0,01	−0,01	0,00	0,00	0,00	0,00	0,00	0,00	0,00		
D_1^1	0,18	0,28	0,18	0,27	0,17	0,27	0,17	0,26	0,17	0,27	0,18	0,29	0,18	0,31		
D_2^1	−0,01	−0,10	−0,01	−0,09	−0,01	−0,09	0,00	−0,08	0,00	−0,07	0,01	−0,04	0,02	−0,01		

Table 1

Values of Universal Constants of Model and Errors in Their Determination

$\alpha_1^{(1)}$	$\alpha_1^{(2)}$	$\alpha_2^{(1)}$	$\alpha_2^{(2)}$	α_3	α_4	α_5	m
8,0	5,0	35,0	6,0	0,65	0,25	8,0	0,035
50%	20%	50%	50%	10%	10%	50%	100%

The values of the weighting coefficients for computing the relative variations of U_* and H_0 for different values of the stability parameter ζ_a are shown in Table 2. Similar coefficients for the turbulent flow of water vapor can be scaled on the basis of the expressions cited above. In the computation of these characteristics z_0 was fixed, proceeding on the basis of some mean conditions (U_* = 0.3 m/sec, z_a = 10 m), and the constant a_T was assumed equal to 300 with a relative error coinciding with the error in determining m (100%). These values of the weighting coefficients can be useful in evaluating the relative error in computing turbulent flows with measurement errors stipulated in each specific case. The relative errors in determining the universal constants of the model can be taken from Table 1. Incidentally, for making this type of computations it is necessary to take the absolute values of the weighting coefficients.

In order to compare the relative contribution of all three sources of errors it is necessary to stipulate some typical values of the errors in measuring wind velocity, temperature, humidity and the numbers M. As a point of departure we will assume that the absolute error in measuring u, T and q on shipboard is usually not less than 0.5 m/sec, 0.1°C and 0.2 g/kg respectively. Under some mean conditions, characteristic, in particular, for the temperate latitudes, it can be assumed that $u \approx 5\text{-}8$ m/sec, $\Delta T \approx -1°C$, $\Delta q \approx 2$ g/kg; the following is the approximately correct:

$$\left|\frac{\delta u}{u}\right| \approx \left|\frac{\delta T}{\Delta T}\right| \approx \left|\frac{\delta q}{\Delta q}\right| \approx 0{,}1.$$

The relative error in measuring M is unambiguously related to the errors in measuring temperature and humidity and also to the Bowen number. As follows from formulas (10) and (16), for the adopted mean values $\delta M/M \approx 0.05$.

The functions F_i^u, F_i^T and F_i^q computed with errors reckoned in this way are shown in Fig. 2. An analysis of this figure shows that the contribution of the errors in standard measurements of wind velocity, temperature and humidity in virtually all cases prevails and averages about 20% for U_* and 40-50% for H_0 and E_0. The error in determining the m and a_T constants makes approximately the same contribution to the total error in computing turbulent flows. The dependence on the stability parameter is not clearly expressed although in the case of stable stratification the contribution of the measurement errors increases somewhat. We note that the contribution of the errors in determining the universal constants of the model against the general background is insignificant and for computations of U_* is 5-10%, whereas for H_0 and E_0 it is about 15%. It can be concluded from this that refinement of the universal functions φ_u, φ_T and φ_q is not the primary task in the plan for

increasing the accuracy in computations of turbulent flows on the basis of standard hydrometeorological measurements. A great success in this direction can be achieved by an improvement in the parameterization of processes of heat and moisture exchange in the immediate neighborhood of the water surface.

The conclusions drawn in this article can also be used in evaluating the errors in computation of turbulent flows on the basis of measurements at two levels within the limits of the near-surface and near-water layers. Here the F_3 values must be assumed equal to zero since the altitudes of the measurement levels are usually known with an adequate degree of accuracy.

We note in conclusion that the developed approach in evaluation of the errors in determining flows does not replace but supplements the direct comparison of the computed values of these parameters with the measured values because it makes it possible to clarify the reasons for the discrepancy between theory and experiment and to define effective ways to improve the model.

BIBLIOGRAPHY

1. Kraus, Ye. B., VZAIMODEYSTVIYE ATMOSFERY I OKEANA (Interaction Between the Atmosphere and Ocean), Leningrad, Gidrometeoizdat, 1976.

2. Monin, A. S. and Yaglom, A. M., STATISTICHESKAYA GIDROMEKHANIKA (Statistical Hydromechanics), Part 1, Moscow, Nauka, 1965.

3. Busch, N. E., "The Surface Boundary Layer," BOUND. LAYER METEOROL., Vol 4, No 2, 1973.

4. Yaglom, A. M., "Comments on Wind and Temperature Flux-Profile Relationships," BOUND. LAYER METEOROL., Vol 11, No 1, 1977.

UDC 551.510.42(261)

CHLORINATED HYDROCARBONS IN THE NEAR-WATER ATMOSPHERIC LAYER OVER THE NORTH ATLANTIC

Moscow METEOROLOGIYA I GIDROLOGIYA in Russian No 4, Apr 81 pp 60-64

[Article by I. G. Orlova, candidate of chemical sciences, and L. P. Fetisov, Odessa Division of the State Oceanographic Institute, manuscript received 29 Jul 80]

[Text]

Abstract: The article gives the results of measurements of chlorinated hydrocarbons in the near-water atmospheric layer over the North Atlantic and regions adjacent to it. Among the broad class of chlorinated hydrocarbons it was possible to detect only DDT, the level of whose content was picogram quantities. An analysis of aerosol samples was made aboard ship by the gas-fluid chromatography method.

The timeliness of investigation of contamination of the biosphere by chlorinated hydrocarbons -- some of the most important contaminants in the environment -- is tied in closely to their highly toxic effect on living organisms, the considerable scale of their use and propagation. In this class of contaminating substances the most dangerous, due to its toxicity, high accumulative properties and stability, is DDT, which belongs to the group of organochlorine pesticides (OCP), and also its metabolic products DDD and DDE.

The stability of individual OCP, such as DDT, is so great that its residues are detected in the soil after 7-15 years [1], and in other media longer [7, 12] after its use.

The broad propagation of OCP, including the sea medium, is an established factor [6, 7, 10, 11]. A considerable role in this process is played by atmospheric transport, for the most part causing their dispersal and propagation over considerable distances. This is evidently responsible for the finding of OCP in regions of the world ocean remote from the contamination sources.

In the atmosphere pesticides are present in the vapor phase or are associated. Usually both phases of pesticides exist simultaneously in the atmosphere. It is without importance whether the pesticides enter the atmosphere in aerosol or vapor form, since in the atmosphere a continuous exchange of molecules between these

phases begins immediately and thus an equilibrium of the concentrations of pesticides in the solid and vapor phases is established [2].

However, there is extremely little factual material confirming this concept. Data on the distribution of chlorinated hydrocarbons in the atmosphere over the sea surface are fragmentary, at times contradictory and clearly inadequate for a study of their migration and the processes of redistribution in the biosphere. In the case of the Atlantic Ocean individual observations of the distribution of OCP in the near-water layer of the atmosphere have been made for the most part primarily in the equatorial, tropical and subtropical zones [5, 8, 10]. Factual data are virtually absent for the higher latitudes. This is attributable to a whole series of difficulties, for the most part of a methodological character, one of which is the time required for analysis when determining ultrasmall concentrations of these substances in the atmosphere over the ocean.

The use of modern gas-chromatographic apparatus aboard scientific research weather ships of the State Oceanographic Institute, having an adequate sensitivity in the determination of OCP, made it possible to attempt to evaluate the concentration level of individual chlorinated hydrocarbons in the near-water atmospheric layer over the North Atlantic.

The investigation was carried out during two expeditionary voyages of the scientific research weather ship "Georgiy Ushakov" (1978-1979). The implementation of this experiment at ocean station "C" (52°45'N, 35°30'W) was of special interest; this was the region of the proposed "biospheric reserve." In addition, on both voyages samples were taken in individual regions of the North Atlantic along the ship's track.

In accordance with the adopted methodology, the extraction of DDT and compounds related to it from the atmosphere is accomplished by blowing a definite volume of air through a solution of an appropriate solvent or by means of use of different filters [10]. We employed the latter method.

The sampling was carried out at the 26-m level from the sea surface at a volume rate 220 m^3/hour employing FPA filter material prepared on the basis of cellulose acetate. The filter diameter was 150 mm.

The filtering material frequently contains impurities which in the subsequent analysis give on the chromatogram peaks with close retention times for DDT and its metabolites. The hindering effect of these impurities is eliminated by means of preliminary washing of the filters with hexane in the following way. The filters were placed in a separatory funnel and extraction was carried out three times using portions of hexane of 250-300 ml for a period of 15-20 minutes. The third extract was used as a "free" experiment.

The filter processed in this way was used in the work. In the case of DDT the coefficient of extraction from the filter material was 81±2%, for DDE it was 84±3%.

After the sampling the filter was separated from its gauze base and it was subjected to the extraction process for 15 minutes each time using portions of hexane of 100, 50 and 50 ml. The combined extract was evaporated to a dry state, purified

of coextracting impurities by concentrated sulfuric acid and a gas chromatographic determination was made [3].

Table 1

DDT Content in Aerosol of Near-Water Atmospheric Layer

No	Sampling date	Coordinate of onset of sample: north latitude	Coordinate of onset of sample: longitude	Exposure hours	Volume of pumped air, m^3	DDT concentration ng/m^3
1	27 Dec 1978 r.	52°45′	35°30′ W	9	1770	0,02
2	28 »	same	same	22	3380	0,005
3	30 »	»	»	16	3340	0,006
4	30 Jul 1979 r.	»	»	24	2940	0,002
5	31 »	»	»	24	4010	0,000
6	14 »	39°30′	27°30′ E	24	3930	0,004
7	15 »	37 43	24 17	24	4100	0,006
8	16 »	36 23	21 54	15	2580	0,018
9	17 »	36 27	16 07	24	4320	0,018
10	18 »	37 33	09 43	24	3980	0,023
11	20 »	36 34	01°21′ W	23	3670	0,000
12	24 »	36 46	08 40	25	4040	0,000
13	25 »	39 23	12 31	24	3880	0,006
14	26 »	42 14	16 59	24	3700	0,000
15	27 »	44 44	21 00	26	4010	0,004
16	28 »	47 33	25 52	23	3260	0,012
17	29 »	49 57	30 11	25	3580	0,017
18	06 Jan	44 15	59 10	11	2180	0,009
19	10 »	41 00	68 13	06	1500	0,007
20	11 »	38 00	71 10	15	3150	0,020

Since the filters do not extract the vapor phase of the OCP, the described sampling method assumes an extraction essentially of aerosol OCP. However, a study of the processes of distribution of OCP in the atmosphere [8-10] indicated that most of the OCP, due to their hydrophobicity and tendency to accumulation at phase discontinuities, will be in a sorbed state.

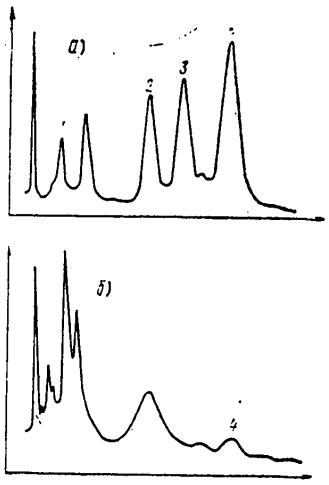

Fig. 1. Chromatogram of standard mixture of OCP (a) and aerosol sample (b). 1) γ-BHC, 2) DDE; 3) DDD; 4) DDT

The conditions for the gas-chromatographic determination ("Tsvet-110" with DPR) were: gas carrier -- nitrogen, high purity; temperature of column thermostat -- 200°C; detector temperature -- 250°C; evaporator temperature -- 220°C; length of column -- 1 m; gas flow through column -- 25 ml/min; electrometer response -- $5 \cdot 10^{11}$ A. The column was filled with chromaton N-AW with a granulation 0.20-0.25 mm, saturated with 5% SE-30.

A chromatogram of a standard mixture and a sample of the near-water layer of the atmosphere is shown in Fig. 1.

A gas-chromatographic analysis was made aboard ship over a period of 24-48 hours after taking of the samples; extraction was carried out immediately after removal of the filters.

In the selected samples of aerosol from the near-water layer of the atmosphere in the North Atlantic only DDT was detected from the class of chlorinated hydrocarbons. Metabolites and polychlorinated biphenyls were not discovered. Nevertheless, their presence in the near-water layer of the atmosphere is possible because DDT under the influence of UV radiation is transformed into polychlorinated biphenyls, forming an intermediate product of photolysis -- DDE [10]. It is realistic to assume that the level of concentration of these substances is considerably lower than the level of DDT content and was beyond the limits of method response.

The absolute DDT concentrations for the investigated region varied from analytical zero (value less than 0.002 ng/m^3) to 0.02 ng/m^3 (Table 1).

Some of the tabulated data (Nos 6-12) characterize the state of DDT contamination of the near-water layer of the atmosphere over the Mediterranean Sea.

In the neighborhood of oceanic station "C" an analysis was made of five samples at different times. The level of DDT content varied from 0 to 0.02 ng/m^3. The mean DDT concentration in this region was 0.007 ng/m^3 with a standard deviation $\pm 7.03 \cdot 10^{-3}$ ng/m^3. In all probability this concentration with a certain amount of caution, due to the small number of observations, can be taken approximately as the background concentration.

The same order of magnitude of DDT concentrations was also found in other regions of the North Atlantic: 0.007-0.009 mg/m^3 for the North American continent and 0.006 for the European continent. Individual high DDT concentrations in the range 0.01-0.02 ng/m^3 were observed both in the open part of the ocean and near the continents.

The level of atmospheric DDT content over the waters of the Mediterranean Sea was higher than over the waters of the Atlantic, which was due primarily to the use of DDT in individual countries of the Mediterranean basin. The mean DDT concentration in samples from this region was 0.012 ng/m^3 (in the North Atlantic it was 0.008 ng/m^3).

It is of interest to compare the collected data with the preceding years of investigations carried out in the near-water layer of the atmosphere in the lower latitudes of the North Atlantic (Table 2).

Table 2

Results of Determinations of Chlorinated Hydrocarbons (DDT) in Near-Water Layer of Atmosphere in Low Latitudes of North America

Place of taking of samples	Air volume	DDT concentration, ng/m^3	Data source
Region of Bermuda Islands and	1070	0.014	[5]
Sargasso Sea	300	0.009	[5]
Northern part of tropical zone of Atlantic	---	0.0007	[9]
Region of Barbados Islands	---	0.0006	[8]

In the region of the Bermudas Islands, according to data published by Bidleman and Olney [5], the DDT concentrations in the near-water layer of the atmosphere correspond to those obtained in this study, whereas the data presented by Risebrough [9], Prospero and Seba [8] for the lower latitudes are approximately an order of magnitude less. This can be attributed to the greater rate of photochemical decomposition of DDT postulated there than in the high latitudes and also the peculiarities of the hydrometeorological conditions and atmospheric circulation during different observation periods.

The low level of the DDT content in the near-water layer of the atmosphere does not mean that it is safe from the ecological point of view. Entering into the water medium, low concentrations of organochlorine pesticides are accumulated in marine organisms, attaining considerable levels of concentration in different links of the marine trophic chain.

Thus, the detected level of DDT content in individual regions, including the open part of the North Atlantic, during different observation periods makes it possible to postulate the constant persence of ultrasmall DDT concentrations in the near-water layer over the North Atlantic and is still another argument in favor of the opinion that atmospheric transport plays a considerable role in the global propagation of DDT in the biosphere [10].

It is evident that for study of long-period changes in the content of organochlorine pesticides in the atmosphere there must be constant observations at base stations, one of which can be the oceanic station "C." In this region continuous observations of the state of the water layer and the near-water layer of the atmosphere have been organized aboard the scientific research weather ships of the State Oceanographic Institute.

BIBLIOGRAPHY

1. Bobovnikova, Ts. I., Babkina, E. I., Mironyuk, G. V. and Yegorov, V. V., "Determination of Organochlorine Pesticides and Their Metabolites in the Soil," TRUDY IEM (Transactions of the Institute of Experimental Meteorology), No 7 (76), 1977.

2. Korapalov, V. M. and Nazarov, I. M., "Regional Transport of Pesticides in the Fergana Valley," TRUDY IPG (Transactions of the Institute of Applied Geophysics), No 39, 1978.

3. RUKOVODSTVO PO KHIMICHESKOMU ANALIZU MORSKIKH VOD (Manual on Chemical Analysis of Sea Waters), Leningrad, Gidrometeoizdat, 1977.

4. Selezneva, Ye. S., "Formulation of Investigations of Background Characteristics of Atmospheric Contamination," METEOROLOGIYA I GIDROLOGIYA (Meteorology and Hydrology), No 1, 1978.

5. Bidleman, T. F. and Olney, C. E., "Chlorinated Hydrocarbons in the Sargasso Sea Atmosphere and Surface Water," SCIENCE, Vol 183, 1974.

6. Harvey, G. R., Steinhaven, W. G. and Teal, J. M., "Polychlorobiphenyls in North Atlantic Water," SCIENCE, Vol 180, 1973.

7. Harvey, G. R., Miklas, H. P., Bowen, V. T. and Steinhaven, W. G., "Observation on the Distribution of Chlorinated Hydrocarbons in Atlantic Ocean Organisms," J. MAR. RES., Vol 32, No 2, 1973.

8. Prospero, J. M. and Seba, D. B., "Some Additional Measurements of Pesticides in the Lower Atmosphere of the Northern Equatorial Atlantic Ocean," ATMOS. ENVIRON., Vol 6, 1972.

9. Risebrough, R. W., Hugget, R. J. and Goldberg, E. D., "Pesticides: Transatlantic Movements in the Northern Trades," SCIENCE, Vol 159, 1968.

10. Spenser, W. F., "Movement of DDT and Its Derivatives Into Atmosphere," RESIDUE REV., Vol 59, 1975.

11. Tatton, G. O. G. and Ruzicka, J. H. A., "Organochlorine Pesticides in Antarctica," NATURE, Vol 215, 1967.

12. Woodwell, G. M., "DDT in Biosphere, Where Does It Go?" SCIENCE, Vol 174, 1971.

UDC 551.465.62

METHODOLOGICAL PROBLEMS IN MEASURING TEMPERATURE AND SALINITY IN THE OCEAN BOUNDARY LAYER

Moscow METEOROLOGIYA I GIDROLOGIYA in Russian No 4, Apr 81 pp 65-70

[Article by A. I. Ginzburg, candidate of physical and mathematical sciences, Institute of Oceanology USSR Academy of Sciences, 5 Aug 80]

[Text]

Abstract: The results of field measurements of boundary changes in temperature ΔT_0 and salinity ΔS_0 in the ocean are compared with the corresponding conditions of heat and mass exchange with the atmosphere on the basis of known semi-empirical expressions [3, 5]. It is shown that in a number of cases considerable discrepancies (even including a change in sign) are a result of the use of measurement methods not taking into account the substantial variability of the vertical thermohaline structure in the near-surface layer with a thickness of 5-10 m. It is noted that this variability can be a source of substantial differences between the results of remote and contact methods for measuring temperature and salinity of the ocean surface.

In order to make a correct interpretation of the results of remote measurements of the physical characteristics of the ocean surface from space vehicles and aircraft it is necessary to know how these characteristics are related, in particular, temperature of the ocean surface (TOS or T_0) and salinity at this horizon (S_0) with the thermodynamic state of the underlying water layers. As a rule numerous comparisons of the results of remote and contact (for the most part shipboard) measurements usually reveal substantial differences between the TOS values restored on the basis of remote data and the temperature usually measured in the limits of the upper 1-3 m under the ocean surface (for example, see [12]). The same can evidently also be said about salinity, although in this case such comparisons are unique [15]. The observed differences are only partially related to the errors in remote measurement methods. Even in a case when the restored T_0 and S_0 values seemingly contain no errors, there are still discrepancies associated, on the one hand, with sharp changes in temperature and salinity in the water near the ocean surface as a result of heat and mass exchange with the atmosphere (changes ΔT_0 and ΔS_0 [2-5]), and on the other hand, with the variability of the thermohaline structure in the near-surface layer of the ocean with a thickness of several meters caused

by a whole series of factors (solar heating, precipitation, convection, internal waves, etc.). This variability not only influences the local instantaneous conditions of heat and mass exchange, and accordingly the ΔT_0 and ΔS_0 values, but also creates conditions under which the imperfection of the employed measurement methods can lead to great errors in determining ΔT_0 and ΔS_0 under field conditions. This article is devoted to an examination of the methodological sources of such errors.

It has been established by laboratory investigations of recent years that in the case of a negative heat balance of the surface the temperature change in the boundary layer ("cold film") with a thickness of approximately 5 mm in water with a temperature $T_w \simeq 20$-$30°C$ and ocean salinity is determined by an expression of the type [3]

$$\Delta \overline{T}_0 = A q^{3/4} (g \alpha c_p \rho \varkappa_T^{1/2} \nu)^{-1/4}. \quad (1)$$

The salinity change as a result of evaporation from the free surface is concentrated in a boundary layer with a thickness of approximately 0.5 mm, which is an order of magnitude thinner than the thermal layer, and as a result of the predominance of thermal instability [5] is always less than the value

$$\Delta \overline{S}_0 = A F^{3/4} \beta^{-1} (g \rho^3 D^2 / \nu)^{-1/4}. \quad (2)$$

In expressions (1) and (2) q and $F = ES\rho$ are the densities of the heat and salt flows through the discontinuity respectively, g is the acceleration of free falling,

$$\alpha = -\frac{1}{\rho}\frac{\partial \rho}{\partial T} \quad \text{and} \quad \beta = \frac{1}{\rho}\frac{\partial \rho}{\partial S}$$

are the contributions of temperature and salinity to density ρ respectively, c_p is specific heat capacity at constant pressure, $\varkappa_T$ is the molecular thermal conductivity coefficient, ν is kinematic viscosity, D is the salt diffusion coefficient, E is the rate of water evaporation.

In accordance with our experimental data on the thermal boundary layer A = 2.82 [3, 4] for the range of wind velocities equivalent to the dynamic velocity in the air $0 \leqslant u_* \leqslant 23$ cm/sec. It decreases in a jump by a factor of approximately 2.8 with $u_* \simeq 23$ cm/sec and with greater wind velocities remains virtually constant [4].

Proceeding on the basis of (1) and (2) and having data on the heat flux q and the evaporation rate E it is possible to estimate the $\Delta \overline{T}_0$ and $\Delta \overline{S}_0$ values for any specific meteorological situation. For example, our $\Delta \overline{T}_0$ estimate based on data on effective backscattering, water temperature, air temperature and humidity, given in an article by Malevskiy-Malevich [8], agreed well with the results of his measurements in the North Atlantic.

As demonstrated in [3], dependence (1) also agrees well with data from in situ measurements of Saunders and Hass. At the same time, there are considerable discrepancies (even with a difference in sign) between the $\Delta \overline{T}_0$ and $\Delta \overline{S}_0$ values

measured by a number of authors and the estimates of these parameters with the q and E values taken from [1] for the corresponding seasons and measurement regions. For example, the $\Delta\overline{T}_0$ and $\Delta\overline{S}_0$ estimates for summer in the Indian Ocean ($q \simeq -130$ W/m^2 and $E \simeq 0.33$ cm/day) gives $\Delta\overline{T}_0 \simeq -0.41$°C and $\Delta\overline{S}_0 \simeq 0.37$°/oo respectively, whereas the measured values (maxima) are equal to -2.9°C and 1°/oo [7]. With a flux $q \simeq -100$ W/m^2 characteristic for the summer months in the Black Sea [13] the computed $\Delta\overline{T}_0$ value is only -0.4°C, whereas the measured [13] value $\Delta\overline{T}_0 = -2$ -3°C. In this same season and also in the Black Sea, according to a communication of other authors [9], there was primarily a "warm film" with a maximum change $\Delta\overline{T}_0 = +1.5$°C. [It must be remembered that in contrast to a "cold film," which is the product of convective instability of the boundary layer and which has a thickness of 5-7 mm or less, the thickness of the "warm film," characteristic for the positive heat balance of the ocean surface with a stable vertical density distribution, is limited only by the magnitude of the flux q and the heating time [2]; it can be more than 1 m and therefore it is undesirable to apply the term "film" to a layer with a positive temperature drop.] In our opinion, such disagreements between the observed temperature and salinity drops in the boundary layer and the existing heat fluxes and evaporation rates are a result of the measurement methods used by the authors of [7, 9, 13].

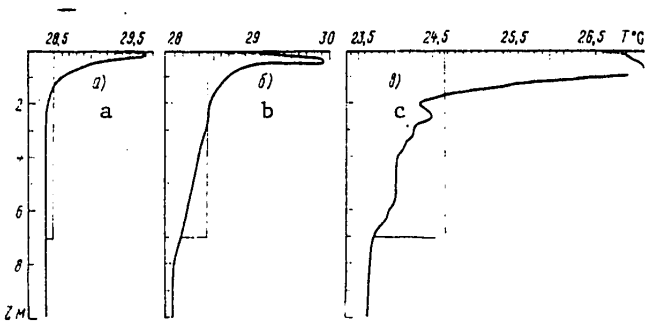

Fig. 1. Temperature profiles registered on 1 October 1977 at 1447 hours (LT) (a), 25 August 1978 on the 27th voyage of the scientific research ship "Akademik Kurchatov" at approximately 1400 hours (LT) (b) and 28 May 1973 at 1840 hours (LT) at a point with the coordinates 28°45'N and 68°25'W (c). The thin line represents the water temperature profile after mixing of the upper seven-meter ocean layer.

First we will examine measurements related to the thermal boundary layer. In the studies mentioned above the temperature drop ΔT_0 was determined as the difference between the surface temperature T_0, measured by the contact method [7-13] or an IR radiometer [9] and the temperature of the lower-lying layer T_{low}, for which we used the temperature of the isothermic layer [13], the temperature at the depth of taking of a sample with a bathometer [7] or the temperature of the upper artificial mixed water layer with a thickness from 1 to 7 m [9]. Naturally, with a correct measurement of T_0 the ΔT_0 value will be determined precisely by measurement of the temperature T_{low}. If at the measurement time the water layer below the boundary layer is isothermic within the limits of several meters, it is evidently of indifference at what depth z_{low} the T_{low} reading is made. Such a situation is possible either with intensive wind mixing or when there is well-developed convection in the absence of solar heating (primarily in the evening and nighttime hours [11, 16]). However, if in the upper several meters there are deviations from

isothermy, as is especially characteristic for intensive solar heating with conditions close to calm [6, 11, 16], the ΔT_0 value will be determined by the depth z_{low} of measurement of T_{low} or by the thickness of the artificially mixed layer. Accordingly, the ΔT_0 value measured by different methods is essentially dependent on the vertical T(z) distribution in the upper several meters of the ocean.

Not having information on the vertical distributions of temperature accompanying measurements [7, 9, 13], we will demonstrate what has been said in the examples of several T(z) profiles (Fig. 1) obtained by a number of researchers in approximately one and the same region in the Atlantic Ocean during a calm or when there was a weak wind. The profile a was obtained by A. V. Solov'yev in the region of the POLYMODE experiment with its center at 29°N and 70°W using a freely floating probe [11]; profile b was obtained by V. T. Paka and K. N. Fedorov in this same region using a "Bumerang" freely falling probe and temperature sensors suspended on floats (at the horizons 0.05 m, 0.30 m, 0.45 m, 0.95 m, etc.); profile c was obtained by Bruce and Firing using a modified XBT probe [16]. Since the mentioned instruments did not make it possible to make measurements of the fine structure near the surface with a resolution of a fraction of a millimeter, information on the drop ΔT_0 near the surface at the time of measurements is lacking. For an approximate determination of T_0 the profiles in Fig. 1 were supplemented (dashed line) in their upper part by the boundary layer (at a distorted vertical scale) with the drop $\Delta T_0 = -0.36$°C, computed using (1) with the value $q = -120$ W/m^2 corresponding to the α profile [11]. Although with such an arbitrary choice of q there can be errors in determining T_0 for profiles b and c, in this case this is unimportant because these errors are considerably less than the methodological errors which are being discussed.

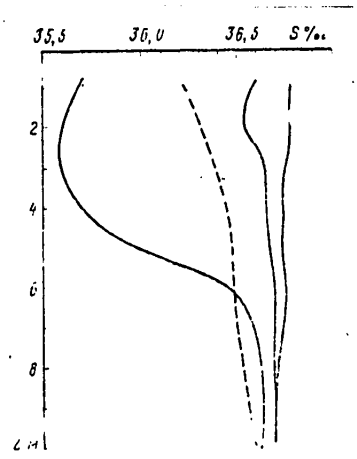

Fig. 2. Salinity profiles obtained in August 1978 on the 27th voyage of the scientific research ship "Akademik Kurchatov" using an AIST probe in a "holding" regime at a number of horizons [6].

Figure 1 shows that with one and the same temperature drop in the boundary layer $\Delta T_0 = -0.36$°C it is possible to obtain, in dependence on the type of the T(z) distribution and using in situ measurement methods, both high negative ΔT_0 values (-1.4°C for the b profile with measurement of the T_{low} temperature at the

0.30 m horizon) and high positive ΔT_0 values (+2.0°C for the profile c when measuring T_{low} at the 1.7-m horizon or with the mixing of water in the 7-m layer). Thus, the lack of information on the variability of temperature in the upper 10-m (and especially in the meter) layer of the ocean at the measurement point can lead to substantial errors in field measurements of ΔT_0 which must be taken into account especially in measurements in the tropical latitudes, since precisely there the maximum variability of temperature in the upper meter of the ocean is observed.

This same conclusion also applies completely to measurements of salinization of the boundary layer ΔS_0. Unfortunately, at the present time there are no instruments making it possible to carry out detailed absolute measurements of the salinity distributions (conductivity) in the upper meter layer of the ocean. However, measurements using the AIST probe, carried out in a regime of holding of the probe at a number of horizons with subsequent averaging [6] on the 27th voyage of the scientific research ship "Akademik Kurchatov" under the POLYMODE program demonstrated a strong variability of salinity in the upper layer 0.7-10 m as a result of showers [6].

Several S(z) profiles obtained in the region of the POLYMODE experiment are represented in Fig. 2, from which it follows that salinity in the limits of the upper meter at closely spaced points can differ by 1°/oo. This variability of salinity can be an important component of the overall methodological error in determining ΔS_0 in measurements, where the reference value used is the salinity value at the depth of taking of the sample with a bathometer [7, 10].

On the other hand, the very method for determining salinity at the ocean surface S_0 in situ, in contrast to temperature measurements, is a serious problem. Remote radiometric methods do not make it possible to measure S_0 with an accuracy better than 1°/oo [14].

The optical interferometry method, which was used successfully in laboratory measurements [5], is not suitable for measurement of the fine vertical structure in situ.

The screen method [7, 10] proposed by Garrett [17] for the collection of films of different origin in an ideal case gives only the mean salinity value in the boundary layer (on the assumption of linearity of the S(z) profile), since the thickness of the layer of collection of the sample by this method ($\simeq$0.4 mm [10]) is approximately equal to the thickness of the boundary layer of increased salinity [5]. However, in a real case the S_0 values determined by this method are exaggerated as a result of evaporation from the screen in the process of taking the sample and the presence of suspensions and petroleum contaminations in it [10]. Thus, the problem of in situ salinity measurements in the thin surface layer of the ocean and its surface with an accuracy better than the possible amplitude of its spatial variability, as a result of the nonuniformity of evaporation from the ocean surface (tenths promille), still requires its solution.

It follows from the above that the variability of the vertical thermohaline structure of the surface layer of the ocean can be the reason for the significant (greater than the ΔT_0 and ΔS_0 differences in the boundary layer) discrepancies

between temperature and salinity measured in the upper meter layer of the ocean (for example, while the ship is proceeding on course at a depth of 0.5-1 m) and with the same parameters measured by remote methods. The greatest discrepancies can be expected when making temperature measurements during the daytime hours, especially under calm conditions with intensive solar heating and in measurements of salinity -- after the passage of heavy showers. This must be taken into account when interpreting the results of in situ measurements of ΔT_0 and ΔS_0 and in formulating investigations for comparing the results of remote and contact methods for measuring temperature and salinity of the ocean surface.

BIBLIOGRAPHY

1. ATLAS TEPLOVOGO BALANSA ZEMNOGO SHARA (Atlas of the Earth's Heat Balance), edited by M. I. Budyko, Moscow, 1963.

2. Ginzburg, A. I., Zatsepin, A. G. and Fedorov, K. N., "Laboratory Investigation of the Fine Structure of the Thermal Boundary Layer in the Water at the Water-Air Discontinuity," MEZOMASSHTABNAYA IZMENCHIVOST' POLYA TEMPERATURY V OKEANE (Mesoscale Variability of the Temperature Field in the Ocean), Moscow, IO AN SSSR, 1977.

3. Ginzburg, A. I. and Fedorov, K. N., "Cooling of the Water From the Surface During Free and Forced Convection," IZV. AN SSSR: FIZIKA ATMOSFERY I OKEANA (News of the USSR Academy of Sciences: Physics of the Atmosphere and Ocean), Vol 14, No 1, 1978.

4. Ginzburg, A. I. and Fedorov, K. N., "Thermal State of the Boundary Layer of Cooling Water With Transition From Free to Forced Convection," IZV. AN SSSR: FIZIKA ATMOSFERY I OKEANA, Vol 14, No 7, 1978.

5. Ginzburg, A. I., Fedorov, K. N. and Vlasov, V. L., "Increased Salinity in the Surface Layer of Sea Water During Evaporation," DOKLADY AN SSSR (Reports of the USSR Academy of Sciences), Vol 243, No 3, 1978.

6. Ginzburg, A. I., Zatsepin, A. G., Sklarov, V. Ye. and Fedorov, K. N., "Effects of Precipitation in the Ocean Surface Layer," OKEANOLOGIYA (Oceanology), Vol 20, No 5, 1980.

7. Yeremeyev, V. N., Bezborodov, A. A. and Romanov, A. S., "Some Characteristics of the Chemical Composition of the Surface Microlayer of Ocean Water," MORSKIYE GIDROFIZICHESKIYE ISSLEDOVANIYA (Marine Hydrophysical Investigations), No 3(86), 1979.

8. Malevskiy-Malevich, S. P., "Characteristics of the Temperature Distribution in the Surface Water Layer," PROTSESSY PERENOSA VBLIZI POVERKHNOSTI RAZDELA OKEAN-ATMOSFERA (Transfer Processes Near the Ocean-Atmosphere Discontinuity), Leningrad, Gidrometeoizdat, 1974.

9. Mel'nikov, G. S. and Mineyev, Ye. N., "Determination of the Surface Temperature Drop at the Discontinuity of the Liquid Phase of the Sea-Atmosphere System," OPTICHESKIYE METODY IZUCHENIYA OKEANOV I VNUTRENNIKH VODOYEMOV (Optical Methods for Study of the Oceans and Internal Water Bodies), Novosibirsk, 1979.

10. Mikhaylov, V. I., "Some Reasons for an Increase in the Salinity of the Surface Microlayer of the Ocean in Individual Parts of the North Atlantic," TRUDY GOIN (Transactions of the State Oceanographic Institute), No 146, 1979.

11. Solov'yev, A. V., "Fine Thermal Structure of the Surface Layer of the Ocean in the POLYMODE-77 Region," IZV. AN SSSR: FIZIKA ATMOSFERY I OKEANA (News of the USSR Academy of Sciences: Physics of the Atmosphere and Ocean), Vol 15, No 7, 1979.

12. Terziyev, F. S., Girdyuk, G. V., Vinogradov, V. V. and Tauber, G. M., "Present Status of Investigations of Sea Surface Temperature," METEOROLOGIYA I GIDROLOGIYA (Meteorology and Hydrology), No 11, 1979.

13. Khundzhua, G. G. and Andreyev, Ye. G., "On the Problem of Determining Heat Fluxes and Water Vapor Fluxes in the Ocean-Atmosphere System According to Observations of the Temperature Profiles in the Thin Surface Layer of the Sea," DOKLADY AN SSSR, Vol 208, No 4, 1973.

14. Basharinov, A. E. and Shutko, A. M., "Research Into the Measurement of Sea State, Sea Temperature and Salinity by Means of Microwave Radiometry," BOUND. LAYER METEOROL., Vol 18, No 1, 1980.

15. Blume, H., Kendall, V. M. and Fedors, J. C., "Measurements of Ocean Temperature and Salinity Via Microwave Radiometry," BOUNDARY LAYER METEOROL., Vol 13, No 1-4, 1978.

16. Bruce, J. G. and Firing, E., "Temperature Measurements in the Upper 10 m With Modified Expendable Bathythermograph Probes," J. GEOPHYS. RES., Vol 79, No 2, 1974.

17. Garrett, W. D., "Collection of Slick-Forming Materials From the Sea Surface," LIMNOLOGY AND OCEANOGRAPHY, Vol 10, 1965.

UDC 551.(526.6+509.33)(261)

POSSIBILITY OF SEASONAL PREDICTION OF WATER TEMPERATURE IN THE NORTH ATLANTIC

Moscow METEOROLOGIYA I GIDROLOGIYA in Russian No 4, Apr 81 pp 71-76

[Article by R. V. Gavrilyuk, USSR Hydrometeorological Scientific Research Center,
manuscript received 29 Sep 80]

[Text]

Abstract: On the basis of an analysis of the spatial-temporal variability of temperature of the water surface layer in the North Atlantic it was possible to determine the seasons in the annual variation and a grid of points is proposed for stipulating the water temperature field. The author demonstrates the possibility of representing the fields of mean seasonal water temperature in the form of series with expansion in natural components. The article describes a method for predicting the mean seasonal water temperature for a period of two months in advance for the spring, summer and autumn seasons and for a period of one year in advance for winter. The results of predictions are presented.

The possibility of using maps of the mean water temperature values for the surface layer of the ocean in the North Atlantic, averaged by five-degree squares, for computations and predictions was demonstrated in [4]. Continuous series of such observations have been available for the period from 1957 through 1974. In order to analyze the spatial-temporal variability of water temperature in the surface layer these series were used in computing the following characteristics: mean monthly water temperature values for a long-term period for each square, standard deviations of water temperature from the mean long-term value, amplitude of the annual variation and the maximum water temperature amplitude for the particular period.

Figure 1 shows the distribution of the mean long-term and maximum (for an 18-year period) water temperature amplitudes. The centers of the maximum amplitude values in both figures coincide and are situated in the middle latitudes along the shores of North America, to the south of Newfoundland. The maximum water temperature amplitude is the difference between the highest mean monthly water temperature in the entire series of observations and the lowest. The years of highly extremal values in each square usually do not coincide, but the coincidence of regions with anomalous amplitudes indicates a universality of the processes causing them. The very same maximum amplitudes indicate a variability of these processes. Such a distribution in the amplitudes of the annual variation of water temperature indicates

that the processes of heating and cooling of the surface water layer transpire differently both in space and in time. In the analysis of the annual variation of water temperature we constructed and analyzed 12 maps of changes in water temperature from month to month. The analysis made it possible to combine months in which the water temperature changes were identical. In discriminating the hydrological seasons we used the V. N. Stepanov method [7], according to which "an allowance is made not only for the absolute water temperature, but also the change in the rate of its increase and decrease (temporal change of the water temperature gradient)." We assign to hydrological winter that segment of the curve of annual variation of temperature where, having lower values, its temporal gradient is close to zero.

Thus, during the period from January through March over the entire area of the ocean there is a gradual decrease in water temperature. As an average for the month the decrease in water temperature is 0.5-1.0°C and therefore these three months were combined into the winter season.

It is easy to trace hydrological spring on the basis of the sharp increase in water temperature. A gradual heating of the ocean surface begins in April-May. However, this heating is not identical in different parts of the ocean. The extreme western band of coastal water is heated most strongly; the water temperature changes from April to May here attain 3.0°C. The remaining part of the ocean area is heated by 1.3-1.5°C. In the southern latitudes the temperature changes in the surface layer of water are 0.5-0.7°C per month. The months of April and May are combined into the spring season.

In the course of the hydrological year there are considerable changes in water temperature. In June, July and August the increase in water temperature is most intense. In the western regions the month-to-month changes are 3.0-4.0°C, in the central regions -- 2.0-3.0°C, in the southern regions -- about 1.0°C from month to month. The months of June, July and August are also combined into the summer season.

The hydrological autumn is characterized by a rapid cooling of the water and ends with the attaining of low temperatures which vary little in the course of time, as is characteristic for the next season. The four last months -- September, October, November and December -- are combined into the autumn season. In the western regions the water temperature decrease from month to month is 2.0-3.0°C, in the central regions -- 1.0-2.0°C, in the southern regions -- 1.0-1.6°C.

We note that such a representation of the annual variation of water temperature by four seasons is not the purpose of this article but was done as a convenience. The breakdown of the seasons with the water temperature gradient taken into account in time makes possible the reverse conversion -- from mean seasonal to mean monthly water temperature value.

Spatially the changes in water temperature in the course of the year transpire very nonuniformly and therefore it is important to select such points which with allowance for spatial variability would most completely characterize the water temperature field. For a solution of this problem we found the correlation between water temperature in each square and the water temperature in the adjacent four squares.

In those places where the correlation coefficients were high the position of the points could be taken with a lesser frequency. In regions with a great water temperature variability the points were situated closer to one another. The position of the points is shown in Fig. 1a.

Thus, spatially the water temperature of the surface water layer in the North Atlantic is stipulated at 28 points and in time four seasons are considered.

During recent years an analytical representation of fields in the form of series with expansion into natural orthogonal functions has been popular. Such a representation of the hydrometeorological information has been discussed in considerable detail in the literature [1-3] and therefore here there is no need for discussing the advantages of this method. In this article the fields of mean seasonal water temperature, stipulated at 28 points, were also expanded into series in natural components. Table 1 gives the eigenvalues of the covariation matrices of the mean seasonal water temperature and the indices of series convergence. The table shows that the contribution of the first expansion term B_1 describes the maximum of the dispersion of the initial field; the additional contribution of expansion coefficients of a higher order is insignificant. The sum of the five expansion terms describes 99.7% of the dispersion of the initial field. Since the first expansion term describes the maximum of the total dispersion, it therefore follows that the proper prediction of the first expansion term B_1 plays a decisive role for the successful prediction of mean seasonal water temperature. The value of a correct forecast B_1 is determined not only by the large contribution to the total dispersion of the predicted field, but also by an entirely definite physical sense. The elementary field corresponding to the first expansion term B_1 characterizes the latitudinal distribution of water temperature. The details in the distribution of water temperature already are reflected in higher-order expansion terms.

Table 1

Eigenvalues of Matrices of Mean Seasonal Water Temperature ($\lambda \cdot 10^2$) and Index of Convergence of A Series

№	Winter		Spring		Summer		Autumn	
	$\lambda \cdot 10^2$	A%	$\lambda \cdot 10^2$	A%	$\lambda \cdot 10^2$	A%	$\lambda \cdot 10^2$	A%
1	175,49	95,7	187,61	98,9	182,23	98,9	171,38	98,4
2	6,05	3,3	0,73	0,3	0,59	0,4	0,95	0,6
3	0,72	0,4	0,46	0,3	0,35	0,2	0,53	0,3
4	0,37	0,2	0,23	0,3	0,32	0,2	0,40	0,2
5	0,21	0,1	0,20	0,1	0,13	0,1	0,26	0,2

In connection with the representation of the predictants in the form of series with expansion in natural components the question arises as to how many expansion coefficients must be predicted. For this purpose the actual fields of mean seasonal water temperature were restored using 2, 3, 4, 5 and 6 expansion coefficients and the guaranteed probability of restoration was computed. As the admissible error we used σ -- the standard deviation of water temperature from the mean long-term

value. The results of the computations indicated that although as an average for the field the guaranteed probability of the restored fields even with restoration using two coefficients is rather high -- 83%, nevertheless, for individual points of the restored field the use of only two coefficients is inadequate. This applies, in particular, to points with a great variability of water temperature. Accordingly, in order to avoid large errors in the restoration of water temperature it is recommended that four or five expansion coefficients be used.

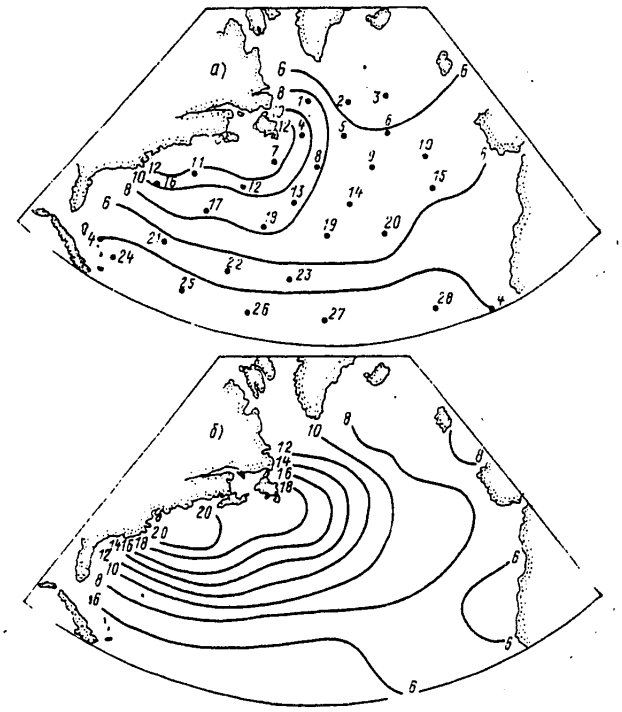

Fig. 1. Mean long-term (a) and maximum (b) amplitude of water temperature in North Atlantic.

In predicting the mean seasonal water temperature in the North Atlantic we made use of the concept of sequential development of processes in the ocean and the atmosphere. In [5] it was demonstrated that it is possible to predict water temperature in the warm part of the year on the basis of heat losses from the ocean during winter and data on atmospheric conditions during the preceding time. In this article an attempt is made to predict the mean seasonal water temperature (spring, summer, autumn) on the basis of the thermal and dynamic state of the atmosphere and the initial water temperature in the preceding season. The advance time of the forecast was 2 months. The general form of the equation for spring, summer and autumn is as follows:

$$B^{t_w}_{i_n} = \sum_j a_j B^{t_a}_{j_{n-2}} + \sum_k b_k B^{\Delta p}_{k_{n-2}} + c_i B^{t_w}_{i_{n-2}} + d_i,$$

where B^{tw}_{in} are the coefficients of expansion of the fields of mean seasonal water temperature,

$$B^{t_a}_{j_{n-2}}, \quad B^{\Delta p}_{k_{n-2}}, \quad B^{t_w}_{i_{n-2}}$$

are the coefficients of expansion of the air temperature field, pressure anomaly field and water temperature field with a shift of two months relative to the month with which the season begins, a_j, b_k, c_i, d_i are the coefficients of the regression equation.

For the winter the water temperature was predicted on the basis of the indices of the thermal and dynamic state of the atmosphere and the water temperature for the winter of the preceding year, that is, for winter the advance time of the forecast is equal to 1 year. The general form of the equation for predicting winter water temperature is as follows:

$$B^{t_w}_i = \sum_j a_j B^{t_a}_{j_{XII-III}} + \sum_k b_k B^{\Delta p}_{k_{XII-III}} + c_i B^{t_w}_{i_{XII-III}} + d_i,$$

where B^{tw}_i are the coefficients of expansion of the water temperature field in winter

$$B^{t_a}_{j_{XII-III}}, \quad B^{\Delta p}_{k_{XII-III}}, \quad B^{t_w}_{i_{XII-III}}$$

are the coefficients of expansion of the fields of air temperature, pressure anomalies and water temperature in the winter of the preceding year; the remaining notations are as before.

When establishing the correlations between different hydrometeorological elements it is sounder to analyze the fields of distribution of these elements, since in this case there is a more complete disclosure of the interrelationship and interdependence of the processes, a clearer manifestation of the influence of the determining factors on the changes in the predicted parameters. Accordingly, the decisive factors -- atmospheric pressure and air temperature in the preceding season -- were stipulated by the fields and were represented analytically by means of expansion into series in natural components.

The air temperature fields were stipulated at nine points (weather ships), expanded into series in natural components and the expansion coefficients were computed.

Atmospheric circulation was examined over the northern part of the ocean (sector I in the northern hemisphere). Pressure was stipulated at 19 points. In finding the natural components we used maps of anomalies of mean monthly pressure over the North Atlantic. The coefficients of expansion of the fields of anomalies of mean monthly pressure into series of natural components were given in [6].

In finding the predictors for predicting the mean seasonal water temperature in the North Atlantic we computed the paired correlation coefficients between the coefficients of expansion of the air temperature field, the field of atmospheric

pressure anomalies and the water temperature field in the next season. The resulting pattern was very mottled. In individual cases there was no correlation at all between some coefficients; in other cases the correlation coefficient attained values 0.50-0.60. We note that with a limited length of the series (n = 18) the significant correlation coefficient $R \geqslant 0.50$.

From among the great number of predictors it was necessary to select those which, first of all, would be uncorrelated with one another, and second, would increase the total multiple correlation coefficient in the regression equation. Such a problem was solved by the multiple correlation method on an M-222 electronic computer for each season of the year and each coefficient of the water temperature field expansion.

Table 2 gives the guaranteed probability of the prediction of six expansion coefficients of the water temperature fields for different seasons of the year. The table shows that the guaranteed probability of the prediction of the first two expansion coefficients B_0 and B_1 is rather high and greatly exceeds the natural guaranteed probability. The coefficients of expansion of a higher order are predicted somewhat more poorly, but the guaranteed probability of their prediction also exceeds the natural value.

Table 2

Guaranteed Probability of Prediction of Coefficients of Expansion of Fields of Water Temperature

B_l	Mean	R from equation	σ	A	B	Mean	R from equation	σ	A	B
	Winter					Spring				
B_0	16,62	0,71	0,14	82	60	17,32	0,78	0,24	100	72
B_1	−31,69	0,86	1,65	93	75	−30,08	0,78	0,91	77	55
B_2	−1,10	0,75	0,81	88	75	−0,60	0,72	2,08	88	66
B_3	0,01	0,93	2,00	100	88	0,03	0,66	1,60	83	55
B_4	−0,02	0,47	1,32	75	88	0,25	0,84	1,66	100	77
B_5	0,01	0,78	1,08	100	88	0,16	0,68	1,20	72	66
	Summer					Autumn				
B_0	21,46	0,81	0,30	100	72	20,35	0,60	0,20	83	72
B_1	−30,00	0,57	1,20	83	77	−30,83	0,81	1,26	94	61
B_2	−0,04	0,71	1,82	88	72	0,03	0,80	2,30	83	83
B_3	0,00	0,59	1,40	83	66	0,01	0,77	1,75	100	83
B_4	0,05	0,69	1,35	88	88	0,01	0,83	1,75	94	77
B_5	0,00	0,45	0,85	77	66	0,01	0,57	1,62	94	77

A) Guaranteed probability of equation, %; B) Natural guaranteed probability, %

The computed expansion coefficients were used in restoring the fields of mean seasonal water temperature. In this article there is no possibility of presenting a detailed table of the guaranteed probability of predicting the mean seasonal water temperature for each field point. We note only that the guaranteed probability of

the prediction of the mean seasonal water temperature with an error of not more than 0.67σ for all field points exceeds the natural value. As an average for the field the guaranteed probability of the prediction of the water temperature fields for different seasons of the year in comparison with the natural value is as follows: for the winter the guaranteed probability of the prediction is 86%, the natural value is 67%; for the spring the guaranteed probability of the prediction is 80%, the natural value is 66%; for the summer -- 84 and 61% and for autumn -- 88 and 73% respectively.

Since these results were obtained for a limited length of the series it would be of interest to check the application of the method on the basis of an independent sample. We had at our disposal the water temperature fields from 1975 through 1980. We computed the expansion coefficients of the air temperature, atmospheric pressure anomalies and mean monthly water temperature fields and then used the regression equations for computing the expansion coefficients of the fields of mean seasonal water temperature. The restoration was accomplished using the computed coefficients. The checking indicated that as an average for the field the guaranteed probability of the prediction in comparison with the natural value is as follows: for spring the guaranteed probability of the prediction was 83%, natural -- 74%, for summer the guaranteed probability of the prediction is 88%, natural -- 75%, for autumn -- 86 and 75% and for winter -- 86 and 66%.

BIBLIOGRAPHY

1. Bagrov, N. A., "Analytical Representation of Fields," TRUDY TsIP (Transactions of the Central Institute of Forecasts), No 64, 1958.

2. Bagrov, N. A., "Analytical Representation of a Sequence of Meteorological Fields Using Natural Orthogonal Components," TRUDY TsIP, No 74, 1959.

3. Belinskiy, N. A., ISPOL'ZOVANIYE NEKOTORYKH OSOBENNOSTEY ATMOSFERNYKH PROTSESSOV DLYA DOLGOSROCHNYKH PROGNOZOV (Use of Some Characteristics of Atmospheric Processes for Long-Range Forecasts), Leningrad, Gidrometeoizdat, 1957.

4. Gavrilyuk, R. V., "Evaluation of 'Thermal Inertia' and Use of Shipboard Observations of Water Temperature in the Ocean," TRUDY GIDROMETTSENTRA SSSR (Transactions of the USSR Hydrometeorological Center), No 241, 1980.

5. Glagoleva, M. G. and Skriptunova, L. I., PROGNOZ TEMPERATURY POVERKHNOSTNOGO SLOYA OKEANA: METODICHESKOYE PIS'MO (Prediction of Temperature of the Surface Layer of the Ocean: Methodological Letter), No 3, Leningrad, Gidrometeoizdat, 1977.

6. Glagoleva, M. G., TABLITSY KOEFFITSIYENTOV RAZLOZHENIYA V RYADY PO YESTESTVENNYM SOSTAVLYAYUSHCHIM POLEY ANOMALIY SREDNEGO MESYACHNOGO DAVLENIYA NAD SEVERNYM POLUSHARIYEM (Tables of Coefficients of Expansion into Series in Natural Components for the Fields of Mean Monthly Pressure Anomalies Over the Northern Hemisphere), Moscow, Gidromettsentr SSSR, 1977.

7. Stepanov, V. N., "Annual Variation of Water Temperature at the Surface of the World Ocean and Hydrological Seasons," OKEANOLOGIYA (Oceanology), Vol I, No 3, 1961.

UDC 551.(465+588)

DELAYING EFFECTS IN THE OCEAN-ATMOSPHERE SYSTEM AND THEIR MODELING

Moscow METEOROLOGIYA I GIDROLOGIYA in Russian No 4, Apr 81 pp 77-84

[Article by O. A. Vladimirov, candidate of geographical sciences, Arctic and Antarctic Scientific Research Institute, manuscript received 8 Aug 80]

[Text]

Abstract: Observations show that climate is not constant. There are a considerable number of facts which show that it is characterized by changes with different time scales. One of the reasons for such variability is the presence of delaying effects in the ocean-atmosphere system. Examples are presented. It is shown that the delaying effects are described by differential equations with a "delaying" argument. Modeling regions are enumerated in which such equations must be used. An example of their use in the modeling of the interrelationship between the low and high latitudes of the Atlantic Ocean by a system of surface currents is cited.

As indicated by observations, many climatic components are not absolutely constant. A sufficient volume of facts has now been accumulated which show that during the course of the earth's entire history climate has repeatedly experienced changes with different time scales.

Climatic fluctuations at scales of $1\text{-}10^2$ years are of the greatest practical interest. This is attributable to the fact that fluctuations with such time scales are of vital importance and fit within the framework of modern planning periods [12].

At the present time several factors have been mentioned which can cause such fluctuations. In the author's opinion, among these there are delaying effects to which particular attention will be devoted below.

The fact is that the temporal development of a number of dynamic processes is determined not only by the forces operative at a particular moment, but is also dependent on effects which existed in the past, that is, is determined by delaying effects. These effects are manifested in the form of consequences and delays.

Aftereffect phenomena must frequently be dealt with when dynamic processes have a singular "memory," in which the consequences of the effects are stored [7].

The appearance of a delay is attributable to the fact that a definite time is required for the movement of any kind of "impulse," for example, along a flow, since the velocity of the latter is finite.

The presence of delaying effects in the investigated system is frequently the reason for the appearance in it of phenomena which exert a significant influence on the very course of the process of system development. For example, delaying effects can cause the appearance of self-exciting oscillations.

It is particularly important that the presence of delaying effects can frequently lead to disruption of system stability if it had such in the absence of similar effects. The reverse is also possible: the appearance of stability as a result of the appearance of delaying effects in the system [10, 16].

Dynamic systems with delaying effects and processes transpiring in such systems in most cases are described by differential equations with a deviating argument or systems of such equations.

A differential equation with a deviating argument is an equation in which there is not only the argument t, but also the sought-for function and its derivatives, taken with different t values. Such an equation is of the delaying type (otherwise known as an equation with a delaying argument) if the value of the higher derivative with any value $t = t'$ is determined through the values of the lower derivatives with $t \leqslant t'$.

An equation of the type

$$c_0 X^{(m)} + c_1 X^{(m-1)} + \ldots + c_m X + d_0 X^{(n)}(t-\tau) + d_1 X^{(n-1)}(t-\tau) + \ldots + d_n X(t-\tau) = f(t),$$

in which the value is called the delaying parameter [6], can serve as an example of differential equations with a delaying argument.

The theory of differential equations with a deviating argument is more complex than the theory of ordinary differential equations without deviations of the argument.

In the study of real systems with delaying effects as the initial approximation it is commonly assumed that the delay τ is constant. Despite this, such an examination is a step forward in comparison with a model of an "ideal" process, which is obtained if it is assumed that "triggering" of the system occurs instantaneously [16].

Differential equations with constant deviations of the argument are usually called differential-difference equations [11].

A differential-difference equation, like an ordinary differential equation, has an infinite set of solutions. The arbitrariness in solutions of the differential-difference equation is greater than for solutions of the ordinary differential equation. In order to eliminate the arbitrariness in the choice of solutions in the

latter case, in addition to the principal equation, there is stipulation of some additional conditions, with initial conditions at a single point most frequently being used for this purpose.

For differential-difference equations the stipulation of initial conditions at a single point with $t = t_0$ is inadequate: the initial conditions must be stipulated in the initial set $[t_0 - \tau, t_0]$, and a solution is sought only with $t \geqslant t_0$.

The principal methods for analysis and solution of differential equations with a delaying argument are given in [1, 4, 10, 16].

Now we will examine those regions of modeling of the ocean-atmosphere system where differential equations with a delaying argument can (or must) find a corresponding application.

First of all we note that the modeling of processes of interaction between the ocean and the atmosphere now meets with great difficulties. The latter also is attributable to the inadequate number of necessary observations and a poor knowledge of the laws of interrelationship of individual phenomena.

For these reasons the use of the classical equations of motion for describing the ocean-atmosphere system is often difficult. Under these conditions the "phenomenological" theory is assuming great importance. By this is meant such a formulation of the patterns in the region of the observed physical phenomena in which no attempt is made to reduce the described correlations to the general laws of nature lying at their basis, through which they could be understood [5].

For the reasons indicated above, in the practical investigation of different types of interactions between the ocean and the atmosphere it is rather common to use phenomenological models, unfortunately without an indication that they are phenomenological and without taking delaying effects into account.

Since, as was indicated above, the ocean-atmosphere system is characterized by the presence of such effects, in the formulation of the corresponding phenomenological models it is necessary to use equations with a delaying argument. Such is necessary in all cases when the dependence of the sought-for characteristics at a particular moment on their values (or the values of other variables) at one of the preceding moments is well expressed.

The satisfaction of this condition is especially necessary when formulating a model of the interrelationship of spatially separated regions connected by currents.

The presence of delaying effects, specifically, delays in the ocean-atmosphere system, can be described by differential equations with partial derivatives, which corresponds to its representation in the form of a system with distributed parameters. In solving these equations it is necessary to have recourse to a simplification involving approximation of a distributed system by a concentrated system.

In such an approximation, from the physical point of view reference is to the breakdown of the spatial region in which the distributed object is determined into an adequate finite number of small regions with averaging of the distributed parameters within each such region, that is, a representation of the system within each small region as a concentrated system. Thus, some interrelated system is

obtained from a series of concentrated systems. However, it must be remembered that this approach must be used with caution because distributed systems have a number of peculiarities which concentrated finite systems do not have or they cannot be adequately modeled.

For this reason with any approximation extremely important questions remain open: precisely to what extent does such a system represent a distributed system and in general is it possible to find any acceptable breakdown of the system into a finite number of concentrated systems which even approximately in a definite sense describes the properties of a distributed system?

It was demonstrated in [3] that the introduction of a delay block (with a constant lag time) into the block diagram of a model with concentrated parameters makes it possible to take into account the "distribution effect," which to one degree or another is characteristic of any real object. The mathematical description of the delay block is with a differential equation with a delaying argument.

In hydrometeorology differential equations with a delaying argument are not yet in use, although they, as already mentioned, more completely reflect the principal properties of the ocean-atmosphere system, in particular, the presence of an aftereffect in it.

As an example, we will examine the change in temperature of surface waters with time in the northern and southern parts of the northern half of the Atlantic Ocean. This region of the world ocean includes the Gulf Stream, North Atlantic, Canaries, Northern Trades and Antilles Currents (Fig. 1).

In the analysis which follows it is assumed that water temperature changes can occur only in the surface (active) layer with the thickness H. Below this layer the temperature is constant in time and space.

The change in the thermal state of waters in each of the regions is dependent on the masses of water entering into it and emerging from it, and also on the quantity of heat arriving from the sun and lost in radiation.

What has been said can be represented rather easily in the form of a model. Accordingly, the change in the thermal state of the active layer of waters in the northern part of the ocean area ΔQ_N during the time Δt, with allowance for the advection of heat with currents, heat losses as a result of radiation, heat receipts due to solar radiation and with the assumption of an equality of the velocities of the currents directed to the north and south, can be represented approximately by the equation

$$\Delta Q_N = cM_N \Delta X = -cm_{N\,\text{вых}} X \Delta t + cm_{N\,\text{вх}} k_N Y(t-\tau)\Delta t - AX'\Delta t + B_N \Delta t,$$

[BX = en(tering);
BbIX = em(erging)]

from which it follows that

$$\frac{dX}{dt} = -\frac{m_{N\,\text{вых}}}{M_N} X + \frac{m_{N\,\text{вх}}}{M_N} k_N Y(t-\tau) - \frac{A}{cM_N} X' + \frac{B_N}{cM_N}. \quad (1)$$

For the southern region similarly

[BX = en(tering); BbIX = em(erging)]

$$\frac{dY}{dt} = -\frac{m_{S\ вых}}{M_S} Y + \frac{m_{S\ вх}}{M_S} k_S X(t-\tau) - \frac{A}{cM_S} Y^4 + \frac{B_S}{cM_S}. \quad (2)$$

In the cited equations: X is water temperature in Kelvin in the north; Y is the same in the south; k_N, k_S are coefficients for taking into account the change in water temperature with its movement from one region to another. Usually during movement of the current from north to south k is greater than unity, with movement from south to north -- less than unity; $m_{N\ em}$, $m_{S\ em}$ are the masses of waters flowing from this region during the adopted unit time; $m_{N\ en}$, $m_{S\ en}$ are the masses of entering waters; M_N, M_S are the masses of the active layer of the ocean in the north and south respectively; A is a coefficient in the formula determining the quantity of heat lost by the mass M_N (or M_S) in the case of radiation from the entire area S during the adopted discreteness time unit (Δt);

$$A = \sigma S \Delta t,$$

where σ is the Stefan-Boltzmann constant; B is the receipt of heat from solar radiation. If it is assumed that the northern and southern halves have one and the same area S, then

$$B_N = s_N S \Delta t; \quad B_S = s_S S \Delta t,$$

where s_N, s_S are the mean solar constant for the northern and southern halves of the considered ocean area respectively; c is the specific heat capacity of water; τ is the delay.

After the linearization of the initial equations (1), (2), and also separation of variables and the introduction of new coefficients we arrive at the equation

$$\frac{d\zeta^3}{dt^3} + A_1 \frac{d\zeta}{dt} + A_2 \zeta - A_3 \zeta(t-\Delta) = 0;$$
$$\frac{d\eta^3}{dt^3} + A_1 \frac{d\eta}{dt} + A_2 \eta - A_3 \eta(t-\Delta) = 0, \quad (3)$$

where $\zeta = x - c_N$, $\eta = y - c_S$, x, y are the temperature anomalies in the north and south, equal to

$$x = X - T_x, \quad y = Y - T_y.$$

T_x, T_y are the mean temperatures in Kelvin in the north and south of the ocean area

$$c_N = \frac{-(m_3 n_1 + m_2 n_3)}{m_2 n_2 - m_1 n_1}; \quad c_S = \frac{-(m_1 n_3 + m_3 n_1)}{m_2 n_2 - m_1 n_1}; \quad \Delta = 2\tau;$$

$$A_1 = m_1 + n_1; \quad A_2 = m_1 n_1; \quad A_3 = m_2 n_2;$$

$$m_1 = a_1 + 4 a_3 T_x^3; \quad m_2 = a_2; \quad m_3 = -a_1 T_x + a_2 T_y - a_3 T_x^4 + a_4;$$

$$n_1 = b_1 + 4 b_3 T_y^3; \quad n_2 = b_2; \quad n_3 = -b_1 T_y + b_2 T_x - b_3 T_y^4 + b_4;$$

$$a_1 = \frac{m_{N\ вых}}{M_N}; \quad a_2 = \frac{m_{N\ вх}}{M_N} k_N; \quad a_3 = \frac{A}{cM_N}; \quad a_4 = \frac{B_N}{cM_N};$$

$$b_1 = \frac{m_{S\,вых}}{M_S};\quad b_2 = \frac{m_{S\,вх}}{M_N}\,k_S;\quad b_3 = \frac{A}{cM_S};\quad b_4 = \frac{B_S}{cM_S}.$$

We will demonstrate a way to analyze such equations. For this purpose we will examine the first equation in system (3) (as for the second analysis). We will investigate stability with the use of a D breakdown [1, 4]. In this case the characteristic equation has the form

$$z^2 + A_1 z + A_2 - A_3 e^{-\lambda z} = 0.$$

We introduce the variable $\theta = \Delta z$. Hence

$$\theta^2 + \alpha_1\theta + \alpha_2 - \alpha_3 e^{-\theta} = 0,$$

where $\alpha_1 = A_1\Delta;\ \alpha_2 = A_2\Delta^2;\ \alpha_3 = A_3\Delta^2.$

Assuming $\theta = i\omega$ and separating the real and fictitious parts, we obtain

$$-\omega^2 + \alpha_2 - \alpha_3\cos\omega = 0,$$

$$\omega\alpha_1 + \alpha_3\sin\omega = 0.$$

Here there are three parameters. It is inconvenient to have a D-breakdown in three-dimensional space. As a simplification of the investigation we will fix one of the parameters. We will assume that α_2 assumes a value equal to 2. This value is not random; it is obtained if one takes into account the most probable values of the coefficients entering into it and if τ is assumed equal to 3 years.

These values (α_2, τ) were computed using the data cited in [2, 8, 9, 13-15]. These studies give information on current velocity and the water masses transported by currents and also indicate the mean current temperatures.

The equations for the boundaries of the D-breakdown into the field of the coefficients α_1 and α_3 can be represented in the form

$$\alpha_1 = \frac{\omega^2 - \alpha_2}{\omega\cos\omega}\sin\omega,$$

$$\alpha_3 = \frac{\alpha_2 - \omega^2}{\cos\omega}.$$

The computed data are represented in Fig. 2a, in which the region of asymptotic stability is shaded.

For different points in Fig. 2a we found the temporal variability of temperatures X and Y on the basis of the initial equations (1), (2). It follows from the computations made that depending on the values of the coefficients entering into them there can be asymptotic stability of the system and instability. As a rule, in the temporal variability there is an oscillatory regime with an amplitude changing with time.

In conclusion we will demonstrate the possibility of practical application of the conclusions drawn above. We will illustrate the finding of the expression for predicting water temperature on weather ships which are latitudinally spaced but situated approximately in the same water flow.

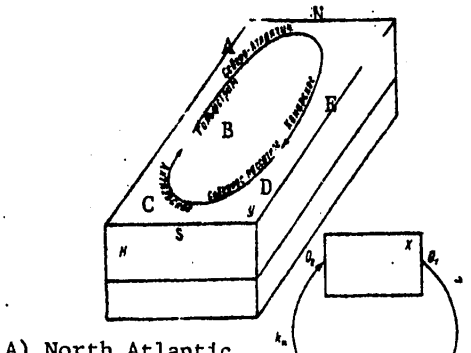

A) North Atlantic
B) Gulf Stream
C) Antilles
D) North Trades
E) Canaries

Fig. 1. Idealized scheme for principal anticyclonic circulatory system of northern half of Atlantic Ocean.

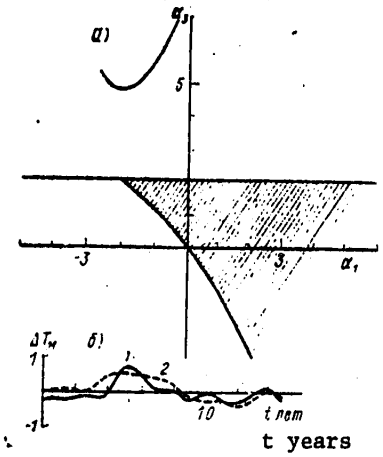

Fig. 2. D-breakdown into the field of coefficients α_1 and α_3 with $\alpha_2 = 2$ (a) and comparison of actual (1) and predicted (2) temperature anomalies (ΔT_M) on weather ship M (b).

In accordance with [1]

$$\frac{dX}{dt} = a_1X + a_2Y(t-\tau) - a_3X^4 + a_4.$$

After conversion to anomalies and subsequent linearization we have

$$\frac{dx}{dt} = -m_1x + m_2y(t-\tau) + m_3.$$

Introducing the ζ and η parameters, we obtain

$$\frac{d\zeta}{dt} = -m_1\zeta + m_2\eta(t-\tau).$$

The values of the coefficients used here (a_i, m_i), and also the ζ and η variables are given above.

If in equation (4) it is assumed that $\eta(t-\tau)$ is known, since this value is related to already elapsed time, then

$$\zeta = \frac{m_2\eta(t-\tau)}{m_1} + Ce^{-m_1t}.$$

In actuality it is assumed that C = 0, since with $\eta(t-\tau) = 0$ ζ must be equal to zero. With this assumption

$$\zeta = a\eta(t-\tau).$$

We will examine the use of this expression for predicting the mean annual water temperature on weather ship M using data from ship J. We recall that the coordinates of the first of these ships is 66.0° and 2.0°E; for the second -- 52.5°N and 20.0°W.

The τ value is determined from the maximum of the cross-correlation function for the above-mentioned ships. The corresponding computations show that $\tau \approx 4$ years.

The following expression can be used for determining a

$$a = \frac{\Sigma |\Delta M|}{\Sigma |\Delta J|},$$

where ΔM is the water temperature anomaly at weather ship M and ΔJ are similar values for ship J. Computations give a = 0.87. Hence, taking into account what has been said,

$$\zeta = 0{,}87\eta(t-4).$$

The results of computations using this formula are represented in the graph in Fig. 2b. It follows from the latter that there is a rather close correlation between water temperature in the region of weather ship J and ship M.

The principal conclusions which can be drawn from these investigations of the role of delaying effects can be reduced to the following:
1. The ocean-atmosphere system in many cases is a system with delaying effects.
2. Such effects exert a substantial influence on the development of the system with time and for this reason they must be taken into account in the modeling.
3. In the modeling of these effects it is best to use differential equations with a delaying argument.
4. An oscillatory regime can develop in the represented model of the interrelationship of the mean annual water temperature anomalies in the high and low latitudes of the world ocean.

BIBLIOGRAPHY

1. Besekerskiy, V. A. and Popov, Ye. P., TEORIYA SISTEM AVTOMATICHESKOGO REGULIROVANIYA (Theory of Automatic Control Systems), Moscow, Nauka, 1975.

2. Budyko, M. I., IZMENENIYA KLIMATA (Climatic Changes), Leningrad, Gidrometeoizdat, 1974.

3. Butkovskiy, A. G., STRUKTURNAYA TEORIYA RASPREDELENNYKH SISTEM (Structural Theory of Distributed Systems), Moscow, Nauka, 1977.

4. Voronov, A. A., TEORIYA AVTOMATICHESKOGO UPRAVLENIYA (Automatic Control Theory), Part 1, Moscow, Vysshaya Shkola, 1977.

5. Geyzenberg, V., "Role of Phenomenological Theories in a Theoretical Physics System," USPEKHI FIZICH. NAUK (Advances in the Physical Sciences), Vol 91, No 4 [year not given].

6. Gnoyenskiy, L. S., Kamenskiy, G. A. and El'sgol'ts, L. E., MATEMATICHESKIYE OSNOVY UPRAVLYAYEMYKH SISTEM (Mathematical Principles of Controlled Systems), Moscow, Nauka, 1969.

7. Guretskiy, Kh., ANALIZ I SINTEZ SISTEM UPRAVLENIYA S ZAPAZDYVANIYEM (Analysis and Synthesis of Control Systems With Delays), Moscow, Mashinostroyeniye, 1974.

8. Ditrikh, G. and Kalle, K., OBSHCHEYE MOREVEDENIYE (General Navigation), Leningrad, Gidrometeoizdat, 1961.

9. Duvanin, A. I., "Model of Interaction Between Macroprocesses in the Ocean and Atmosphere," OKEANOLOGIYA (Oceanology), Vol VIII, No 4, 1968.

10. Norkin, S. V., DIFFERENTSIAL'NYYE URAVNENIYA VTOROGO PORYADKA S ZAPAZDYVAYUSHCHIM ARGUMENTOM (Second-Degree Differential Equations With a Delaying Argument), Moscow, Nauka, 1965.

11. Rubanik, V. P., KOLEBANIYA KVAZILINEYNYKH SISTEM S ZAPAZDYVANIYEM (Oscillations of Quasilinear Systems With a Delay), Moscow, Nauka, 1968.

12. FIZICHESKIYE OSNOVY TEORII KLIMATA I YEGO MODELIROVANIYE: TRUDY MEZHDUNARODNOY NAUCHNOY KONFERENTSII. STOKGOL'M, 29 IYULYA-10 AVGUSTA 1974 (Physical Principles of the Theory of Climate and Its Modeling: Transactions of the International Scientific Conference. Stockholm, 29 July-10 August 1974), Leningrad, Gidrometeoizdat, 1977.

13. Khromov, S. P. and Mamontova, L. M., METEOROLOGICHESKIY SLOVAR' (Meteorological Dictionary), Leningrad, Gidrometeoizdat, 1974.

14. Shokal'skiy, Yu. M., OKEANOGRAFIYA (Oceanography), Leningrad, Gidrometeoizdat, 1959.

15. Shuleykin, V. V., FIZIKA MORYA (Marine Physics), Moscow, Nauka, 1968.

16. El'sgol'ts, L. E. and Norkin, S. B., VVEDENIYE V TEORIYU DIFFERENTSIAL'NYKH URAVNENIY S OTKLONYAYUSHCHIMSYA ARGUMENTOM (Introduction Into the Theory of Differential Equations With a Deviating Argument), Moscow, Nauka, 1971.

UDC 556.555.4(470.12)

METHOD FOR COMPUTING THE THERMAL DIFFUSIVITY COEFFICIENT OF BOTTOM DEPOSITS OF LARGE SHALLOW-WATER LAKES (IN THE EXAMPLE OF LAKE KUBENSKOYE)

Moscow METEOROLOGIYA I GIDROLOGIYA in Russian No 4, Apr 81 pp 85-92

[Article by S. M. Shishkayev, candidate of technical sciences, and A. N. Yegorov, candidate of geographical sciences, Limnological Institute USSR Academy of Sciences, manuscript received 15 Jul 80]

[Text]

Abstract: In the example of Lake Kubenskoye the authors have formulated physical and mathematical models of formation of the temperature profile in the bottom deposits of large shallow-water lakes. Computations were made of the coefficients of effective thermal diffusivity of bottom deposits during periods of summer heating and summer-autumn cooling in 1973 and 1974. It is shown that during the cooling period of a water body, in the presence of a temperature maximum situated in the depths of the mass of bottom deposits, there is an intensification of heat transfer in comparison with the period of heating of the water body. The detected effect is related to the migration of the water component in porous water-saturated ground.

In this article an attempt is made to develop an experimental-theoretical method for determining the thermal diffusivity coefficient and also make a quantitative evaluation of the postulated temporal variation of this parameter in porous water-saturated ground of a large shallow water body. Use is made of data from in situ temperature measurements in the thickness of the thermally active layer of ground for periods of summer heating and autumn cooling.

During the period of autumn cooling of a shallow water body it can be found that as a result of the rapid cooling of the upper layers of bottom deposits the temperature maximum will move into the depths of the bottom deposits. In a layer of some thickness the temperature of the lower layers will be greater than in the above-lying layers. Under such conditions in the porous water-saturated bottom material there can be a convective transfer of heat caused by the migration of the water component.

In the example of Lake Kubenskoye we will examine the factors exerting an influence on the thermal regime of the bottom material in a relatively small water body.

Formulation of Physical Model of the Processes of Forming of the Temperature Field in Bottom Deposits of Large Shallow-Water Lakes

1. We will assume that all the changes in the temperature regime of bottom deposits occur only by means of heat exchange with the water mass of the lake. In other words, a change in atmospheric conditions is reflected initially in the temperature of the water mass and the latter directly determines the formation of the temperature field of the bottom material.

2. We will neglect the influence of geothermal heat and also the migration of ground water. We exclude the direct incidence of solar radiation on the surface of the bottom material.

3. In this formulation of the problem we will assume that in the bottom deposits there are no additional heat sources, such as of a biological nature.

4. The heat flow in the bottom deposits will be considered unidirectional and having only a vertical component.

5. We will assume that the coefficient of effective thermal diffusivity a_{eff} is constant within the limits of each of the considered periods of heating and cooling of the water body and is dependent neither on the coordinate (depth at which the layer is situated) nor on time.

Validation of Formulation of Boundary Condition

In accordance with the first assumption the condition at the boundary of the contact of bottom deposits with the water mass of the lake must be stipulated in the form of a third-order boundary condition:

[B = water]
$$x = 0; \quad -\lambda \frac{\partial T}{\partial x} = \alpha (T_{x=0} - T_{в}). \tag{1}$$

Here λ is the thermal diffusivity coefficient for bottom deposits, α is the coefficient of heat exchange between the ground and the water mass; $T_{x=0}$ is the temperature at the surface of the bottom deposits; T_{water} is the temperature of the water mass.

The x coordinate is reckoned from the surface of the bottom deposits into the depth of the bottom material.

From the formulated boundary condition we find the temperature difference between the water mass and the surface of the bottom deposits:

[B = water]
$$T_{в} - T_{x=0} = \frac{\lambda}{\alpha} \frac{\partial T}{\partial x} = \frac{\lambda}{\alpha} \frac{T_{x=0} - T_{x=H}}{H} = \frac{T_{x=0} - T_{x=H}}{\mathrm{Bi}}. \tag{2}$$

Here $T_{x=H}$ is the temperature at the depth H of the so-called thermally neutral layer; Bi is the BIO criterion, determining the ratio of the intensity of heat transfer from the surface of the bottom material into the water to the intensity of heat transfer in the bottom deposits within the limits of the thermally active layer.

We will agree that the thermally active or active layer of bottom deposits is that in which there are seasonal temperature fluctuations. Accordingly, the depth at which the thermally neutral layer is situated determines the upper boundary of the layer in which there is a virtual absence of seasonal temperature fluctuations, at least within the limits of the time periods considered below. As demonstrated by temperature measurements in the bottom deposits, for Lake Kubenskoye it can be assumed that the depth at which the thermally neutral layer H is situated is 3 m.

A quantitative evaluation of the order of magnitude of the BIO criterion, made in accordance with the formulas in [3], shows that $Bi > 150$. Without making a major error, on the basis of experimental measurements of temperature in the bottom deposits of Lake Kubenskoye it can be assumed that $|T_{x=0} - T_{x=H}| < 20°C$.

Using expression (2) we find that within the limits of the total error in measuring the temperature of bottom deposits the temperature of the surface of the bottom material coincides with the temperature of the water mass of the lake.

It is important to note that in the formulation of the mathematical model a boundary condition of the third kind degenerates into a boundary condition of the first kind, when it is necessary to stipulate not the intensity of heat exchange α, but the temperature variation at the surface of the bottom deposits. It was established that the latter virtually coincides with the temperature of the water mass in the lake.

It is also known that in relatively shallow large water bodies of the Lake Kubenskoye type, as a result of wind mixing of the water body and turbulent free convection, homothermy is observed in the depth of the water mass.

As a result, we come to the conclusion that the variation of the temperature of the surface of bottom deposits necessary in the formulation of the problem coincides with the variation of water mass temperature.

Mathematical Formulation and Solution of the Problem for the Thermally Active (Active) Layer of Bottom Deposits

Proceeding on the basis of a physical model of the process, in general form we cite a mathematical formulation and solution of the problem of formation of the temperature field in bottom deposits.

The equation for heat propagation in the bottom material is:

$$\frac{\partial T}{\partial t} = a_{эфф} \frac{\partial^2 T}{\partial x^2}, \qquad (3)$$

where T is temperature; t is time; x is a coordinate directed from the surface of the bottom material into the depth of the mass of bottom deposits; a_{eff} is the effective thermal diffusivity coefficient.

The temperature distribution in the ground at the time used as the origin of reckoning is:

$$t=0; \quad T=f(x). \tag{4}$$

The variation in temperature at the surface of the bottom deposits, coinciding, as was demonstrated, with the variation of temperature of the water mass in the lake is:

$$x=0; \quad T=\varphi(t). \tag{5}$$

The condition for the constancy of temperature at the depth H of the thermally neutral layer is:

$$x=H; \quad T=\text{const}. \tag{6}$$

A solution of the problem (3)-(6), obtained with use of the finite integral transforms method [2], was obtained in the following form:

$$T=\frac{2}{H}\sum_{n=1}^{\infty}\left\{\int_0^t \frac{a_{эфф}\,\pi n}{H}\left[\varphi(\xi)-(-1)^n T_H\right]\exp\left[-a_{эфф}\left(\frac{\pi n}{H}\right)^2\times\right.\right. \tag{7}$$

$$\left.\left.\times(t-\xi)\right]d\xi+\left(\int_0^H f(x)\sin\frac{\pi n}{H}x\,dx\right)\exp\left[-a_{эфф}\left(\frac{\pi n}{H}\right)^2 t\right]\right\}\times$$

$$\times\sin\frac{\pi n}{H}x.$$

With a known value a_{eff} and definite initial and boundary conditions solution (7) determines the temperature field T = f(x, t) in the bottom deposits in dependence on the depth of the layer x and time t.

Expression (7) can also be used for solving the inverse problem of determining the coefficient of effective thermal diffusivity of the bottom material. The direct purpose of this study is a determination of a_{eff}. For this it is first necessary to stipulate the temperature distribution in the bottom material f(x) in the initial condition (4) and the temperature variation at the surface of the bottom deposits (t) in the boundary condition (5), or, as is the same, the variation of the mean mass water temperature in the lake.

The function f(x) was determined in analytical form on the basis of direct measurements of temperature in the bottom material of Lake Kubenskoye, carried out by one of the authors of this study in the course of expeditions of the Limnological Institute USSR Academy of Sciences [4].

The function $\varphi(t)$ was stipulated on the basis of the known variation of mean ten-day temperatures of the water mass in Lake Kubenskoye [1].

With stipulated initial and boundary conditions, and also with a distribution of temperature at the end of the considered period of time, also known from direct measurements, using expression (7) it is easy to determine the a_{eff} value.

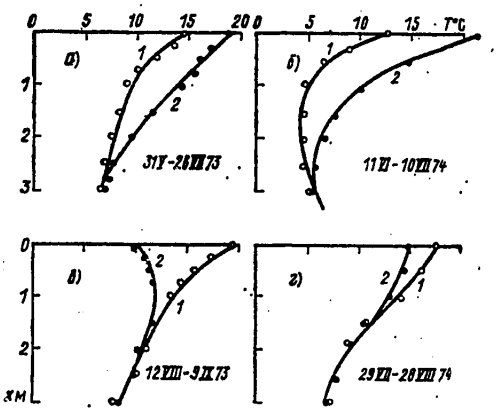

Fig. 1. Temperature profiles in bottom deposits of Lake Kubenskoye. a, b) periods of heating, c, d) periods of cooling.

In actuality, the left-hand side of expression (7) in such a case is known and the a_{eff} value with any prestipulated error is found by trial and error and by comparison of the right- and left-hand sides of equation (7) by solution of the direct problem.

For the purpose of clarifying the possible seasonal change in the thermal diffusivity coefficient of bottom deposits we will determine a_{eff} in periods of heating and cooling of Lake Kubenskoye arbitrarily selected taking into account available experimental data: for 1973 we examined the period of heating from 31 May through 26 July and then a period of cooling from 12 August through 9 September; during 1974 -- the period of heating from 11 June through 10 July and the period of cooling from 29 July through 28 August. In order to evaluate the possible influence of free convection on the intensity of heat transfer in the bottom deposits the periods of cooling were selected in such a way that in one case there was a temperature maximum in the bottom deposits situated at some depth from the surface (period of cooling 12 August 1973 - 9 September 1973), and in the other case the maximum temperature was situated near the surface of the bottom (period of cooling 29 July 1974-28 August 1974).

Figure 1 shows the results of direct temperature measurements in the bottom deposits of Lake Kubenskoye during the above-mentioned periods of time in dependence on the depth x at which the layer is situated. The x coordinate is reckoned from the surface of the bottom material into the depths of the mass. The index 1 denotes the initial temperature distribution and 2 denotes the final temperature distribution in the

bottom deposits in each of the considered periods.

For each of the periods we will determine in analytical form the initial temperature distribution in the ground f(x) and the variation of water temperature $\varphi(t)$.

Period of heating (31 May - 26 July 1973)

$$f(x) = 14{,}8 - 8x + 2{,}4x^2; \quad 0 < x < 1{,}5 \text{ м};$$

$$f(x) = 9{,}9 - 1{,}13x; \quad 1{,}5 < x < 3 \text{ м};$$

$$\varphi(t) = 14{,}8 + 0{,}37t - 5{,}32 \cdot 10^{-3} t^2; \quad 0 < t < 56 \text{ days}.$$

Period of cooling (12 August - 9 September 1973)

$$f(x) = 19{,}4 - 7{,}8x + 2x^2; \quad 0 < x < 1{,}5 \text{ м};$$

$$f(x) = 16{,}3 - 2{,}73x; \quad 1{,}5 < x < 3 \text{ м};$$

$$\varphi(t) = 19{,}4 - 0{,}29t - 1{,}78 \cdot 10^{-3} t^2; \quad 0 < t < 28 \text{ days}.$$

Period of heating (11 June - 10 July 1974)

$$f(x) = 12{,}8 - 17{,}6x + 9{,}6x^2; \quad 0 < x < 0{,}5 \text{ м};$$

$$f(x) = 9 - 6{,}4x + 2{,}4x^2; \quad 0{,}5 < x < 1{,}5 \text{ м};$$

$$f(x) = 4{,}6 - 0{,}3x + 0{,}2x^2; \quad 1{,}5 < x < 3 \text{ м};$$

$$\varphi(t) = 12{,}8 + 0{,}42t - 4{,}35 \cdot 10^{-3} t^2; \quad 0 < t < 29 \text{ days}$$

Period of cooling (29 July - 28 August 1974)

$$f(x) = 17{,}5 - 1{,}95x - 1{,}71x^2; \quad 0 < x < 1{,}25 \text{ м};$$

$$f(x) = 23{,}18 - 10{,}94x + 1{,}85x^2; \quad 1{,}25 < x < 3 \text{ м};$$

$$\varphi(t) = 17{,}5 - 9{,}33 \cdot 10^{-2} t; \quad 0 < t < 30 \text{ days}.$$

First we will compute the value of the effective thermal diffusivity coefficient of bottom deposits in Lake Kubenskoye during periods of heating and cooling in 1973.

The a_{eff} values are computed at those horizons for which there are experimental measurements of the temperature of bottom deposits. The results of computations of the temperature profile in the bottom deposits during the period of summer heating are given in Table 1.

It was found that with a stipulated initial temperature profile the finite distribution of temperature in the bottom deposits during the considered heating period is satisfactorily described by expression (7) if it is assumed that $a_{eff} = 2 \cdot 10^{-2}$ m^2/day.

Table 1 also gives computations of the temperature profile in the bottom deposits of Lake Kubenskoye during the period of summer-autumn cooling.

The considered period, as indicated in the figure, is characterized by the presence of a temperature maximum in the depths of the bottom deposits.

The computations show that it is possible to achieve a quite satisfactory correspondence between the experimental and computed temperature values in the bottom deposits during the considered cooling period if in the solution (7) it is assumed that $a_{eff} = 5 \cdot 10^{-2}$ m^2/day. At the same time, if during the considered cooling period $a_{eff} = 2 \cdot 10^{-2}$ m^2/day, then it is impossible to attain such a correspondence (values in parentheses).

A comparison of the values of the effective thermal diffusivity coefficients during the above-mentioned periods of heating and cooling indicates an intensification of heat transfer in the bottom deposits of Lake Kubenskoye during the period of cooling of the water body. As already noted, the most probable reason for this is the initiation of free convective heat transfer in porous water-saturated ground with the presence of a corresponding temperature profile in it, and specifically the presence of a temperature maximum situated at some depth from the bottom surface.

In order to confirm the results we made computations of the coefficients of effective thermal diffusivity for the periods of summer heating and autumn cooling of Lake Kubenskoye during 1974. The period of cooling of the water body in 1974 was characterized by the absence of a temperature maximum in the bottom deposits.

With such a temperature profile, in contrast to the period of cooling of 1973 considered earlier, the initiation of free convection in bottom deposits is impossible.

The results of the computations of the temperature profile in the bottom deposits of Lake Kubenskoye during the period of summer heating in 1974 and comparison with the experimentally determined temperature values at different horizons are given in Table 2.

As in computations made earlier for the period of summer heating of Lake Kubenskoye during 1973 the temperature distribution in the bottom deposits during the period of summer heating of Lake Kubenskoye in 1974 is also described quite well by means of expression (7) with a value $a_{eff} = 2 \cdot 10^{-2}$ m^2/day.

The results of computations of the temperature profile in the bottom deposits during the period of summer cooling of Lake Kubenskoye in 1974 are also presented in Table 2. The temperature values T_{comp} were computed for the purpose of comparison with two values of the coefficients of effective thermal diffusivity, and specifically with $a_{eff} = 2 \cdot 10^{-2}$ m^2/day and $a_{eff} = 5 \cdot 10^{-2}$ m^2/day (values in parentheses).

Table 1

Comparison of the Computed (T_{comp}) and Experimental (T_{ex}) Temperature Values in Bottom Deposits of Lake Kubenskoye on 26 July 1973 During Period of Heating (31 May-26 July 1973) and on 9 September 1973 During Period of Summer-Autumn Cooling (12 August-9 September 1973)

x m	T_{comp} °C	T_{ex} °C	x m	T_{comp} °C	T_{ex} °C
	Period of heating			Period of cooling	
0.5	16.8	16.4	0.5	11.7(13.0)	11.7
1.0	14.1	14.2	0.7	11.8	11.8
1.5	11.5	11.4	1.5	11.7(12.3)	11.7
2.0	9.5	9.6	2.0	10.8	10.7
2.5	7.9	7.6	2.5	9.7	9.6

Table 2

Comparison of Computed (T_{comp}) and Experimental (T_{ex}) Temperature Values in Bottom Deposits of Lake Kubenskoye on 10 July 1974 During Period of Summer Heating (11 June-10 July 1974) and on 28 August 1974 During Period of Cooling (29 July-28 August 1974)

x m	T_{comp} °C	T_{ex} °C	x m	T_{comp} °C	T_{ex} °C
	Period of heating			Period of cooling	
0.5	14.6	14.8	0.5	14.3(14.0)	14.3
1.0	10.1	10.1	1.0	13.0(12.8)	13.0
1.5	7.7	7.7	1.5	11.5(11.5)	10.8
2.0	6.5	6.5	1.9	9.0(8.8)	9.4
2.5	5.9	5.7	2.5	8.4(8.5)	7.8

FOR OFFICIAL USE ONLY

APPROVED FOR RELEASE: 2007/02/09: CIA-RDP82-00850R000400040041-8

Table 2 shows that computations of the temperature profile with a value $a_{eff} = 2 \cdot 10^{-2}$ m^2/day lead to a better correspondence of the computed and experimentally determined temperature values in bottom deposits than computations with $a_{eff} = 5 \cdot 10^{-2}$ m^2/day.

The result is easily explained from the point of view of the hypothesis expressed on the possible contribution of free convection to heat transfer in porous water-saturated ground. In actuality, the convective transfer of heat is possible only when there is a temperature maximum situated in the depth of the mass of bottom deposits. In the absence of such heat transfer within the framework of the considered mathematical model of the process there is a conductive (molecular) regime, regardless of what period (heating or cooling) is considered.

The proposed computation thus makes it possible to determine the value of the effective thermal diffusivity coefficient of bottom deposits of large shallow-water lakes within the framework of the formulated assumptions, using as a basis data from simple measurements of the temperature of bottom deposits.

In computing a_{eff} in each specific case it is necessary to evaluate the correctness of these assumptions. For example, a considerable nonuniformity of the structure of bottom deposits can lead to a dependence of the thermal diffusivity coefficient on the depth at which the layer is situated. In such a case the experimentally determined temperature profile of bottom deposits will differ appreciably from the computed profile obtained from a solution of the direct problem with a constant value of the thermal diffusivity coefficient.

In the first approximation it is possible to determine the error arising as a result of assumption of the vertical constancy of a_{eff}. In the case of a structure of bottom deposits uniform in depth in order to determine the thermal diffusivity coefficient it is sufficient to have data from temperature measurements at one horizon.

After determining the thermal diffusivity coefficient during the periods of heating and cooling of a water body it is possible, as demonstrated, to determine the presence or absence of a seasonal variation of this parameter. Allowance for the seasonal variation of the effective thermal diffusivity coefficient of bottom deposits is a reserve for increasing the accuracy of the evaluation of the heat supply in the bottom deposits of large shallow-water lakes.

In conclusion the authors take the opportunity to thank Doctor of Geographical Sciences V. N. Adamenko for constant attention to the work and valuable comments expressed during its discussion.

BIBLIOGRAPHY

1. GIDROLOGICHESKIYE YEZHEGODNIKI (Hydrological Yearbooks), T. O., Nos 2, 3, 5-7, Arkhangel'sk, 1975.

2. Grinberg, G. A., IZBRANNYYE VOPROSY MATEMATICHESKOY TEORII ELEKTRICHESKIKH I MAGNITNYKH YAVLENIY (Selected Problems in the Mathematical Theory of Electrical and Magnetic Phenomena), Moscow, 1948.

3. Kutateladze, S. S. and Borishanskiy, V. M., SPRAVOCHNIK PO TEPLOPEREDACHE (Handbook on Heat Transfer), Moscow, Gosenergoizdat, 1958.

4. Tikhomirov, A. I. and Yegorov, A. N., "Thermal Regime and Heat Reserves," OZERO KUBENSKOYE (Lake Kubenskoye), Part I, GIDROLOGIYA (Hydrology), Leningrad, 1977.

UDC 551.5:63

DIRECTIONS IN RESEARCH FOR THE PURPOSE OF SUPPLYING THE NATIONAL ECONOMY WITH AGROCLIMATIC INFORMATION

Moscow METEOROLOGIYA I GIDROLOGIYA in Russian No 4, Apr 81 pp 93-102

[Article by I. G. Gringof, candidate of biological sciences, and L. S. Kel'chevskaya, candidate of geographical sciences, All-Union Scientific Research Institute of Agricultural Meteorology, manuscript received 10 Jul 80]

[Text]

Abstract: the article outlines the principal means for carrying out agroclimatic research for the purpose of supplying the national economy with agroclimatic information. It is proposed that systematic supply of information be ensured by the creation of a USSR State Agroclimatic Survey.

Agroclimatic information is assuming ever-greater importance in solution of practical problems in the development of agriculture in our country.

At the present time the basis for agrometeorological data for the USSR State Committee on Hydrometeorology is inadequately informative for the support of the national economy at a high technical level. In particular, the lack of agrometeorological data on technical carriers precludes the use of electronic computers for the processing, analysis, generalization and output of different types of agroclimatic information, supporting scientific research and the broad servicing of organizations important in the national economy.

The manual preparation of materials for the publication of agroclimatic scientific reference literature does not favor its rapid appearance and affords no possibility for using observational data of recent years and also limits the set of agroclimatic parameters and their generalization in space and time.

Earlier published reference-regime materials have been based on observational data only for the 1960's and series of observations through 1972 have been used only for the reserves of productive moisture [23]. Agrometeorological observations for the most part are short series (7-20 years), and in individual years they are nonrepresentative for a number of reasons. The methodology for the processing of such observation series has not been adequately investigated, first because specifically

such a problem has not been posed before agroclimatologists. Second, for most agrometeorological elements and their complexes no study has been made of the patterns of temporal and spatial variability, which makes impossible the use of the statistical and mathematical methods for their description. In the literature there are generalized studies relating directly to the methods of agroclimatic processing of data [5, 10], but they do not completely correspond to modern scientific and technical requirements.

Many studies have been published which have been devoted to the creation of new methods for the collection, processing, analysis and generalization of hydrometeorological information in general by means of an electronic computer, as well as the problems involved in the accumulation and storage of this information on technical carriers. Many studies have also been published on the automated processing of agrometeorological information [3, 4, 8-12, 15, 18-22, 24 and others]. However, the entire experience of creating an automated agrometeorological data system and its prospects have been discussed only in [11]. It was demonstrated in this study that in the majority of the enumerated studies there was formulation and solution of special problems in the automation of agrometeorological computations, checking of data and the output of individual tables. Only two studies have been raised in part to the level of practical applications [3, 8].

There are also serious gaps in investigations devoted to the agroclimatic regime of different territories: there is a lack of complex agroclimatic characteristics as well as inadequate development of agroclimatic recommendations for the optimum distribution of agricultural crops over the country, agroclimatic support of major meliorative measures, etc.

Serious difficulties also arise as a result of a shortage of agrometeorological information obtained in the system of the State Committee on Hydrometeorology and for evaluating agroclimatic resources. Accordingly, the need arises for employing information from different institutes of the USSR Agriculture Ministry and the USSR Academy of Sciences on the yields and strain testing of crops, quantities of applied fertilizers, soil quality, etc. This information, not constituting a unified state archives, is used only sporadically, for carrying out individual studies. The general agreement between the Main Administration of the Hydrometeorological Service and the USSR Agriculture Ministry [5] includes only traditional forms of exchange of information, which does not to a full degree meet the increasing demands of the day. In this agreement, in particular, no provision is made for the output of the information necessary for the preparation of regime-reference literature.

Thus, as already noted in [6], the base of agrometeorological data, although quite broad, for the time being is poorly organized.

In connection with what has been said above, agroclimatology is faced with the problems involved in the optimum ways to carry out scientific investigations for the purpose of agroclimatic support of the national economy and for the corresponding distribution of available work and material resources within the framework of the State Committee on Hydrometeorology.

The task is as follows: correctly organize the agrometeorological base and reduce it to technical carriers, at the same time creating mathematical support for the effective use of this base. In addition, it is necessary to carry out a search for fundamentally new methods for the interpretation of agroclimatic data in a form convenient for direct use in practical work [6].

The problem of more effective use of scientific personnel and material resources involves the development of an optimum structure for carrying out a complex of investigations in the field of agroclimatology, taking into account their great practical significance. The following points should be considered necessary: programmed coordination of investigations, their systematic and complex nature, and also automation of the processes of collection, processing and analysis of agrometeorological information and the creation of norm-setting and reference literature on the agroclimatic regime. The implementation of this program is possible within the framework of an agroclimatic survey of the USSR, the creation of which is provided for simultaneously with the development and introduction of an automated system for the collection, processing and checking of agrometeorological information [6].

The adoption of a resolution by the State Committee on Hydrometeorology on the creation of an agroclimatic survey of the USSR was determined by the All-Union Conference on the Development of Research in the Field of Agroclimatology and Improvement in the System for the Support of Agriculture With Data on Agroclimatic Resources (Moscow, April 1979).

The Administration for Hydrometeorological Support of the National Economy of the State Committee on Hydrometeorology proposed a draft of the structure of an agroclimatic survey of the USSR in which it was pointed out that the USSR agroclimatic survey will be a systematized, constantly supplemented summary of information on the agroclimatic resources of a territory.

At the same time it should be noted that an agroclimatic survey is not only a passive summary of agrometeorological information (on soil moisture content, phenology, agrohydrological properties of soils), but also the production of specialized works, the handbooks AGROKLIMATICHESKIYE RESURSY OBLASTI (Agroclimatic Resources of the Oblast) and the atlas-monographs KOMPLEKSNAYA AGROKLIMATICHESKAYA KHARAKTERISTIKA TERRITORII (Complex Agroclimatic Description of a Territory), containing specific recommendations on the use of agroclimatic resources. Thus, the survey calls for investigations which cannot be made by the user, who has only passive information. This creates a definite complexity in carrying out an agroclimatic survey in comparison with climatic and water surveys [25 and others].

The goals of an agroclimatic survey are quite extensive and include the scientific support of complex planning of agricultural production of the country and also the use of a systematic approach and analysis directly in the implementation of scientific research in the field of agroclimatology and the organization of these investigations in the system operated by the State Committee on Hydrometeorology. These goals are also outlined in the program for long-range scientific research in the field of applied climatology.

Thus, the creation of a USSR agroclimatic survey provides for a thorough agroclimatic support of agencies concerned with the national economy, to an equal degree taking in production and individual branches of science, furnishing them with appropriate information.

The survey will be used in the following:
-- in current and long-range planning of the development of agriculture;
-- in the distributing of productive forces over the territory of the country;
-- in the planning of the multisided use of agroclimatic resources for increasing the productivity of agriculture and its effectiveness;
-- in developing measures for the rational use of favorable agroclimatic conditions and the rational overcoming (lessening) of the effect of unfavorable agroclimatic conditions;
-- in the exploitation of sown agricultural areas;
-- in the development of new methods for agrometeorological observations and the implementation of scientific investigations in all aspects of agrometeorology;
-- in predicting changes in agrometeorological and agroclimatic conditions;
-- in solving problems related to the production, upgrading and processing of agricultural production.

The solution of the enumerated problems within the framework of the USSR agroclimatic survey is possible in a case if its creation is accomplished in a system which is unified for the entire country. Moreover, since the information obtained by other departments is a component part of the survey, the need arises for including materials on the creation and implementation of the USSR agroclimatic survey as among the most important subjects. Thus, on the one hand, the direction for implementation of the agroclimatic survey as a state document is defined, but in this connection it is desirable that its name be made more precise: "USSR State Agroclimatic Survey (USSR SAS)"; on the other hand, the overall organizational structure of its creation and implementation is outlined, that is, the USSR SAS implementation should be assigned to the USSR State Committee on Hydrometeorology and Enovironmental Monitoring (agroclimatic information). However, other ministries are to ensure the collection of additional information necessary for the creation of the survey. For example, the Agriculture Ministry should provide information on the yields of agricultural crops, the USSR Academy of Sciences -- on the quality of soils, cartographic information, etc., and the State Inspectorate on Strain Testing of Agricultural Crops -- on the yield of standard varieties of agricultural crops, on varieties to be introduced and on promising varieties in agreement with and in accordance with the model of the survey.

Next we must consider the following specific characteristics of support of the national economy with agroclimatic information. The use of survey data in planning the multisided use of agroclimatic and natural resources for increasing the productivity of agriculture, and also for other purposes will be effective in a case when the agroclimatic resources, in combination with natural resources, will be considered as the integrated "Agroclimate - Agricultural Production" system. This is one of the important and new directions in research for the purpose of ensuring the availability of agroclimatic information, governed by a number of factors.

First, traditional agrometeorology has recently substantially broadened the subject matter with which it deals. Whereas earlier studies were made of individual factors, such as frosts, droughts, heat supply, moisture supply, etc., now there is a tendency to investigate a series of interrelated factors constituting whole formations -- systems and structures. Examples of this are the models "weather-yield" [22], "weather-soil-yield" [16] and others.

Agroclimatic conditions as a system can be studied not only using mathematical models, but also by means of atlas-monographs, which are also models. Agroclimatic and natural resources are modeled in a system of atlas maps, combined by sections. The unity of the sections is ensured by their subject matter.

Second, at the present stage new disciplines have been developed which make it possible to investigate agroclimatic systems: the theory of information, the theory of image recognition, etc.

Third, at the present level of development of the sciences systems analysis is widely introduced in any research. In implementing the survey atlas-monographs will become a means for systems analysis of the natural complex. More details will be given about this below.

Programmed coordination in creation of the USSR SAS provides for a clear organizational structure, a unified program and a methodological base, as well as a centralized coordination by the creation and implementation of the survey at a union-wide scale.

Since up to the present time there is no rigorous and clear-cut system in creating regime-reference literature in the field of agrometeorology, the first stage in research should be work on creating a draft of the USSR State Agroclimatic Survey. First of all it is proposed that the following problems be solved:
-- analysis and generalization of earlier investigations on the creation of regime-reference literature and the automated processing of agrometeorological data;
-- determination of the volume of finalized agrometeorological research;
-- determination of the types and volume of information necessary for preparing survey reference materials;
-- development of an automated system for collection, accumulation, analysis, generalization and output of agroclimatic information for the parts of the survey to be published and not to be published;
-- development of the fundamental principles, structure and content of the part of the survey to be published;
-- development of the organizational structure for implementing the survey;
-- development of methods for creating and implementing the survey;
-- development of models of reference manuals and atlas-monographs;
-- development of stages in priority scientific research necessary for creating a survey.

The preliminary structure of the part of the USSR SAS, proposed by the Administration for Hydrometeorological Support of the National Economy of the State Committee on Hydrometeorology, contains the following publications.

Structure and Periodicity of Publications to be Published by USSR SAS

Name of publications	Periodicity of publications
Series 1. Annual Data	
Agrometeorological Yearbook, Nos 1-35	Published annually for preceding year.
Series 2. Five-year data	
Agrometeorological Conditions for Formation of the Yield of Agricultural Crops Over the Territory of the USSR During a Five-Year Period	Published once in five years.
Series 3. Long-term data	
Agroclimatic Resources of Oblast, Kray, Republic	Published once in 20 years.
Agroclimatic Atlas-Monographs. Individual agroclimatic characteristics:	One-time publications.
Part I. Soil Moisture Content. Mean long-term probabilistic characteristics of reserves of productive moisture in soil under main agricultural crops (including atlas of maps).	Published once in 20 years.
Agrohydrological properties of soils, Nos 1-34	Published once in 20 years.
Part II. Phenology. Phases of development and state of main agricultural crops (including atlas of maps)	One-time publications.

Notes. In conformity to the coordinated resolution of the USSR State Committee on Hydrometeorology and Environmental Monitoring and USSR Agriculture Ministry there can also be other publications of materials from the agroclimatic survey not provided for in this structure.

A debatable point in the survey structure is the periodicity of the publications. For example, the need for republishing the handbook "Agroclimatic Resources of an Oblast" in the years immediately ahead is dictated not only by the lengthening of the agrometeorological series by 15-20 years and the inclusion of anomalous years (1972, 1975, 1976), but also a reexamination of the model relative to its information content.

We have proposed a generalized structure of the USSR State Agroclimatic Survey, taking into account the development of an automated system for creating a bank of agroclimatic data and the proposals of a number of institutes of the State Committee on Hydrometeorology (USSR Hydrometeorological Center and others) (Fig. 1).

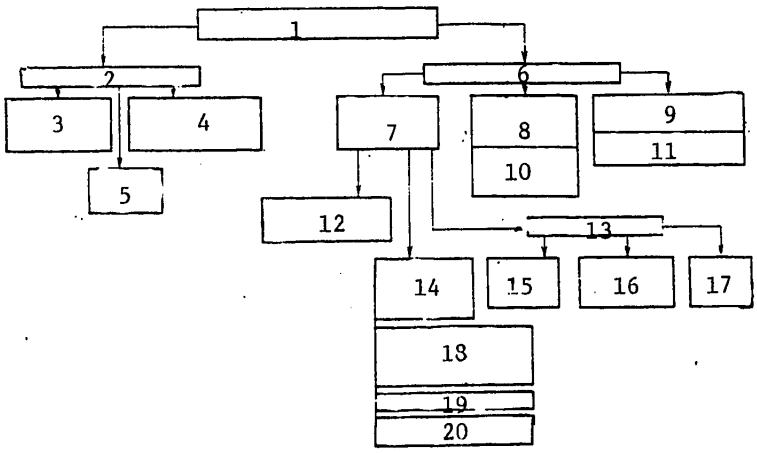

Fig. 1. Draft of structure of "USSR State Agroclimatic Survey."

KEY:

1. USSR State Agroclimatic Survey (SAS SSSR)
2. Part not to be published
3. Banks of agrometeorological data
4. Mathematical support (methods and programs)
5. Catalogues and dictionaries
6. Part to be published
7. Series 3. Long-term data
8. Series 2. Five-year data
9. Series 1. Annual data
10. Agrometeorological conditions for five years
11. Agrometeorological Yearbook, Nos 1-34
12. Agroclimatic resources of oblast, kray and republic
13. Atlas-monographs
14. Individual agroclimatic characteristics
15. Territory of USSR
16. Territory of economic regions
17. Oblast, kray, republic
18. Part 1. Moisture content and agrohydrological properties of soils
19. Part 2. Phenology
20. Part 3. Conditions for the wintering of winter crops

The unpublished part of the survey includes only some subsystems of the entire automated information system, specifically:

-- mechanized archives of agrometeorological data on long-term technical carriers which are centrally prepared at the union and regional centers (information base of survey -- IB SAS USSR);
-- dictionaries and catalogues, that is, specialized reference-catalogue materials for ensuring the automatic recovery and classification of information available in the information base of the survey;
-- methods and computer programs for the exploitation of data banks, that is, mathematical support of the processing, recovery and output of survey information.

The priority task in the organization of work on the unpublished part of the survey is the preparation of a long-range plan for creating an information base of the data bank (IB DB USSR Agroclimatic Survey), in accordance with which the work of the published part of the survey will be coordinated.

The principal organizational tasks in the preparation of the published parts of the survey involve a study of the requirements on agroclimatic information on the part of its different users, development of models of reference-regime literature and methods for their preparation.

At the State Committee on Hydrometeorology definite experience is already available in the preparation of a number of reference publications on the agroclimatic regime and on the development of an automated system for the collection and processing of agrometeorological information. However, the atlas-monographs will be produced for the first time. There are no such publications in related branches of science nor in other countries, except for the agricultural atlas-monograph of the world [26]. Although the maps of this atlas were compiled using a small number of elements, the publication is unique.

The importance and direction of research for the purpose of creating cartographic scientific-reference literature in agroclimatology was already noted in our earlier article [14]. Accordingly, in this article it is desirable to discuss in greater detail the cartographic publications of the survey and examine their proposed content.

What exactly are atlas-monographs, their importance and purposes?

Agroclimatic atlas-monographs constitute a complex evaluation of agroclimatic and natural resources of a territory, as was noted in [1].

The scientific basis for evaluating the agroclimatic resources of different territories is a recognition of the patterns of natural complexes. Maps make it possible to clarify these patterns. Accordingly, atlases are not only the scientific basis for the planning of agricultural production, but also a scientific method for investigating the spatial variability of natural complexes.

For an overall evaluation of the natural and climatic conditions the following maps are provided for in the atlas: landscape, vegetation, soils, hydrographic, water volume in rivers, ground water, agriculture, climatic and climate-forming factors important for the evaluation of agroclimatic resources (radiation balance, temperature regime, precipitation, dangerous hydrometeorological phenomena, etc.).

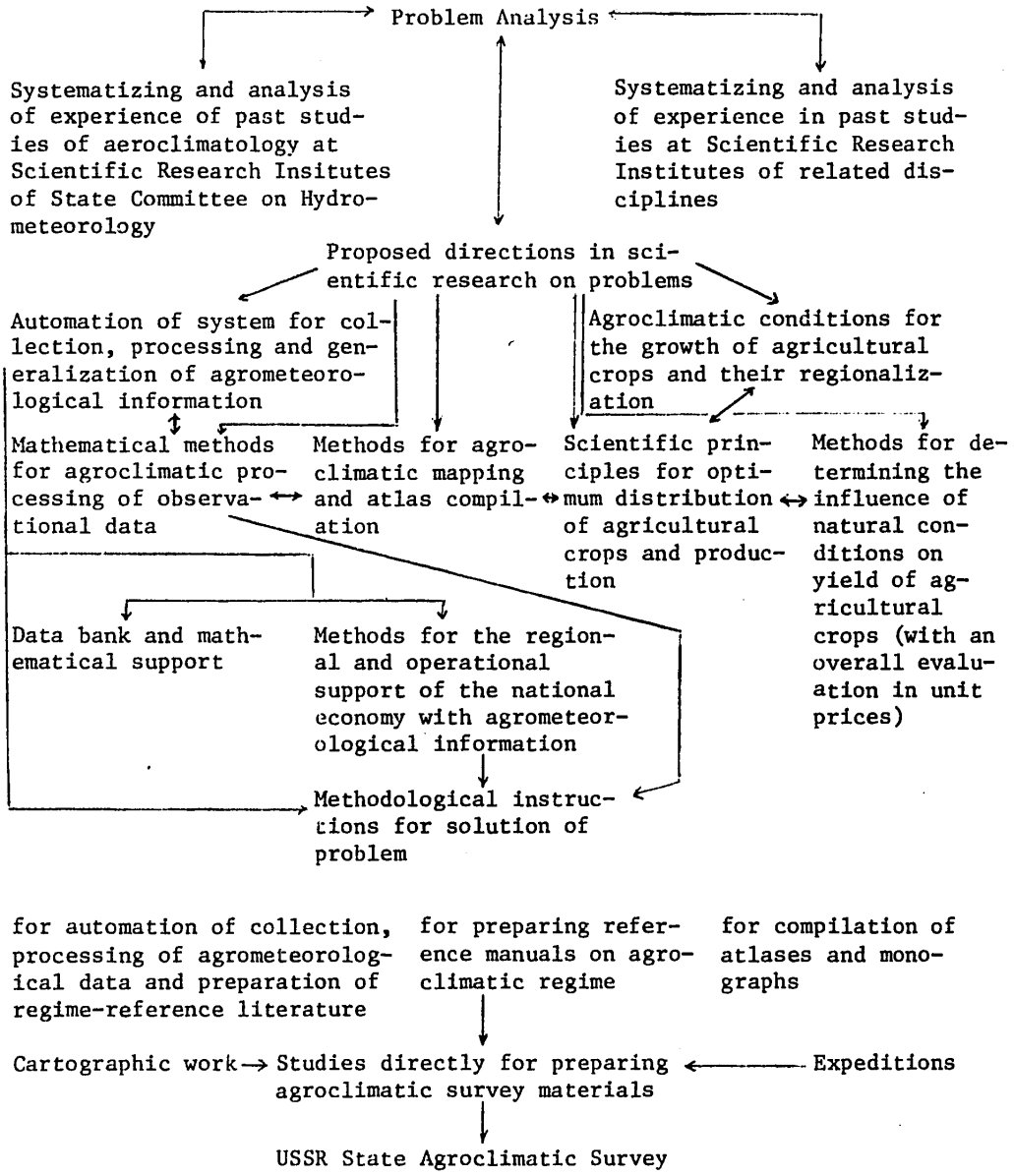

Fig. 2. Diagram of structure of complex of investigations in field of agroclimatology for effective support of national economy with scientific agrometeorological information.

Then an evaluation of agroclimatic resources is given: map of agroclimatic regionalization and agroclimatic elements and their complexes (photosynthetically active radiation, sums of active and effective temperatures, complex moistening index, and others). This is followed by sections on the agroclimatic resources for the cultivation of agricultural crops by groups: grains, industrial crops, fiber, vegetable and melon crops, root crops and tubers, fruit and berry crops, pastures and hay.

In order to evaluate the agroclimatic resources for the cultivation of crops a complex of maps will be compiled for characterizing the heat supply of early-, intermediate- and late-maturing varieties of crops, their supply with reserves of productive moisture by 10-day periods and the principal phases of development, and an agrohydrological regionalization map; the conditions for crop development are characterized by a series of phenological maps. In addition, this same section includes evaluation, recommendation and prognostic (probabilistic) maps. The recommendation maps include maps of the optimum times for the sowing and planting of crops, etc. The evaluation maps include those with an evaluation of the productivity of climate, that is, maps of the regionalization of a crop by productivity, taking into account the principal climatic factors, soil fertility and level of agricultural engineering. The prognostic maps will be maps of the potential yields of crops, which will become the basis for the programming of optimum yields. A map of economic stimulation of plant cultivation as a function of agroclimatic conditions will also be of exceptionally great importance.

Maps of the prognostic type can also include maps of the probabilistic characteristics of the factors most important for agricultural production (soil moisture, unfavorable weather phenomena, etc.).

The monograph accompanying the atlas will give climatic and agroclimatic descriptions, descriptions of maps and digital data, as well as recommendations on the use of the agroclimatic resources of a territory against the background of the natural complex, a description of the possibilities of taking into account and contending with dangerous or unfavorable weather and climatic phenomena.

In order to supply agroclimatic information for agricultural production for territories at all levels the atlas-monographs should be produced for the country, economic regions, republics and oblasts.

The differences in multisided agroclimatic characterization of territories are related to the specifics of content, the choice of agroclimatic indices and scale.

Thus, the agroclimatic atlas includes a system of maps which are organically interrelated and which supplement one another. Accordingly, in such an atlas there will be reflection of the entire "Agroclimate - Agricultural Production" system. This is its scientific and methodological sense, that is, the atlas will be a systems analysis tool. No such an analysis has been made in agroclimatology.

It must be noted once again that the scientifically sound implementation of agricultural production and the collection of stable yields of cultivated crops is possible when there is a detailed and thorough investigation of agroclimatic conditions against a background of other components of the natural complex [1].

On this basis the development of recommendations and optimum variants of use of climatic resources in agriculture is becoming realistic.

In the successful implementation of work for the creation of the USSR State Agroclimatic Survey the most proper approach, in our opinion, is the programming of the practical use of the results of studies of the All-Union Scientific Research Institute of Agricultural Meteorology and other scientific research institutes through the USSR State Agroclimatic Survey in accordance with the scheme shown in Fig. 2.

The central place in the scheme is occupied by problem analysis, constituting a set of definite procedures (expert evaluation, informative, mathematical-statistical and cartographic models, etc.), making it possible to solve a number of problems. The most important of these are: clarification of the problems, finding the most realistic and optimum methods for solving them, choice of the best variant of investigations, foreseeing of results, etc. In our opinion the subject of problem analysis is partially covered in this article.

Since no studies have been made in the field of agroclimatic survey on a modern technological basis, in this article it does not seem possible to set forth a developed organizational structure for implementing the survey. This problem can be considered after a preliminary coordination of the organizational structure in different instances at the USSR State Committee on Hydrometeorology, USSR Agrilculture Ministry and the USSR Academy of Sciences. But in general, it must be said that the implementation of the survey must be carried out on a national (interdepartmental) basis with the organizational forms following from this.

****

BIBLIOGRAPHY

1. Brodskiy, Ye. G., Gringof, I. G., Kogay, N. A. and Muminov, F. A., "Multisided Agroclimatic Characterization of Central Asia," TRUDY SARNIGMI (Transactions of the Central Asian Scientific Research Hydrometeorological Institute), No 67(148), 1979.

2. Vakulenko, A. V. and Zhukov, V. A., "Informational Support and Structure of the 'Agrometeorologiya' Data Bank," TRUDY IEM (Transactions of the Institute of Experimental Meteorology), No 11(79), 1977.

3. VREMENNYYE METODICHESKIYE UKAZANIYA PO MASHINNOY OBRABOTKE I KONTROLYU DANNYKH GIDROMETEOROLOGICHESKIKH NABLYUDENIY (Interim Methodological Instructions on Computer Processing and Monitoring of Data From Hydrometeorological Observations), Obninsk, No 11, Part I, Section 2, 1971.

4. Gayvoronskaya, L. S. and Turbayevskaya, N. K., "Algorithm for the Processing of Agrometeorological Information," TRUDY GIDROMETTSENTRA SSSR (Transactions of the USSR Hydrometeorological Center), No 1, 1967.

5. GENERAL'NOYE SOGLASHENIYE MEZHDU GLAVNYM UPRAVLENIYEM GIDROMETSLUZHBY PRI SOVETE MINISTROV I MINISTERSTVOM SEL'SKOGO KHOZYAYSTVA SSSR (General Agreement Between the Main Administration of the Hydrometeorological Service of the Council of Ministers and the USSR Agriculture Ministry), Moscow, GIMIZ, 1975.

6. Gringof, I. G. and Khvalenskiy, Yu. A., "Principal Results and Long-Range Prospects for the Continued Development and Improvement of the Agrometeorological Investigations at the All-Union Scientific Research Institute of Agricultural Meteorology," TRUDY VNIISKhM (Transactions of the All-Union Scientific Research Institute of Agricultural Meteorology), No 1, 1980.

7. Gulinova, N. V., METODY AGROKLIMATICHESKOY OBRABOTKI NABLYUDENIY (Methods for the Agroclimatic Processing of Observations), Leningrad, Gidrometeoizdat, 1974.

8. Zhukov, V. A., Tomin, Yu. A. and Grintsevich, L. M., "Automated System for the Processing of Regime Agrometeorological Information," TRUDY IEM (Transactions of the Institute of Experimental Meteorology), No 1(50), 1973.

9. Zhukov, V. A., "Automated Monitoring of Agrometeorological Information," TRUDY IEM, No 1(60), 1973.

10. Zhukov, V. A. and Velichko, N. N., "Some Problems in the Automation of Output of an Agrometeorological Yearbook," TRUDY IEM, No 1(50), 1973.

11. Zhukov, V. A. and Tomin, Yu. A., "Status and Prospects for Automation of the Processing of Data From Agrometeorological Observations," TRUDY IEM, No 11 (79), 1977.

12. Zhukov, Yu. A., "Primary Monitoring of Data on Moisture Reserves in the Soil With the Use of an Electronic Computer," TRUDY IEM, No 13, 1969.

13. Kel'chevskaya, L. S., METODY OBRABOTKI NABLYUDENIY V AGROKLIMATOLOGlI (Methods for the Processing of Observations in Agroclimatology), Leningrad, Gidrometeoizdat, 1971.

14. Kel'chevskaya, L. S., "Basic Directions in Investigations for Creating Cartographic Scientific Reference Literature in Agroclimatology," TRUDY VNIISKhM, No 1, 1980.

15. KOD DLYA SOSTAVLENIYA PERVICHNOY I ITOGOVOY AGROMETEOROLOGICHESKOY INFORMATSII KN-21M (Code for Compiling Primary and Summary Agrometeorological Information -- KN-21M), Leningrad, Gidrometeoizdat, 1970.

16. Konstantinov, A. V., POGODA, POCHVA I UROZHAY OZIMOY PSHENITSY (Weather, Soil and Yield of Winter Wheat), Leningrad, Gidrometeoizdat, 1978.

17. MATERIALY XXV S"YEZDA KPSS (Materials of the Twenty-Fifth Congress CPSU), Moscow, Politizdat, 1976.

18. Mel'nik, Yu. S., "Experience in Computing the Correlation Between the Yield of Sunflower and Moistening Conditions on a High-Speed Computer," METEOROLOGIYA I GIDROLOGIYA (Meteorology and Hydrology), No 11, 1963.

19. Mel'nik, Yu. S., "Criteria in Checking Data on the Height of Sunflowers With the Automated Processing of Data," TRUDY NIIAK (Transactions of the Scientific Research Institute of Aeroclimatology), No 51, 1969.

20. Novikov, A. G., "Some Problems in the Objective Analysis of Agrometeorological Information and Prediction of the Moisture Supply of Spring Wheat," TRUDY IEM (Transactions of the Institute of Experimental Meteorology), No 8, 1969.

21. Novikov, A. G., MEKHANIZIROVANNAYA OBRABOTKA DANNYKH AGROMETEOROLOGICHESKIKH NABLYUDENIY PRI AGROKLIMATICHESKIKH ISSLEDOVANIYAKH: METODICHESKOYE POSOBIYE (Mechanized Processing of Data From Agrometeorological Observations in Agroclimatic Research: Methodological Handbook), Moscow, Gidrometeoizdat, 1966.

22. Sirotenko, O. D., Boyko, A. P. and Abashina, Ye. V., "Development of Theoretical Investigations in Agrometeorology," TRUDY VNIISKhM, No 1, 1980.

23. SREDNIYE MNOGOLETNIYE I VEROYATNOSTNYYE KHARAKTERISTIKI ZAPASOV PRODUKTIVNOY VLAGI POD OZIMYMI I RANNIMI YAROVYMI ZERNOVYMI KUL'TURAMI (Mean Long-Term and Probabilistic Characteristics of Supplies of Productive Moisture Under Winter and Early Spring Grain Crops), Vol 1, edited by L. S. Kel'chevskaya, Leningrad, Gidrometeoizdat, 1979.

24. Tomin, Yu. A., "Problems in the Microfilming of Agrometeorological Information," TRUDY IEM, No 1(60), 1973.

25. Cherkavskiy, S. K., "State Inventory of Waters and Their Use in Hydrological Computations and Forecasts," METEOROLOGIYA I GIDROLOGIYA, No 9, 1973.

26. WORLD ATLAS OF AGRICULTURE, Printed in Italy by I. G. D. A., Novara, 1969.

UDC 551.(507.362+506.24)

REMOTE SENSING OF THE ATMOSPHERE FROM SATELLITES DURING THE FGGE PERIOD

Moscow METEOROLOGIYA I GIDROLOGIYA in Russian No 4, Apr 81 pp 103-111

[Article by K. Ya. Kondrat'yev, corresponding member USSR Academy of Sciences, Main Geophysical Observatory, manuscript received 16 Sep 80]

[Text]

Abstract: This is a review of the results of remote sensing of the atmosphere during the FGGE period, including the two principal directions in remote sensing: reconstruction of the wind vector field on the basis of cloud movement registered by means of processing of successive images of the cloud cover obtained using geostationary satellites; reconstruction of the vertical profiles of temperature and humidity on the basis of data from spectral measurements of outgoing radiation from satellites in polar orbits. The article briefly examines the results of stratospheric sensing for the purpose of reconstructing both structural parameters and composition of the stratosphere. Data are given characterizing the accuracy of different remote sensing methods. The preliminary results of satellite observations of the earth's radiation balance are discussed.

Remote sensing of the atmosphere from satellites has made a very important contribution to the collection of a global mass of information during the FGGE period. The purpose of this article is a review of the results of remote sensing based on materials from a symposium on the preliminary results of the FGGE held within the framework of the COSPAR congress of 2-14 June 1980 at Budapest.

The exceptionally important contribution to the mass of FGGE data made by satellite data on the wind and pressure makes necessary a careful analysis of the reliability of methods for reconstructing the temperature and wind fields and the value of satellite data for numerical weather forecasting. A large group of reports was devoted to a discussion of these matters: V. Sharov and G. Ganev (Bulgaria), F. Rakotzi and E. Kovach (Hungary), T. Tantser and D. Hegedyush (Hungary), N. Eigenwilling and H. Fischer (West Germany), F. Mosher (United States) and N. Kodaira (Japan).

Considerable attention was devoted to an examination of the methods and the results of reconstruction of the wind field. Although the processing of successive images obtained using geostationary satellites is in principle simple, existing processing methods are extremely diversified: from manual to completely automated computer processing.

F. Rakotzi and E. Kovach proposed a new variant of automated processing with monitoring by an operator, using images from the "Meteosat" in a direct transmission regime and which were then subjected to photometric measurements for the purpose of obtaining matrices of the brightness fields. The automated choice of tracer clouds was accomplished by selecting image sectors with a brightness contrast exceeding a stipulated threshold value. The suitability of the method was illustrated in the example of processing a series of five images for 25 November 1979 relating to a sector of the Atlantic Ocean with the coordinates 38-48°N, 12-24°W. This sector was broken down into sections measuring 200 x 100 km, for each of which the wind velocity vector was reconstructed. The vertical tie-in of data was accomplished using the results of aerological sounding at one point situated within the limits of the considered sector. The following data characterize the wind velocity values and standard deviation (SD) for different times:

Greenwich Mean Time	0900-1000	1000-1130	1130-1230	1230-1330
Wind velocity, m/sec	19	23	24	26
SD	4.96	5.00	6.50	6.50

N. Kodaira (Japan) described an interactive automated method for the processing of data for the Japanese geostationary meteorological satellite (GMS) for reconstructing the wind vector (WV) fields and the altitude of the upper cloud cover boundary (AUCB). This method relies on the choice of a tracer cloud by the operator and subsequent automated computer processing for the purpose of reducing the errors associated with the choice of the tracers and evaluation of the emissivity of clouds in reconstructing the WV and the AUCB. The processing of data from the "Himawari" geostationary meteorological satellite was made difficult by a malfunction causing an inclination of the satellite axis by 1.6°. However, the use of surface landmarks for the precise geographical tie-in of images made it possible to check the position of the axis of rotation with an accuracy to about 0.01°, which approximately corresponds to the instantaneous field of view of the IR channel of the scanning radiometer. The initial material in discriminating clouds and the underlying surface (or the cloud cover layer situated below) was two-modal histograms of the brightness temperature T_B, computed for squares with a side of 85 km (17 x 45 image elements) and clearly revealing two modes, which correspond to cloud cover at a high altitude and the underlying surface.

For an objective separation of the modes the empirical threshold value $T_B = T_S - A$ (T_S is the temperature of the ocean surface, A is a constant) is introduced. If values $T_B > T_S - A$ are excluded, a single-peak histogram remains, making it possible to determine the temperature of the clouds (the minimum measured T_B value is used for a vertical tie-in of the reconstructed wind field). In evaluating the emissivity e of clouds use is made of an empirical expression relating it to the type of clouds.

Table 1 gives the corresponding results. It is assumed that thin cirrus clouds are situated at the level of the tropopause. The temperature of the upper cloud boundary is determined by the values of the measured brightness temperature, reconstructed temperature of the ocean surface and cloud emissivity. The altitude of the upper cloud boundary (AUCB) is computed using the climatological vertical temperature profiles (mean monthly profiles for squares 5° in latitude x 5° in longitude). The AUCB is reconstructed both with large-scale averaging and with more detailed averaging -- for the region of Japan and adjacent seas. In the latter case the spatial resolution corresponds to a sector of 9 x 23 image elements and T_B is determined from the minimum measured values.

The principal source of errors in reconstructing the wind is the spatial noncoincidence of two successive images, used in computing the vector of movement of tracer clouds. The operator chooses the tracers on the basis of a visual analysis of the images appearing on three display screens for the visible and IR channels, represented in a black-and-white variant and in conventional colors.

Table 1

Emissivity of Clouds of Different Types (T -- Thin, I -- Intermediate, D -- Dense)

Cloud type	Dense cirrus	Altostratus			Altocumulus			Cumulus			Stratocumulus			Stratiform		
		T	I	D	T	I	D	T	I	D	T	I	D	T	I	D
Emissivity, %	60	-	70	90	50	80	90	80	90	100	30	70	90	60	80	100

Two or three successive images are compared in this process. This makes it possible to take into account the dynamics of cloud cover for more reliable choice of a tracer. Simultaneously with the choice of the tracer (about 200 tracers are selected) an estimate is made of the corresponding emissivity. The movement of the tracers is calculated employing an electronic computer using the cross-correlation method. Two or three successive images are used for this purpose. With allowance for the parameters of the geostationary satellite orbit the reconstructed wind field is tied in to terrestrial coordinates. One of the methods for checking the quality of the reconstructed wind field is a comparison with rawin data. Different checking procedures are also used in each stage in the computer processing of data. Some differences in the regimes of functioning of satellite instrumentation and processing

Table 2

Determination of Quantity of Clouds for Individual Layers in Range 1000-300 gPa

Quantity of clouds	Layer, gPa				
	1000-850	850-700	700-500	500-400	400-300
	Critical relative humidity, %				
0.05	64	50	36	31	28
0.55	79	71	62	59	57
0.95	89	87	83	80	80

methods determine the timeliness of analysis of the comparability of wind fields reconstructed using satellite data. F. Mosher (United States) for this purpose used data relating to overlapping parts of the fields scanned by different satellites. The main reason for the noncomparability of the reconstructed wind vector fields is the lack of a precise spatial coincidence of successive cloud cover images, causing the appearance of systematic errors. Usually in processing FGGE data there was tracking of movement of reliably identified cloud cover sectors of 20 to 80 km for 30-90 minutes.

Most of the wind information at the lower level was obtained on the basis of tracking of the clouds over the ocean. Their characteristic spatial-temporal scales correspond well to the spatial-temporal resolution of satellite images. Clouds over the land usually are of a lesser size and are more dynamic, which makes difficult reconstruction of the wind field. However, in the case of American observation series there is some number of short-interval image series for the tropical regions allowing processing with a high spatial-temporal resolution.

The most important error in wind field data is associated with their altitudinal tie-in, which is usually accomplished using information on the IR brightness temperature of the upper cloud boundary and the vertical temperature profile for the reconstruction of the altitude of the upper cloud boundary (AUCB). Difficulties arise which in the case of cirrus clouds are associated with their nonblackness (need for taking cloud emissivity into account) and in the case of lower-level clouds with the fact that the movement of clouds characterizes the wind field at the level of their lower boundary, whereas IR data make it possible to reconstruct only the AUCB (an evaluation of cloud thickness is necessary).

An analysis of the results indicated that despite the absence of a standardized reconstruction method, the comparability of the wind fields was entirely satisfactory. In all cases of spatially coinciding wind vectors during the period 15 January-13 February 1979 the statistical characteristics of the discrepancy for pairs of geostationary meteorological satellites are close. An analysis of the systematic discrepancies led to the conclusion that the spatial mismatch of images generates errors not greater than 2 m/sec, except for data from the National Center of Environmental Satellites (United States), when the mean systematic discrepancy somewhat exceeds 3 m/sec (evidently the increase in error was caused by the use of manual matching of images). A comparison of the vertical tie-in of the wind fields revealed a systematic exaggeration of the level of tie-in by approximately 100 gPa in the case of processing of data from the Japanese geostationary meteorological satellite (in comparison with the other four geostationary meteorological satellites). This systematic discrepancy is probably associated with different methods for the vertical tie-in of the wind field.

N. Eigenwilling and H. Fischer (West Germany) presented the results of reconstruction of the wind field on the basis of tracking of the movement of nonuniformities in the distribution of water vapor on successive images in the band 6.3μm H_2O, obtained using the "Meteosat." It was found that water vapor "clouds" are quite conservative. The weighting function corresponding to the H_2O channel is rather broad and the level of its maximum varies in the temperate latitudes from 400 gPa (in summer) to 500 gPa (in winter). The processing of series of four images in three days revealed a good correspondence between the reconstructed wind field and synoptic charts. A quantitative comparison with radiosonde data gave a SD equal to 5 m/sec (wind velocity) and 16° (direction).

D. Raymond, et al. (France) made an attempt at reconstructing the field of vertical movements in the upper troposphere using data for the "Meteosat" channel 6.3μm, using for this purpose additional synoptic information on the jet stream. A representative series of reports was devoted to the method and results of atmospheric sounding for the purpose of reconstructing the vertical profiles of temperature, humidity and different gas and aerosol components of the stratosphere.

These investigations rely on the use of different experimental geometries: scanning in the nadir zone, atmospheric scanning near the horizon, "eclipse" experiments for determining the attenuation of solar radiation by the thickness of the atmosphere. A group of reports by Hungarian specialists (D. Molnar, R. Roth, M. Tsazar) examined the problems involved in evaluating the characteristics of the cloud cover on the basis of satellite data and the use of the results for determining the radiant heat influx.

D. Molnar proposed a method for reconstructing the altitude of the upper cloud boundary (AUCB) and the effective quantity of clouds (EQC) using data from a radiometer with selective modulation carried aboard the "Nimbus-5" satellite, relating to the channels 707.4 cm^{-1} (I_1) and 726.5 cm^{-1} (I_2) in the band 15μm CO_2 and the transparency window 11μm (I_3). The first two channels are suitable for the detection of tropospheric clouds of both the upper and lower levels, since the maxima of their weighting functions are situated near the levels 300 and 500 gPa. Computations of outgoing radiation for three channels (I_1, I_2, I_3), made on the assumption of a nondependence of the transmission of IR radiation by clouds on wavelength for different models of the atmosphere (in the case of one-layer cloud cover), indicated that in the temperate latitudes (30-60°N, 30-60°S) the value $s = (I_3 - I_2)/(I_2 - I_1)$ correlates well with the AUCB and EQC values. In the tropical and high latitudes a high correlation is observed for $s^1 = (I_3 - I_2)(I_2 - I_1)$; the regression coefficients for the stipulated latitude zone in both cases virtually do not have an annual variation. The processing of global data for the purpose of reconstructing the AUCB and EQC requires the use of only 176 regression coefficients. A comparison of the results of processing of data from a radiometer with selective modulation during five months of 1974 with data from aerological soundings, and also the images of the cloud cover from the "ESSA-8" satellite; revealed a systematic understatement of the reconstructed AUCB, but the discrepancies were usually very small. An important advantage of the considered method is the use of only the measured values of outgoing radiation in the absence of a need for computed estimates of any parameters. Also of great importance is the possibility of a simultaneous reconstruction of the AUCB and EQC.

R. Roth (Hungary) carried out statistical processing of television images of cloud cover from the "ESSA" satellites, reduced to digital form, for five years (1968-1972) for the purpose of obtaining the climatological characteristics of spatial-temporal variability of cloud cover in Europe and adjacent regions. The considered data relate to the zone 30-60°N in summer and in the cold half of the year occupy the zone 30-50°N with a longitudinal extent of 20°W-40°E. For each point in a 5° geographic grid the author computed the quantity of clouds, taking into account data in a radius 250 km relative to a grid point of intersection. The statistical characteristics of the climatology of the cloud cover are the mean monthly variability values, regional spatial structural functions and time structural functions for the grid points of intersection (in a time interval up to 15 days). The results make possible a detailed characterization of the peculiarities of the spatial-temporal variability of the cloud cover. For example, in winter in the high latitudes there is a great cloud cover stability. There are no significant contrasts between the land and the ocean: the regional structure of cloud cover is very uniform. The reverse situation (considerable differences in temporal dynamics of the cloud cover over the land and ocean) is characteristic for the low latitudes. The "land-ocean" contrast is manifested clearly during summer.

Whereas in the low latitudes over the ocean there is a strong variability, in North Africa there is an exceptionally stable cloud cover (this stability also extends into the Mediterranean Sea region), which is attributable to the northward propagation of the subtropical cyclone. In the high latitudes of the Atlantic Ocean the influence of the Icelandic Low determines the increase in the quantity of clouds and an increase in the stability of the cloud cover.

M. Tsazar (Hungary) proposed a method for reconstructing the type and quantity of clouds and also the altitudes of the upper and lower boundaries of the cloud cover, relying on the use of satellite images of cloud cover, data from radiation measurements and the results of aerological soundings. The quantity of clouds was reconstructed using an eight-layer model of the atmosphere on the basis of an analysis of satellite images ("ESSA-8") and data from aerological soundings for 1200 hours (GMT) for the period 20-30 April 1969 within the limits of the region 35-70°N, 30°W--40°E. The reconstruction method relies on determination of the empirical relationship between the quantity of clouds (data from satellite nephanalysis) and relative humidity (Table 2).

The thickness of the clouds (excluding cumulonimbus clouds) is determined from the geopotential values (radiosonde data) corresponding to the cloud cover boundaries. The availability of nephanalysis data, allowing an estimate of the quantity of clouds, made it possible, having information on the albedo of the "earth's surface-atmosphere" system A_S with a known quantity of clouds n, to compute the albedo of clouds: $A_C = A_S - (1 - n) A_0$, where A_0 is the albedo of the underlying surface. A nomogram was constructed representing isolines of outgoing radiation F, plotted in the coordinate system (A_0, n), clearly classifying the different types of clouds as determined by nonintersecting subsets of values (A_0, n, F). A method is proposed for recognizing the type of clouds. Estimates of the quantity and altitudes of the cloud boundaries can be used in computing the radiant influx of heat as a result of long-wave radiation.

The launching of an interferometer spectrometer (IS) on the satellites "Meteor-25, -28 and -29," carried out on the basis of cooperation of specialists in the GDR and the USSR, afforded possibilities for the further analysis of optimum conditions for reconstructing the vertical temperature profile (VTP). D. Spenkuch, W. Dohler and M. Guldner (GDR) discussed the influence exerted on the accuracy of reconstruction by the following factors: 1) instrument functions for different channels of radiometers used in thermal sounding; 2) choice of "optimum" channels in the band 15μm CO_2; 3) the role of the contribution of additional absorbing components of the atmosphere during reconstruction of the VTP.

The basis for the examination was spectra of outgoing radiation registered from the "Meteor-28" satellite with a nominal resolution equal to 5 cm^{-1}. The analysis of spectra in the region of the atmospheric transparency window 8-12μm, relating to different geographical regions, revealed a small variability of the contribution of selective absorption, which made it possible to draw conclusions on the possibility of use of a constant correction for absorption in the window governed by the lines. However, this correction was negligible for the ocean zone in the high latitudes (more than 60°), where there is a specific spectral variation of outgoing radiation. Confirmation was obtained for the conclusion drawn earlier that with a spectral resolution of about 20 cm^{-1} the intervals at 936 and 961 cm^{-1} are most transparent (in comparison with 899 cm^{-1}).

Averaging of the spectrum of outgoing radiation by intervals with a half-width of 150 cm^{-1}, corresponding to the VTP radiometer used on American meteorological satellites, indicated that in the zone of the high-latitude oceans (more than 55°) there are systematic discrepancies of brightness temperature T_B within the range from -0.4 to +0.5°C for broad channels in comparison with data for the channel 899 cm^{-1} with a width of 5 cm^{-1}. If it is taken into account that for this channel there are systematic discrepancies from 0.4 to 0.7°C relative to the most transparent channel 961 cm^{-1}, the total discrepancies in the case of broad channels attain -0.9 - -1.2°C if corrections are not introduced for the influence of thickness of the atmosphere.

Comparison of radiosonde data and the results of reconstruction of the VTP on the basis of data for 40 spectra with the use of different "optimum" combinations of spectral intervals (the statistical regularization method was employed) led to the conclusion that in all cases the results were very close (the only exception are the data from the VTP radiometer carried on the "Nimbus-5"). It must therefore be assumed that the problem of the choice of the "optimum" spectral intervals is primarily of academic interest. An increase in the width of the spectral intervals accomplished for the purpose of ensuring a higher signal-to-noise ratio in actuality does not provide advantages because in such a case the need arises for taking into account the additional absorbing components. Numerical modeling was carried out for the purpose of evaluating the influence of errors in determining the transmission functions on the accuracy in reconstructing the VP. The evaluations obtained with and without allowance for the contributions of H_2O and O_3 indicate that the use of "pure" CO_2 transmission functions leads to systematic errors in reconstruction of the VTP in the lower and middle troposphere, attaining -2°C. It is shown that with the use of the most reliable information on the transmission functions the systematic errors in reconstruction disappear. The random errors are associated primarily with incorrectness of the inverse problem.

As already noted, the main contribution of atmospheric remote sensing data to the global mass of FGGE data was determined by functioning of the American third-generation meteorological satellites TIROS-N and (in part) NOAA-6. It is therefore of special interest to ascertain the informational contribution of the data from these satellites in weather diagnosis and forecasting. W. Smith, et al. (United States) discussed the results of analysis of the three-dimensional fields of mass and moisture content reconstructed on the basis of data from the satellites TIROS-N (launched on 13 October 1978) and NOAA-6 (launched on 27 June 1979) with the use of spectral measurements of infrared and radiothermal outgoing radiation. Each of these satellites separately ensures the collection of global masses of data on the vertical profiles of temperature and humidity each 12 hours (thus, the simultaneous availability of two satellites made it possible to accumulate global masses of data each 6 hours).

The processing of data for their inclusion in the FGGE (level II-b) data mass was carried out by the National Service of Environmental Satellites with averaging for a grid with an interval of 250 km for the purpose of subsequent use of the reconstructed fields of mass and moisture content for analysis and numerical forecasting of large-scale atmospheric processes. However, for special observation periods (SOP) in the FGGE program processing also was carried out for a finer mesh with a 50-km interval. In the course of the FGGE the reconstruction method was regularly improved for the purpose of minimizing errors.

However, despite this, the global standard deviations (SD) of the values reconstructed from radiosonde data remained surprisingly stable from month to month, varying in the range 2-3°K with an increase in the SD both near the underlying surface (up to 4°K in the case of continuous cloud cover when the errors in reconstruction were maximum) and in the stratosphere. The examined SD to a considerable degree characterize the real variability of the atmosphere and caused a spatial-temporal noncorrespondence between satellite and radiosonde data. The actual reconstruction errors were less than the SD.

The results of an analysis of the global fields of the moisture content mass obtained using the following were compared: 1) only data from satellite remote sensing of the atmosphere; 2) maps routinely produced by the National Meteorological Center, taking into account all data from ordinary and satellite observations, but with the exclusion of satellite information over the continents. The assimilation of asynchronous data was accomplished during the time of one revolution (102 minutes). A comparison indicated that TIROS-N data ensure a reliable analysis of the fields of relative geopotential 100-500 gPa for processes on a synoptic scale and have an adequate spatial resolution. There is an especially good agreement of the analysis over the continents, where the initial masses of data are completely different. The use of a four-dimensional assimilation scheme is necessary for the effective use of asynoptic satellite information jointly with data from ordinary observations. In this connection a study was made of the desirability of using a Kalman filter. The use of the results of reconstruction of the profiles of temperature, humidity and geopotential with a high resolution with the use of interactive analysis of data and employing an electronic computer (Makaydas system) clarified the information yield of this type of results for a detailed study of the processes of a subsynoptic scale and the tracing of small-scale disturbances responsible for dangerous weather conditions in the temperate latitudes which cannot be analyzed using routinely produced low-resolution maps. Even under tropical conditions the considered data have adequate reliability for recognition of the structures of general circulation characterized by a low amplitude of temperature and geopotential. Thus, for example, the geopotential field 850-200 gPa was entirely reliable when the isolines are plotted each 30 m (this corresponds to a difference in mean temperature of the layer equal to 0.7°C).

D. Peak and D. Brownscombe (Great Britain) discussed the preliminary results obtained using instrumentation carried aboard the TIROS-N for remote sensing of the stratosphere on the basis of measurements of thermal radiation of the atmosphere in the horizon zone using a radiometer with pressure modulation (PMR). The maxima of the weighting functions of the PMR correspond to the levels 15, 5 and 1.5 gPa and the radiometric noise varies in the range 0.3-0.6 $W/(m^2 \cdot sr \cdot cm^{-1})$. Due to the leakage of gas present in the cell there is a drift of the maxima of the weighting functions in the course of PMR functioning. The reconstruction of the temperature profiles revealed an entirely satisfactory agreement with data from rocket measurements. Data for a period of 450 days reveals a strong variation of zonal and global mean brightness temperature values for the zone 65°N-85°S; this must be attributed to the influence of dynamic factors.

****

F. Taylor, et al. (Great Britain) described a sounding unit for the stratosphere and mesosphere (SMS) carried aboard the "Nimbus-7." This radiometer with pressure modulation accomplishes vertical and horizontal scanning (the latter is employed for using the Doppler effect for the purpose of "tuning" the channels to a definite level of the maximum of the weighting function). The SMS has nine channels: 15 μm (two channels in the CO_2 band used for the vertical tie-in of data, reconstruction of the temperature profile and deviations from local thermodynamic equilibrium -- LTE); 4-5μm (CO band); 4-5μm (NO); 2.7μm (H_2O); 25-100μm (H_2O); 7.7μm (N_2O); 7.7μm (CH_4); 4.3μm (CO_2 band, study of deviations from LTE). The channel 4-5μm (NO) was unreliable, since in the operational work there is a partial transformation of NO into NO_2. A meridional section of the temperature field of the layer 100-0.001 gPa was constructed. Deviations from LTE already begin to appear above 45-50 km. Their influence dominates at an altitude of 90 km. Fluorescence is observed in the band 4.3 μm during the daytime. Near the equator there is an increase in the ratio of the mixture with altitude to about 10^{-5} at an altitude of about 40 km (still higher the ratio of the mixture decreases). The reconstructed vertical profiles of nitrous oxide at different latitudes are given.

D. Gilly, et al. (United States) presented the results of reconstruction of the profiles of temperature, ozone concentration, water vapor, nitric acid and NO_2 gas in the stratosphere on the basis of data from a limb-type IR stratospheric sounding unit carried aboard the "Nimbus-7" and D. Russel and E. Remsberg (United States) discussed similar data for ozone and nitric acid vapor making it possible to construct global maps of the concentration of these components at different levels. The accuracy in reconstructing the ratios of the O_3 and HNO_3 mixture varies in the range 0.05-0.15 and 0.20-0.55 $mill^{-1}$ (by volume). The results agree well with data from balloon and rocket soundings.

H. Fischer (West Germany) undertook a comparison of the vertical profiles of the H_2O mixture, reconstructed using data from an IR limb-type sounding unit, with the results of direct balloon measurements. The increase in the ratios of the mixture observed near the level 30 km must be attributed to the formation of water vapor as a result of methane oxidation. In reconstructing the H_2O profile on the basis of data for the 6.3μm band it is important to have simultaneous reliable results of reconstruction of the temperature profile. Comparison with balloon data sometimes reveals very important discrepancies (including systematic). However, these discrepancies to a considerable degree can be attributed to the spatial-temporal noncorrespondence of satellite and balloon data. In the southern hemisphere the field of the water vapor mixing ratio was very uniform at different altitudes in the stratosphere.

D. Loville (United States) reviewed the results of satellite observations of the fields of concentration and total content of ozone. A comparison of satellite and surface data (Dobson spectrometers) for the FGGE revealed discrepancies attaining 5-6%. A comparison of global maps of the total content of ozone and temperature during the period of the strong stratospheric warming in January-February 1979 revealed a strong increase in O_3 content in late January near 80°N and then a rapid dropoff (at this same time there was a temperature decrease at the level 30 gPa). The global map of the total content of ozone, averaged using all available data, reveals variations in the range 200-400 dobson units. Subsatellite measurements of the vertical profiles of ozone concentration at Koln and other points, made by

A. Gazi (West Germany), gave a good agreement with data from the "Sage" satellite, intended for measurements of the content of small gas components and aerosol in the stratosphere. In particular, there was an entirely satisfactory agreement of the meridional profiles of total ozone content in March 1979.

P. McCormick (United States) analyzed the results of reconstruction of aerosol content in the stratosphere using data from "eclipse" measurements from the "Sage" satellite with a four-channel radiometer having channels at wavelengths 0.38, 0.55 and 0.6μm (ozone reconstruction) and 1μm (water vapor reconstruction). There is a strong variability in the content of stratospheric aerosol, especially in winter in the polar regions and after volcanic eruptions. In order to tie in data from remote sensing to the results of direct measurements subsatellite observations were organized at 11 points (the most important were two points situated in Greenland and in Alaska). The results agree well with data from lidar soundings. During a period of stratospheric warming (January-February 1979) in the region of the temperature minimum there was found to be variable aerosol clouds which persist over a period of 1-3 days. A similar phenomenon is observed in the high latitudes of the southern hemisphere. During the period of functioning of this instrumentation there were three volcanic eruptions: La Soufriere (April), Sierra Negra (December) and Saint Helens (June 1980). A seven-channel instrument is being prepared within the framework of the program of ERB research which will make it possible to reconstruct the content of different small gas components and aerosol in the stratosphere.

The prospects for improving the instrumentation on geostationary meteorological satellites, discussed by V. Suomi, provides for the preparation of a 12-channel filter radiometer for the purpose of accomplishing thermal and humidity remote sensing of the atmosphere. By 1990 plans call for the preparation of geostationary meteorological satellites with a triaxial orientation system which will carry a Fourier spectrometer (spectral resolution about 0.35; 0.7 or 2 cm^{-1}, depending on the scanning zone) for reconstructing the vertical temperature profile with an accuracy to about 1 K with a spatial resolution of 10 km.

An extremely productive session within the framework of the symposium on the results of the FGGE was devoted to the results of investigations of the earth's radiation balance. In a thorough report by T. Vonder Haar, et al. (United States), presented by E. Rashke (West Germany), due to the absence of the authors, there was a summarization of the results of observations of the earth's radiation balance (ERB) during the FGGE period. One of the masses of data on the ERB was obtained using wide- and narrow-angle scanning radiometers carried aboard the "Nimbus-7" satellite. The complex of actinometric instrumentation carried aboard this satellite also included a precision band radiometer for measuring the solar constant. The interpretation of data from scanning radiometers on geostationary meteorological satellites (GMS) also made it possible to carry out an analysis of the patterns of variability of the ERB with a high spatial-temporal resolution. Plans for the future provide for observations under the program for experimental study of the ERB, the implementation of which will begin in the mid 1980's, and the use of different space platforms from the "Spacelab" station to operational geostationary meteorological satellites.

Table 3

Summary of Results of Measurements of Solar Constant (SC)

Author	Platform	Year	Volume of data, number of series	Altitude, km	Mean correction, W/m^2		Reduced SC value, in W/m^2	Initial SC, in W/m^2
Vonder Haar	Explorer	1965	120 days	750	0	0		1389
Drummond,et et al.	B-578	1966-1967	6	13.0	80	5	1387±17	1359
Drummond, et al.	Convair-990	1967-1968	7	12.0	79	164	1387±19	1359
Krueger	Convair-990	1967	6	11.6	85		1372±24	1364
Danken, et al	Convair-990	1967	4	11.6	133		1377±40	1349
McNatt, et al.	Convair-990	1967	5	11.6	95		1375±30	1343
Kendall	Convair-990	1968	6	12.2	77	150	1373±14	1370
Kondrat'yev, Nikol'skiy	Balloon	1962-1967	12	28-34	35	10	1376±18	
Murcray	Balloon	1967-1968	4	31-35	24	4	1373±12	1339
Willson	Balloon	1969	1	36.0	14	0	1369±11	1366
Drummond	X-15	1967	1	78-81	0	5	1385±14	1361
Plamondon	Mariner-6, 7	1969	145 days	1-1.4 a.u.	0	0	1362±18	1352
Hickey	Nimbus-6	1975	180 days	1100	0	0	1388±14	1392
Hickey	Nimbus-6	1975	5	1100	0	14	1382±14	1381

Table 3 gives a summary of the results of measurements of the solar constant (SC) during recent years. The SC values indicated here have been reduced to the new pyrheliometer scale. The mean SC value based on all data is 1377±20 W/m^2 with a standard deviation (SD) 8 W/m^2. Averaging of the initial values leads to a mean value 1360 (14) W/m^2. Comparison with "Nimbus-7" data with respect to the SC indicates a possible small increase in the SC during the period from the minimum to the maximum of solar activity, which could be associated with darkening of the photosphere in the years of the activity minimum due to a decrease in sunspot number. Observations using a band radiometer carried aboard the "Nimbus-7" for the first time made it possible to trace the variability of the SC over a long period of time (similar observations were made on the "Solar Maximum Mission" satellite). An analysis of data for the first year of functioning of the "Nimbus-7" indicated that the SC was virtually constant: with an average value 1375.7 W/m^2 the solar constant was 0.99 W/m^2. Within the limits of stability of radiometer readings (±0.2%) there was no detectable trend or cyclicity. Only on about 15 August 1979, over the course of several days, was there registry of an appreciable decrease in the SC (about 0.3%), but this result requires checking.

Global maps of the ERB, albedo of the "earth's surface - atmosphere" system and outgoing radiation were reproduced on the basis of observational data for 48 individual months (1964-1977) for illustrating the known patterns of the planetary field of the ERB. In the southern hemisphere there is a wave structure of the ERB field (wave number about 3) whose nature requires further investigations. At the present time the key aspect of investigation of the ERB has become an analysis of the variability (especially interannual) of the ERB and its components. Global maps have been constructed showing the variability of the ERB and its components, which can be attributed to the influence of the annual variation (with separate allowance for the annual, semiannual and total periodicity). In the case of the ERB in latitude zones greater than 20° the contribution of the annual variation to variability is about 95%, but in the equatorial zone the leading role is played by the semiannual component.

Although there is a clearly manifested "mirror" relationship between the annual variation of albedo and outgoing radiation, the problem of a reciprocal compensation of the variability of ERB components requires further careful study. The noncompensating effect of such clouds as cirrus and low stratus clouds on components of the ERB can be of great climatological importance. Allowance for the annual and semiannual cycles in an analysis of outgoing radiation data will, in general, make possible a better explanation of the variability of outgoing radiation over the continents than over the oceans. In many cases the percentage of variability of albedo and outgoing radiation governed by the annual and semiannual variation is relatively small, dropping to values less than 50% (this applies, in particular, to the monsoon zone). In some cases there is an interannual variability of the ERB in a number of regions attaining 40 W/m^2.

Analysis of the annual variation of the mean monthly meridional ERB profiles separately for the continents and oceans made it possible to characterize heat transfer from the continents to the oceans in summer in the northern hemisphere and in the opposite direction in winter. The processing of data from geostationary meteorological satellites for the first time afforded a possibility for studying the patterns

of diurnal variation of the ERB and its components. Over the continents and some regions of the ocean the amplitude of the diurnal variation attains tens W/m^2. A detailed analysis of the spatial-temporal variability of the ERB and its components on the basis of data for the second special observation period (May-June 1979), relating primarily to the latitudes 60°S-60°N was made by K. Rao (United States) on the basis of data from the TIROS-N satellite. Comparison with data for the period 1974-1977 revealed differences which are partially attributable to changes in general circulation of the atmosphere.

A study by G. Ohring, et al. (Israel, United States) was of great importance for the theory of climate. On the basis of data from satellite observations of the earth's radiation balance (ERB) and its components for 45 individual months (results of measurements using scanning radiometers carried aboard the "NOAA" satellites) it was possible to obtain climatological evaluations of the degree of reciprocal compensation of the dependence of solar radiation Q absorbed by the "earth's surface-atmosphere" system, as well as outgoing radiation F, on cloud cover n. This dependence, characterizing the response of the ERB to the quantity of clouds, is determined by the parameter $\delta = \partial Q/\partial n - \partial F/\partial n = \partial R/\partial n$ (R is the radiation balance). It can be demonstrated that $\partial Q/\partial n = Q_0(A_c - A_0)$, where Q_0 is the exoatmospheric insolation; A_c, A_0 is the albedo of the system with a continuous cloud cover and with a cloudless sky. The processing of data on the ERB, carried out earlier by R. Sess, led to a value $\partial F/\partial n = -91$ W/m^2 for the northern hemisphere and an almost zero value $\delta = +2.6$ W/m^2 (in the southern hemisphere $\delta = -0.6$ W/m^2). It therefore followed that the ERB is not responsive to changes in the quantity of clouds, that is, an allowance for "cloud" feedback is not important. In some other studies it was found that $\partial F/\partial n \simeq 40$ W/m^2 and $\delta < 0$, which indicates a predominance of the response of Q to cloud albedo. The initial material for the new computations is time series of the mean monthly values Q and F for the points of intersection of a global grid 10° in latitude x 10° in longitude. The observational data were subjected first of all to processing for the purpose of excluding the influence of annual and semiannual cycles and also the long-term trend of Q and F. The measured system albedo A_s was used as an indicator of the quantity of clouds.

Analysis of the distribution $\partial F/\partial n$ and $\partial R/\partial n$ in the zone 60°S-60°N indicated that outgoing radiation is most sensitive to the quantity of clouds (from -60 to 90 W/m^2) in the low latitudes, which is attributable to the high upper boundary of equatorial cloud cover. In the zone of latitudes greater than 40° the $\partial F/\partial n$ usually vary in the observable range 0-30 W/m^2; there are significant deviations from zonality. The values of the horizontal and vertical gradients $\partial F/\partial n$ are comparable. In the entire considered latitude zone $\delta < 0$, that is, the effect of sensitivity of absorbed radiation to the albedo of clouds predominates. The maximum values δ = -100 - -125 W/m^2 are observed primarily in those regions of the oceans in the low latitudes where the response of outgoing radiation to the quantity of clouds is small, insolation is high and the surface albedo is low. In general, δ decreases with latitude to values -50 - -75 W/m^2 in the high latitudes.

In summarizing the results, it must be emphasized that the materials presented at the symposium were very informative and indicate that in a number of countries (especially in the United States and at the European Intermediate-Range Forecasts Center) energetic work is being carried out on the analysis and use of the mass of

FGGE data. The results indicate a successful, for the most part, completion of the FGGE. A decisive contribution to the global mass of data (especially in the southern hemisphere) was from satellite observations of three categories: a) remote temperature and humidity sounding of the atmosphere from the TIROS-N and NOAA-6 satellites, b) reconstruction of the wind field at two levels on the basis of the movement of clouds registered on successive images of the cloud cover from geostationary meteorological satellites (the experience of tracking "clouds" of water vapor on the basis of "Meteosat" data was also successful). In connection with the asynoptic character of satellite information great attention is being devoted to the improvement of four-dimensional assimilation methods. The effectiveness of assimilation methods is also of great importance for increasing the accuracy of data from satellite remote sensing, which still do not satisfy the required accuracy criteria.

UDC 551.(558.1+576.31+577.1)(265.6)(267)

THERMODYNAMIC CONDITIONS ACCOMPANYING CONVECTIVE CLOUD COVER AND PRECIPITATION NEAR THE EQUATOR (ACCORDING TO DATA FROM THE REGIONAL MONSOON EXPERIMENT (MONEX))

Moscow METEOROLOGIYA I GIDROLOGIYA in Russian No 4, Apr 81 pp 111-116

[Article by B. Ye. Peskov, candidate of geographical sciences, A. A. Zhelnin, candidate of physical and mathematical sciences, and A. B. Shupyatskiy, doctor of physical and mathematical sciences, USSR Hydrometeorological Scientific Research Center and Central Aerological Observatory, manuscript received 10 Jul 80]

[Text]

Abstract: The thermodynamic characteristics of the troposphere are examined in relation to convective activity and their diurnal variation in the neighborhood of the intertropical convergence zone along the southeastern shores of Asia in the winter of 1978-1979.

The conditions for the development of powerful convective clouds and precipitation have not been studied adequately. This is indicated by the contradictory nature of the information of the influence of even such fundamental factors as the instability of stratification of temperature and humidity in the troposphere and the convergence of wind velocity in the atmospheric boundary layer [1-6]. In many regions where convection is characterized by a great intensity and variability the atmospheric conditions nevertheless have not been investigated at all. Everything which has been said applies to places where MONEX work has been carried out near the equator, where exceptionally intensive cloud convection alternated with its weakening without appreciable changes in the stratification of temperature and humidity in the troposphere when there were small but important changes in divergence in the atmospheric boundary layer.

In this article we generalize some data from investigations carried out on Soviet scientific research ships in the winter of 1978-1979 near the intertropical convergence zone (ICZ) in the South China and Java Seas (polygons I and II), and also in the Indian Ocean (polygon III) at a distance of several hundreds of kilometers from Singapore.

Each polygon had the configuration of a triangle with vertices separated from one another by a distance of 400-500 km. The results of radiosonde observations and data on precipitation were averaged for three points in each polygon. This increased their reliability and comparability with areal radar data and the characteristics of large-scale horizontal divergence of wind velocity Div $\vec{V}$ and vertical

velocity w, computed using these same three points. In the interpolation of the aerological characteristics to the isobaric levels we used all the initial radiosonde data (isobaric surfaces, singularities, etc.).

An analysis of observations in polygons I and II revealed an exceptionally clear diurnal variation of climatic activity in zones distant 70-250 km from the shores of Kalimantan Island. Figure 1 shows the diurnal variation of the altitude of cloud tops H, maximum at each of the hourly times in the regions of two ships in polygon I with a radius of 50 km. The solid curve 1 shows the means of H_{max} for 12 days in December 1978 in the neighborhood of the southern point of polygon I with the coordinates 4°N and 111°E at a distance of about 200 km to the north of Kalimantan Island. The dashed curve 2 characterizes the mean 10-day H_{max} values in a region situated 100 km closer to Kalimantan. In both regions at about 0800 hours (LT) $H_{max} \gtrsim 10$ km. In the evening, however, after 1600 hours the convective clouds were 8-13 km lower, and as a rule after 2000 hours disappeared entirely at the first point.

The mean diurnal precipitation sums using data for 21 days are also given in Fig. 1 (rectangles enclosed in the solid line 3). A precipitation maximum in the morning hours and a minimum in the evening hours are clearly defined. A similar diurnal variation is characteristic of the horizontal convergence of wind velocity (Div $\vec{V} < 0$) at the sea surface, computed on the basis of hourly data (dashed rectangles) and the thickness of the tropospheric layer in which convergence was noted (dashed curve 8).

Judging from the diurnal variation curves at all levels, including those cited in Fig. 1, the diurnal variation of convective activity to the maximum degree is synchronized with the convergence of wind velocity in the lower layer of the troposphere. Small changes in instability energy can be significant for convection in the lower layers of the troposphere where its value is closest to zero [1].

Increased Div $\vec{V}$ values near the 200 gPa surface (the role of which is emphasized in [3]) were noted during a period of active convection, but the Div $\vec{V}$ maximum is displaced into the period of a dropoff in activity. The appearance of convergence and ascending movements in the layer 600-300 gPa also falls in this period, that is, occurs later than in the lower layers. It evidently follows from this that the noted processes in the upper troposphere, including increased divergence at the 200 gPa level, are caused by the development of convection.

A similar pattern of change in the diurnal variation of the altitude of the tops of convective clouds and precipitation against a background of weakened convective activity was noted in polygon II (southern point 0°S, 107.5°E, 250 km from the shores of Kalimantan and Sumatra, Table 1). The sum of precipitation here in the morning period was twice as great as in the evening period. There was a substantial change in convergence in the near-water layer (by $6 \cdot 10^{-6}$ sec^{-1}), the altitude of the layer of ascending movements in the lower part of the troposphere (from 870 to 980 gPa) and the sign of vertical movements near the condensation level (950-900 gPa). At the same time, the instability energy and the dew point spread were virtually identical. The temperature and absolute humidity were higher during

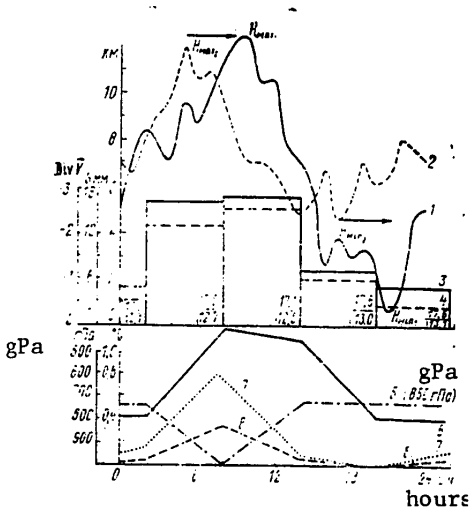

Fig. 1. Diurnal variation of convective activity and thermodynamic characteristics in polygon I.

1 and 2) H_{max} of clouds, km; 3) precipitation sum, mm; 4) Div $\vec{V} \cdot 10^{-6}$ sec^{-1}; 5) dew point spread, °C; 6) deviation of curve of state from stratification curve, °C; 7 and 8) upper boundary of layer of ascending movements and wind velocity convergence, gPa. The figures denote: in the numerator -- air temperature, °C, in the denominator -- specific humidity, 10^{-3} g/g at level 850 gPa.

Table 1

Mean 30-Day Characteristics at 0800 and 2000 Hours (LT) in Polygon II (January-February 1979)

Characteristic	Time hrs	Level, gPa					
		1008—1009	950	850	700	500	200
Sum of precipitation in polygon 6 hours before and after time, mm	8	1,5	—	—	—	—	—
	20	0,7	—	—	—	—	—
Div $\vec{V}$, 10^{-6} sec^{-1}	8	—8,7(2,0)	0,2(8,1)	2,6(9,6)	—4,8(7,7)	2,2(8,3)	8,1(10,4)
	20	—3,0	2,6	—2,5	4,4	2,1	8,2
Vertical velocity, 10^{-4} gPa/sec	8	0,0	—1,8(5,1)	0,8(11,7)	—1,0(17,2)	2,4(22,6)	6,5(50,1)
	20	0,0	0,6	1,1	1,8	—0,7	—2,4
Deviation of curve of state from stratification curve, °C	8	0,0	0,0	1,0	1,3	3,2	1,8
	20	0,0	0,0	1,2	1,5	4,0	4,2
Dew point spread, °C	8	3,0	2,5	3,0	7,5	7,0	8,0
	20	4,5	2,5	3,0	7,0	7,0	7,0
Specific humidity, 10^{-3} g/g	8	18,0(0,6)	15,5(0,7)	11,8(0,9)	6,4(1,4)	2,9(0,6)	0,05(0,01)
	20	18,2	16,2	12,5	6,8	3,1	0,06
Temperature, °C	8	25,8(0,4)	21,9(0,5)	16,9(0,8)	9,5(0,5)	—6,0(0,8)	—53,6
	20	27,5	22,8	17,3	10,1	—5,3	—53,6

Note. The standard deviation is given in parentheses.

a period of weakening of convection. The observed altitude of the tops of clouds (about 6.5 km) differed appreciably from the altitude computed by the particle method ($H > 12$ km); its actual changes correlate with convergence of wind velocity in the boundary layer. The divergence of velocity at the 200 gPa level during the period from 0800 to 2000 hours did not change since convection evidently developed far lower.

A confirmation of the existence of a correlation between convective activity and the convergence of wind velocity and ascending movements is the absence of a diurnal variation of all these characteristics in polygon III. An increase in the diurnal variation of convective activity corresponded to an increase by several times in the diurnal variation of convergence in the layer 980-800 gPa in polygon II in comparison with polygon III, and in polygon I in comparison with II. Such a correspondence cannot be found in the peculiarities of the diurnal variation of stratification in three polygons: in a large part of the troposphere from morning to evening there was an increase in temperature by 0.5-0.9°C and specific humidity by 0.2-$0.8 \cdot 10^{-3}$ g/g (Table 2).

The monthly precipitation sum in polygon III was four times greater than in polygon II. The corresponding mean values of the maximum altitude of the tops of clouds were 8.5 and 6.2 km. The positive instability energy in both polygons extended to an altitude greater than 12 km; in the lower 2-km layer, especially important for convection, it was a little greater in polygon II. Only above 2 km the deviations of the curve of state from the stratification curve in polygon III were 0.4-0.6°C greater than in polygon II (with a value of the deviations themselves 2-5°C).

Table 2

Morning-to-Evening Changes in Thermodynamic Characteristics at 900-gPa Level

Characteristic	Polygon		
	I	II	III
Temperature, °C	0.4	0.7	0.5
Specific humidity, 10^{-3} g/g	0.4	0.8	0.2
Div $\vec{V}$, 10^{-6} sec^{-1}	6.7	2.8	0.6
w, 10^{-4} gPa/sec	5.9	2.3	0.5

The differences between the polygons with respect to the dew point spreads were 0.5-1.5°C; in the layer up to 2 km the dew point spreads were less in polygon II and greater in polygon III. The specific humidity in the main part of the troposphere differed by less than $0.5 \cdot 10^{-3}$ g/g. Both the specific humidity and the air temperature were somewhat higher in polygon III (Table 3). After jointly analyzing the data in Figure 1 and Tables 1-2 it can be concluded that there is no stable correlation between convective activity and any peculiarities of stratification, as coincides with the data in [5, 6].

It should be noted that with a well-expressed diurnal variation the ascending movements and Div $\vec{V}$ are related to convective activity only in the period of its maximum. For example, in polygon I these values are greater than in polygon II only at

0800 hours; however, in polygons I and III they are approximately equal. In all probability the explanation of the latter fact is that in polygon I at the times of the absolute maxima of convective activity (0500 and 1000 hours) no radiosonde observations were made and the thicknesses of the layers occupied by convergence and ascending movements at these times were far greater than those noted at 0800 hours.

Table 3

Mean 30-Day Characteristics at 850-gPa Level in Polygons II and III (the Standard Deviation is Given in Parentheses)

Characteristic	Polygon II	Polygon III
Deviation of curve of state from stratification curve, °C	1.2	1.0
Dew point spread, °C	3.0	4.0
Specific humidity, 10^{-3} g/g	12.1	12.1(0.9)
Air temperature, °C	17.1	17.9(0.5)
Div $\vec{V}$, 10^{-6} sec^{-1}	-0.1	-0.7(7.3)
w, 10^{-4} gPa/sec	0.9	-6.9(9.7)
Upper boundary of wind velocity convergence layer, gPa	960	800
Upper boundary of layer of ascending movements, gPa	920	490

Table 4

Percentage of Cases With Precipitation (Numerator), Mean Quantity of Precipitation (mm in 6 hours), Number of Cases (in Parentheses) Under Different Humidity Conditions

Mean dew point spread in layer 850-500 gPa, °C	Mean deviation of curve of state from stratification curve at level 950 gPa, °C: 0.0-0.8	0.9-3.5
0.0-2.9	$\frac{22}{1.5}$ (24)	$\frac{82}{11.2}$ (20)
3.0-5.9	$\frac{20}{0.0}$ (27)	$\frac{21}{0.4}$ (16)

In polygons I and II three classes of situations in which the activity of convection differed substantially (with 20-30 cases in a class) were observed. The analysis indicated that weakened convection is accompanied by an increase in the dew-point spreads and the appearance of small stability in the lower 500-m layer. With an identically unstable stratification of temperature and humidity convective activity was entirely determined by the convergence of wind velocity and ascending movements in the atmospheric boundary layer. In this case Div $\vec{V}$ at the 200-gPa level changed insignificantly.

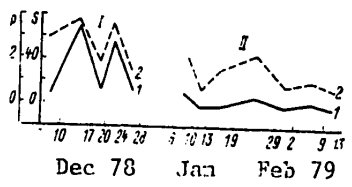

Fig. 2. Mean diurnal precipitation sums 8 mm (1) and Laplacian of surface pressure $\nabla^2 p$ [gPa x (500 km)^2] (2) by periods in polygons I and II.

In addition to data averaged by polygon we examined data from radiosonde observations on individual ships. We analyzed 60 cases of positive deviation of the curve of state from the stratification curve ΔT in the middle troposphere and 153 cases when $\Delta T > 0$ in the entire troposphere, including the layer near the condensation level (950-900 gPa) and the layer 150-200 gPa. At the 850-gPa level $\Delta T > 2°C$ and the mean dew-point spread in the layer 850-500 gPa is less than 6°C.

An analysis of these cases indicated the following: despite increased instability, in approximately 50% of the cases precipitation did not fall. Precipitation was not noted in more than 75% of the cases when at the level 950 gPa $\Delta T < 0.9°C$ (with allowance for a virtual temperature from 0.5 to 1.4°C) or the mean dew-point spread was 3-6°C (Table 4).

With Div $\vec{V} > 0$ at the sea surface the probability of falling of rain was 33%, and with Div $\vec{V} < 0$ -- 67%. The altitude of the cloud tops was dependent on the convergence value. In cases of an equality of the temperature and humidity stratification conditions in the entire troposphere, including near the condensation level, the falling of rain for the most part occurred with $\vec{V} < -9 \times 10^{-6}$ sec^{-1}.

In the considered cases of increased instability there was the same diurnal variation of convective activity as in all the cases considered above. For example, in polygon I in evening, despite instability, there was no precipitation more than 15 mm and clouds with $H_{max} > 10$ km. Toward morning there was a sharp increase in both the number of cases of increased instability and the probability of rains and thick clouds in each of them. The apparent reason for this was an increase in the convergence of wind velocity in the lower layer of the troposphere.

The role of horizontal convergence of wind velocity in the development of well-developed cloud convection is confirmed by an analysis of the pressure field. The plane pressure Laplacian $\nabla^2 p$ was computed using data read from synoptic charts with grid squares having a side of 500 km. There was a correlation between $\nabla^2 p$ and convection: precipitation was observed only with $\nabla^2 p < 0$. With an increase in $\nabla^2 p$ there was an increase in the quantity of precipitation and the altitude of the cloud tops. A decrease in $\nabla^2 p$ during the course of the day from 4.0 gPa·(500 km)^2 in the morning to 2.8 gPa·(500 km)^2 in the evening in polygon I and from 3.4 to 0.8 gPa·(500 km)^2 in polygon II was accompanied, as already mentioned, by a sharp weakening of convective activity. The $\nabla^2 p$ values and precipitation quantities S, averaged for sufficiently long time intervals, are given in Fig. 2. In polygons I and II $S > 50$ mm was observed with a mean value of the pressure Laplacian more than 3.5 gPa·(500 km)^2, whereas with $\nabla^2 p \leq 1.0$ gPa·(500 km)^2 there was no precipitation. In polygon I with $\nabla^2 p > 4.0$ gPa·(500 km)^2 clouds attained altitudes 12-19 km, and with $\nabla^2 p < 2.0$ gPa·(500 km)^2 -- only 7-9 km. It should be noted that the maximum altitude of the cloud tops for the region to a greater degree than precipitation was associated with velocity convergence and the pressure Laplacian and was not dependent

on any stratification characteristics. Only with a very great convergence $H_{max} >$ 12.0 km was the level predicted by the particle method attained (there where negative instability energy becomes equal to the positive energy [2]). We also emphasize that even with such a great cloud thickness thunderstorms are almost not noted. There were no squalls with an intensity greater than 16 m/sec.

Generalizing everything mentioned above, we can point out the following.

In the investigated regions, in the neighborhood of the southeastern shores of Asia, near the ICZ, an almost constant great instability of temperature stratification and high air humidity in the entire troposphere. Nevertheless, convective activity in polygons I and II had a sharply expressed diurnal variation with a maximum in the morning hours and a minimum in the evening hours.

Convective activity and its diurnal variation were greater in regions of high values and diurnal variation of horizontal convergence of wind velocity and ascending movements.

Aperiodic changes in convective activity, like periodic changes, were associated with changes in convergence and ascending movements in the lower part of the troposphere and also with pressure field changes. An increase in the positive Laplacian of near-water pressure $\nabla^2 p$ (cyclonicity) corresponded to an intensification of wind velocity convergence and active development of convective clouds.

In polygons I and II an increase in $\nabla^2 p > 0$ in the premorning hours was associated with a temperature decrease and pressure increase over the land with its lesser change over the water in the investigated regions. In the second half of the day the $\nabla^2 p < 0$ value was governed by an increase in temperature and a decrease in pressure over the land with its lesser change over the water surface of the polygons.

A diurnal variation of convective activity with a morning maximum appeared only at a distance of less than 250 km from the land, which was evidently associated with the breeze effect.

Aperiodic intensifications of cyclonicity were caused by cold intrusions causing a pressure increase northward from the polygons with its lesser change in the polygons.

Among the stratification peculiarities exerting an influence on convection in the investigated region we should note: 1) an upper level of equalization of negative and positive energy determining the maximum possible altitude of the tops of clouds with a very great wind velocity convergence in the lower part of the troposphere; 2) a dew-point spread in the layer 950-500 gPa; 3) a deviation of the curve of state from the stratification curve near the condensation level (950 gPa).

BIBLIOGRAPHY

1. Inagamova, S. I., Chasova, K. I., Gruzinova, L. G. and Lineva, N. N., "On the Problem of Precipitation Over the Tropical Latitudes of the Atlantic Ocean," TROPEKS-74 (TROPEX-74), Vol 1, Leningrad, Gidrometeoizdat, 1976.

2. Peskov, B. Ye., "Some Problems in Investigations and Prediction of Thunderstorms," TRUDY GIDROMETTSENTRA SSSR (Transactions of the USSR Hydrometeorological Center), No 225, 1979.

3. Fal'kovich, A. I., DINAMIKA I ENERGETIKA VNUTRITROPICHESKOY ZONY KONVERGENTSII (Dynamics and Energetics of the Intertropical Convergence Zone), Leningrad, Gidrometeoizdat, 1979.

4. Kuo, H. L., "Instability Theory of Large-Scale Disturbances in the Tropics," J. ATMOS. SCI., Vol 32, 1975.

5. Ruprecht, E. and Gray, W. M., "Analysis of Satellite-Observed Tropical Cloud Clusters," TELLUS, Vol 28, 1976.

6. Williams, K. T. and Gray, W. M., "Statistical Analysis of Satellite-Observed Trade Wind Cloud Clusters in the Western North Pacific," TELLUS, Vol 25, 1973.

UDC 551.5:621.396.96

OPTIMUM MEASUREMENT OF RADAR PARAMETERS OF METEOROLOGICAL FORMATIONS

Moscow METEOROLOGIYA I GIDROLOGIYA in Russian No 4, Apr 81 pp 117-121

[Article by B. S. Yurchak, Institute of Experimental Meteorology, manuscript received 17 Jun 80]

[Text]

Abstract: On the basis of the results of theoretical investigations of the spectral characteristics of echo signals it is demonstrated that it is possible to match the radio channel of a meteorological radar receiver on the basis of similar characteristics only of the sounding pulse. The spectral approach is used in analyzing all the quality indices of reception of radiometeorological echo signals and validating the choice of the optimum relationship between the receiver bandwidth and the duration of the meteorological radar transmitter pulse.

In radar measurements of microphysical and geometrical characteristics of meteorological formations there must be a precise evaluation of the absolute value and spatial distribution of radar reflectivity.

In this study we examine the optimality of measurements of these parameters by modern meteorological radar stations (MRS) by an analysis of distortions of the spectral-temporal characteristics of echo signals in the radio channel of the receiver and allowance for the finite spatial extent of the transmitter sounding pulse.

The temporal distribution of the mean power (form) of the radar echo signal from the meteorological formation at the input of the meteorological radar input $\overline{P(t)}$ is related to the spatial distribution of radar reflectivity Z(R) by the expression [6]

$$\overline{P(t)} = A \int_0^\infty \frac{Z(R)}{R^2} P_0\left(t - \frac{2R}{c}\right) dR, \qquad (1)$$

where A is a coefficient, R is range, t is time, c is the velocity of propagation of electromagnetic waves, $P_0(t)$ is the shape of the sounding pulse.

Expression (1) illustrates the well-known phenomenon of distortion of the shape of the distribution of radar reflectivity of a meteorological formation as a result of the finite spatial extent of the sounding pulse (for example, see [10]).

In accordance with [7], the signal at the receiver output can be written in the form

[BbIX = out(put)] $$\overline{P(t)_{out}} = \int_{-\infty}^{\infty} B(x)\,\overline{P_0(t+x)}\,dx, \qquad (2)$$

where $$B(x) = \int_{-\infty}^{\infty} H(t)\,H(t+x)\,dt$$

is the instrument function and H(t) is the "pulsed" transfer function (PTF) of the meteorological radar respectively. Taking (1) into account, (2) can be written in the form

$$\overline{P(t)}_{вых} = A\int_{0}^{\infty}\frac{Z(R)}{R^2}\,U\left(t-\frac{2R}{c}\right)dR, \qquad (3)$$

where $$U(t) = \int_{-\infty}^{\infty} B(x)\,P_0(t+x)\,dx$$

is the meteorological radar instrument function. It follows from (3) that the shape of the echo signal at the receiver output reproduces the Z(R) distribution the more precisely the "narrower" the instrument function U(t). The U(t) characteristics can be evaluated experimentally since in the sounding of a point target the shape of the echo signal with an accuracy to a constant factor is equal to the instrument function. As follows from (3), with $Z(R) \sim \delta(0)$ $\overline{P(t)}_{out} \sim U(t)$. For the special case when $P_0(t)$ and the amplitude-frequency characteristic (AFC) of the receiver can be approximated by Gaussian functions, the instrument function is

$$U(t) = P_0\left[\left(\frac{4\ln 2}{\pi^2\tau_0^2\Pi^2}\right)^2 + 1\right]^{-\frac{1}{2}} \times \exp\left(-4\ln 2\,\frac{t^2}{T^2}\right), \qquad (4)$$

where

$$T^2 = \frac{16(\ln 2)^2 + (\pi\Pi\tau_0)^2}{(\pi\Pi)^2},$$

Π and τ_0 are the width of the AFC band and the duration of the sounding pulse at the 3 db level. As indicated by measurements with the MRL-2 meteorological radar, having Π = 1.5 MHz and τ_0 = 1 μsec [2], the shape of the echo signal from the point target coincided within the limits of estimated errors with the corresponding theoretical function $U(t) \sim \exp(-2.05\ t^2)$ (t in μsec). The approximation of U(t) to a delta function is the better the lesser is τ_0 and/or the greater is Π.

In radar sounding of meteorological formations it is necessary not only to reproduce the form of Z(R) correctly, but also to ensure precise absolute measurements of its value, and also the possibility of detecting meteorological formations with a low radar reflectivity. Accordingly, it is necessary to examine as well the dependence of the accuracy of the absolute measurements of the mean power of the echo signal and the receiver response (signal-to-noise ratio) on τ_0 and Π.

The measurement of the mean power of the echo signal from a meteorological formation is usually accomplished by a comparison of the amplitude of the echo signal with the value of the calibration pulse of a known power [1, 3, 10]. In such a measurement method errors can arise due to the inadequacy of the echo signal and calibration pulse losses in the meteorological radar receiving channel caused

by the finite character of the width of the amplitude-frequency characteristic band. In order to take these losses into account we [13] introduced a coefficient of conversion losses (CCL), equal to the ratio of the power of echo signals at the output of a real receiver and an ideal receiver with an amplitude-frequency characteristic uniform and unlimited in the transmission band, having identical amplification factors:

$$\mu = \overline{P}_{out}/\overline{P}_{out\ ideal} = \int_{-\infty}^{\infty} S(f)|K_0(f)|^2 df \Big/ \int_{-\infty}^{\infty} S(f)\, df \qquad (5)$$

where S(f) is the power spectrum of the incoherent echo signal component at the meteorological radar receiver input.

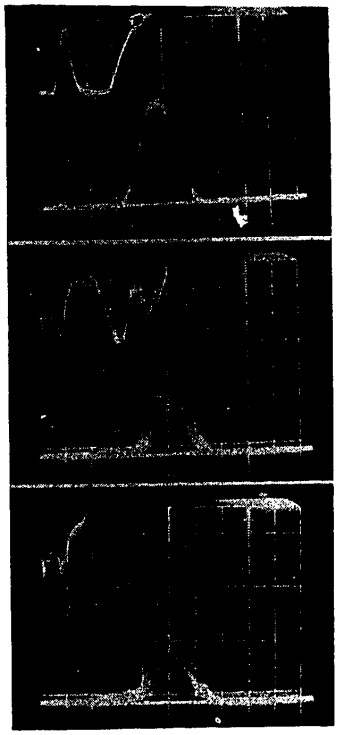

Fig. 1. Videosignals (upper scan) and envelopes of "mean" radiospectra (lower scan) of echo signals from point target (a) and stratocumulus cloud (b, c). (The scale on the upper scan is 5 μsec/graduation, on the lower scan -- 0.67 MHz/graduation.)

$K_0(f)$ is the amplitude-frequency characteristic normalized to the maximum amplification factor. In determining the CCL the stipulation of the S(f) form is a first step. It is usually assumed that the spectral width S(f) is determined by the duration of the echo signal τ_{es} (extent of the meteorological formation) [5, 10, 11].

On this basis, in particular, for the processing of the echo signal it is proposed that the passband of the amplitude-frequency characteristic be narrowed to a value $\sim\tau_{es}^{-1}$ [5, 10]. However, the theoretical examination which we made revealed that the width and shape of S(f) in the case of incoherent scattering are determined only by the spectrum of the sounding pulse, regardless of the extent of the meteorological formation [14].

In order to obtain experimental confirmation of this conclusion we carried out measurements of the spectral characteristics of echo signals using a spectral analysis apparatus. The basis for this apparatus was a dispersion-type spectrum analyzer of the S4-47 type [9]. The experiment was carried out using an MRL-2 meteorological radar [2]. An analysis was made of the radio signal from the output of the intermediate frequency preamplifier. The apparatus made it possible to register the amplitude radio spectra and their envelopes for each echo signal and represent them on an oscillograph screen either individually or in the form of superposed records. Due to some modernization of the S4-47 the range of durations of the signals to be analyzed was broadened to 28μsec, which corresponds to an extent of a sector of the meteorological formation of 4.2 km.

Figure 1 shows the measured envelopes of the radiospectra of echo signals from a point target (Fig. 1a) and a stratocumulus cloud (Fig. 1b,c). The radiospectra are shown in the lower scan (scale 0.67 MHz/graduation) and the corresponding segments of the videosignal are shown on the upper scan (scale 5μsec/graduation). Figure 1b shows a typical radiospectrum "averaged by records." The envelope of this spectrum coincides with the spectrum of the sounding pulse (compare with Fig. 1a). Changes in the shape and width of the spectra with a change in the durations of the segments of the echo signals to be analyzed were not noted (compare Fig. 1b and Fig. 1c). It follows from this result, and also from a theoretical analysis [14], that $\Delta f_{es}\,\tau_{es}\approx\Delta f_0\,\tau_{es}\gg 1$ (Δf_{es} and Δf_0 are the widths of the spectra for the echo signal and the sounding pulse respectively). Accordingly, meteorological echo signals must be assigned to the class of complex, wide-band signals, whereas the meteorological formation is assigned to the class of highly disperse targets (according to the classification in [4]). Thus, the equality of the power spectra of the echo signal and the sounding pulse even makes it possible with an a priori unknown nature of the meteorological formation to accomplish matching of the receiver for reception of the incoherent component of the echo signal exclusively on the basis of the characteristics of the sounding pulse (that is, as in classical radar).

For a rectangular sounding pulse and a Gaussian amplitude-frequency characteristic the determination of $\overline{P}_{out}$ for the most part is reduced to computation of an integral in the form

$$I=\int_0^\infty\left(\frac{\sin x}{x}\right)^2 e^{-\alpha x^2}\,dx,$$

where

$$\alpha=\frac{4\ln 2}{(\pi\Pi\tau_0)^2}$$

Expanding the exponent into a Fourier integral

$$e^{-\alpha x^2}=\frac{1}{\sqrt{2\pi}}\int_0^\infty e^{-\frac{y^2}{4\alpha}}\cos yx\,dy$$

after a number of transformations we obtain

$$I=\frac{1}{2}\pi\left[\Phi\left(\frac{1}{\sqrt{a}}\right)-\right.$$
$$\left.-\sqrt{\frac{a}{\pi}}\left(1-e^{-\frac{1}{a}}\right)\right], \quad (6)$$

where

is the integral of errors. $$\Phi(u)=\frac{2}{\sqrt{\pi}}\int_0^u e^{-t^2}\,dt$$

Since in the considered case of a rectangular pulse the denominator of expression (5) is equal to $1/2\Pi$, then

$$\mu=\Phi\left(\frac{1}{\sqrt{a}}\right)-\sqrt{\frac{a}{\pi}}\left(1-e^{-\frac{1}{a}}\right). \quad (7)$$

A graph of the dependence $\mu(\Pi\tau_0)$ is shown as Fig. 2 (curve 1). With $\Pi\tau_0>1$ it can be assumed that the CCL is

$$\mu\approx 1-\sqrt{\frac{a}{\pi}}. \quad (7a)$$

The calibration method employed in the operation of the meteorological radar does not make it possible to take into account the errors due to limitation of the pass-band. The standard calibration method involves the feeding of a radio pulse of a known power with a duration of 6μsec [3, 12] or 10μsec [1] to the receiver input. It is easy to show that the error in such a calibration method will be equal to the ratio of the CCL of the sounding and calibration signals: $\delta\overline{P}=\mu(\Pi\tau_0)/\mu(\Pi\tau_{con})$. For example, for the MRL-2 in measurements with $\tau_0=1\mu$sec

$$\delta\overline{P}=\frac{\mu(1,5)}{\mu(9)}\approx\mu(1,5),$$

that is, $\delta\overline{P}$ = -0.97 db.

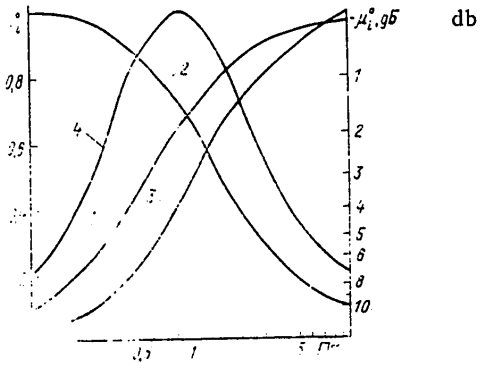

Fig. 2. Dependence of indices of quality of reception of radiometeorological echo signals on the characteristics of the meteorological radar with a rectangular sounding pulse and a Gaussian amplitude-frequency characteristic.

Accordingly, for the MRL-5 $\delta\overline{P} = \mu(1)/\mu(10) \approx \mu(1)$, that is, $\delta\overline{P} = -1.55$ db. As is indicated by the data in the table, the CCL values differ not only for different types of meteorological radar stations, but also for different regimes for the operation of one station. This circumstance is reflected in the results of radar measurements of microphysical characteristics of meteorological formations and naturally makes difficult the carrying out of a comparative analysis of the results obtained by different authors.

In order to eliminate this shortcoming in calibration of meteorological radars the calibration of the receivers of the meteorological radar station must be carried out using signals whose spectral-temporal characteristics coincide with or are close to the similar characteristics of echo signals from meteorological formations.

It would be possible to decrease the requirements on the coincidence of the spectral-temporal characteristics of the calibration and echo signals when making measurements of mean power and also to improve reproduction of the form of Z(R) when using in meteorological radars receivers with a broad bandwidth ($\Pi > \tau_0^{-1}$). However, the following problems arise here: up to what point is it possible to widen the band without there being a considerable decrease in receiver response? Adhering to the traditional approach, we will analyze the dependence of the signal-to-noise ratio at the output of the meteorological radar receiver on the bandwidth of the amplitude-frequency characteristic.

As the radiometeorological signal-to-noise ratio we will examine the ratio of the mean power of the incoherent component of the echo signal to the mean noise level:

[ВЫХ = out(put); Ш = noise]

$$\mu_1 = \left(\frac{S}{N}\right)_p = \frac{\overline{P}_{вых}}{\overline{P}_ш} = \frac{\int_{-\infty}^{\infty} S(f)\,|K_0(f)|^2 df}{kT_e\Pi_ш}, \tag{8}$$

where k is the Boltzmann constant; T_e is the equivalent noise temperature, Π_{noise} is the noise bandwidth of the amplitude-frequency characteristic.

For a rectangular sounding pulse and a Gaussian amplitude-frequency characteristic, taking (6) into account, and also that $\Pi_{noise} = 1.06\Pi$, we obtain

$$\mu_1 = \frac{\overline{a^2}\tau_0}{kT_e}\left[\sqrt{\alpha\pi}\,\Phi\left(\frac{1}{\sqrt{\alpha}}\right) - \alpha\left(1 - e^{-\frac{1}{\alpha}}\right)\right], \tag{9}$$

where $\overline{a}^2$ is the mean square of echo signal amplitude.

The function (9), normalized to

$$(S/N)_{p,max} = (S/N)_{p_1}\Big|_{\substack{\Pi\tau_0 = 0 \\ \tau_0 \neq 0}} = \frac{\overline{a^2}\tau_0}{kT_e}$$

is shown in Fig. 2 (curve 2). The same as for the CCL, with $\Pi\tau_0 > 1$ (9) can be represented approximately in the form

$$\mu_1 \approx \frac{\bar{a}^2\tau_0}{kT_e}(\sqrt{2\varkappa} - 1). \tag{9a}$$

The resulting dependences μ, $\mu_1 = f(\Pi\tau_0)$, computed using formulas (7) and (9), accurately coincide with the results of numerical computations of the similar parameters in [15], whereas the approximate formulas (7a) and (9a) are far simpler than the expressions proposed in this study.

It follows from the cited data that a widening of the bandwidth by more than $\Pi^* = \tau_0^{-1}$ leads to a considerable decrease in the signal-to-noise ratio. However, its narrowing to a value below Π^* leads to an increase in the spatial correlation radius of the output signal, which worsens the range resolution of the meteorological radar station [15, 16] and increases the error in reproduction of echo signal shape (see (4)) with an insignificant increase in the signal-to-noise ratio. Thus, the optimum method for measuring the mean power of the echo signal involves a comparison of the amplitudes of the echo signal and the calibration pulse of a known power, whose spectrum is close to the spectrum of the sounding pulse, whereas the duration corresponds to the extent of the meteorological formation.

It is of interest to clarify whether there is some optimum $(\Pi\tau_0)_{opt}$ value which would be a compromise choice between the requirements of an increase in the radiometeorological signal-to-noise ratio, on the one hand, and a decrease in the increment of the spatial correlation radius of the echo signal, on the other. In [15] for this purpose the authors examined the ratio $\mu_2 = (S/N)p/r_6 = f(\Pi\tau_0)$, where r_6 is the increment of echo signal duration in space coordinates at -6 db. The indicated function had a maximum with $(\Pi\tau_0)_{opt} = 0.72$. However, the considered parameter carries little information because when going on the basis, for example, of the results in [8] it can be shown that with levels below -6 db the $(\Pi\tau_0)_{opt}$ values change and with a level -3 db and above the $(N/S)_p/r_n$ function in this case in general does not have a maximum as a result of the well-known phenomenon of accentuation of the wide-band signal with passage through a narrow-band filter. Therefore, it is better to analyze the increment of the correlation interval, determined as

$$\Delta\tau_{cal} = \tau_{cal\ out} - \tau_{cal}, \tag{10}$$

where

$$\tau_к = \Delta f_{эфф}^{-1}, \quad \Delta f_{эфф} = \int_{-\infty}^{\infty} \frac{S(f)}{S_0}\,df,$$

$$\tau_{к\ вых} = \Delta f_{эфф\ вых}^{-1},$$

$$\Delta f_{эфф\ вых} = \int_{-\infty}^{\infty} \frac{S(f)\,|K_0(f)|^2\,df}{S_0},$$

$$S_0 = S(f)|_{f=f_0}.$$

[K = cal(ibration);
ВЫХ = out(put;
ЭФФ = eff(ective)]

Using the already cited results of computation of the corresponding integral, for a rectangular sounding pulse and a Gaussian amplitude-frequency characteristic we obtain

[K = cal; HOP = nor]

$$\frac{\Delta\tau_{\kappa}}{\tau_0} = \frac{\sqrt{2\pi}}{\left(\frac{S}{N}\right)_{P,\,\text{нор}}} - 1, \tag{11}$$

where $(S/N)_{P,\,nor}$ is the normalized radiometeorological signal-to-noise ratio. Using the dependence of the relative increment of the correlation interval on $\alpha(\Pi\tau_0)$ (11), in each specific case it is possible to estimate the increment $\Delta\tau_{cal}$. For example, for the MRL-2 $\Delta\tau_{cal} = 0.25\mu$sec.

Similarly, we can obtain

$$\mu_3 = \frac{(S/N)_p}{\Delta\tau_{\kappa}} = \frac{\overline{a^2}}{kT_e} \frac{\left(\frac{S}{N}\right)_{P,\,\text{нор}}}{\sqrt{2\pi} - \left(\frac{S}{N}\right)_{P,\,\text{нор}}}. \tag{12}$$

A graph of the function (12), normalized to $\overline{a^2}/kT_e$, is shown in Fig. 2 (curve 3). In particular, it follows from the graph that it is not possible to select $(\Pi\tau_0)_{opt}$ for this case since the function (12) does not have a maximum but increases monotonically with an increase in $\Pi\tau_0$. This occurs because the decrease in $\Delta\tau_{cal}$ with an increase in $\Pi\tau_0$ transpires more rapidly than the decrease in $(S/N)_{P,\,nor}$.

Meteorological Radar Station Coefficients of Conversion Losses for Family of Meteorological Radars

Type of meteorological radar	Parameters of meteorological radar station τ_0 μsec	Π MHz	CCL μ db	CCL $-\mu$ db
MRL-1	0.45	3	0.76	1.2
	1.0	2.3	0.87	0.6
	2.0	2.3	0.94	0.3
MRL-2	1.0	1.5	0.8	0.97
	2.0	1.5	0.9	0.46
MRL-5	1.0	1.0	0.7	1.55
	2.0	1.0	0.85	0.7

It is desirable that optimality be evaluated using the parameter $\mu_1 = (S/N)_p \mu$, characterizing simultaneously response of the receiver and the energy losses of the echo signal (see curve 4 in Fig. 2). The function $\mu_4(\Pi\tau_0)$ has a maximum with $\Pi\tau_0 \approx 0.8$. Accordingly, from this point of view a change in the bandwidth in comparison with the usually adopted $\Pi = (0.65\text{-}1.5)\tau_0^{-1}$ is also undesirable for the receivers of meteorological radars.

The parameters $\mu - \mu_4$ examined in this study are in effect indices of the quality of reception of radiometeorological echo signals. Due to the known analogy between radar and acoustic sounding the results can also be used in the development of acoustic sounders and a correct method for measuring the corresponding acoustic parameters of the atmosphere.

The author thanks a group of specialists at the State Design and Planning Institute imeni A. A. Zhdanov, headed by G. D. Den'gin and I. D. Krotov, for assistance in creating the apparatus for spectral analysis of echo signals.

BIBLIOGRAPHY

1. Abshayev, M. T., Burtsev, I. I., Vaksenburg, S. I. and Shevela, G. F., RUKOVODSTVO PO PRIMENENIYU RADIOLOKATOROV MRL-4, MRL-5 I MRL-6 V SISTEME GRADOZASHCHITY (Manual on the Use of the MRL-4, MRL-5 and MRL-6 Radars in a Hail-Protection System), Leningrad, Gidrometeoizdat, 1980.

2. Belov, N. P., METEOROLOGICHESKIYE RADIOLOKATSIONNYYE STANTSII (Meteorological Radar Stations), Leningrad, Gidrometeoizdat, 1976.

3. Brylev, G. B. and Sal'man, Ye. M., RUKOVODSTVO PO PROIZVODSTVU NABLYUDENIY I PRIMENENIYU INFORMATSII S RADIOLOKATOROV MRL-1 I MRL-2 (Manual on Making Observations and Using Information From MRL-1 and MRL-2 Radars), Leningrad, Gidrometeoizdat, 1974.

4. Van Tris, G., TEORIYA OBNARUZHENIYA, OTSENOK I MODULYATSII (Theory of Detection, Evaluations and Modulation), Vol III, Moscow, Sovetskoye Radio, 1977.

5. Gornostayev, N. V., "On the Problem of the Threshold Response of Meteorological Radar Receivers), TRUDY GGO (Transactions of the Main Geophysical Observatory), No 327, 1974.

6. Isimaru, A., "Propagation and Scattering of Waves in Randomly Inhomogeneous Media. Theory and Applications," TIIER, Vol 65, No 7, 1977.

7. Levin, B. R., TEORETICHESKIYE OSNOVY STATISTICHESKOY RADIOTEKHNIKI (Theoretical Principles of Statistical Radio Engineering), No 1, Moscow, Sovetskoye Radio, 1974.

8. Livshits, A. R., "Determination of the Duration of a Pulse Propagating Through a Channel With a Bell-Shaped Frequency Characteristic," ELEKTROSVYAZ' (Electrocommunication), No 9, 1959.

9. Mardin, V. V. and Krivonosov, A. I., SPRAVOCHNIK PO ELEKTRONNYM IZMERITEL'NYM PRIBORAM (Handbook on Electronic Measuring Instruments), Moscow, Svyaz', 1978.

10. Stepanenko, V. D., RADIOLOKATSIYA V METEOROLOGII (Radar in Meteorology), Leningrad, Gidrometeoizdat, 1966.

11. Fedorov, A. A., "Optimum Reception of Signals From Meteorological Targets," TRUDY GGO, No 395, 1977.

12. Endryus, D. F. and Senn, Kh. V., "Semiautomatic Calibration of a Receiver and Videostages of Meteorological Radars," PROBLEMY RADIOLOKATSIONNOY METEOROLOGII (Problems in Radar Meteorology), Leningrad, Gidrometeoizdat, 1971.

13. Yurchak, B. S., "Influence of the Characteristics of the Receiver of a Meteorological Radar on the Accuracy in Measuring Radar Reflectivity of Meteorological Formations," TRUDY IEM (Transactions of the Institute of Experimental Meteorology), No 9(52), 1975.

14. Yurchak, B. S., "Radar Observation of a Multiple Meteorological Target," TRUDY IEM (Transactions of the Institute of Experimental Meteorology), No 19(72), 1978.

15. Doviak, R. J. and Zrnic, D. S., "Receiver Bandwidth Effect of Reflectivity and Doppler Velocity Estimates," J. APPL. METEOROL., Vol 18, No 1, 1979.

16. Natanson, F. E. and Smith, P. L., "A Modified Coefficient for the Weather Radar Equation," PREPRINTS 15th RADAR METEOROLOGY CONFERENCE, Champaign-Urbana, AMS, 1972.

REVIEW OF MONOGRAPH BY YU. A. IZRAEL': 'ECOLOGY AND MONITORING THE STATE OF THE ENVIRONMENT' ('EKOLOGIYA I KONTROL' SOSTOYANIYA PRIRODNOY SREDY'), LENINGRAD, GIDROMETEOIZDAT, 1979

Moscow METEOROLOGIYA I GIDROLOGIYA in Russian No 4, Apr 81 pp 122-123

[Review by I. K. Dibobes, doctor of medical sciences, and I. M. Nazarov, candidate of technical sciences, laureates of the USSR State Prize]

[Text] A highly important organizational measure related to monitoring of the state of the environment was the transformation of the Main Administration of the Hydrometeorological Service of the USSR Council of Ministers into the USSR State Committee on Hydrometeorology and Environmental Monitoring, which became the principal agency in our country responsible for monitoring the state of the environment, in 1978.

The book by Corresponding Member USSR Academy of Sciences Yu. A. Izrael' entitled EKOLOGIYA I KONTROL' PRIRODNOY SREDY (Ecology and Monitoring the State of the Environment) is devoted to the scientific principles of new directions in the activity of the State Committee on Hydrometeorology, the most important of which are monitoring of the state of the environment, determination of admissible ecological loads and their normalization. However, the title, in our opinion, conveys only the narrower initial intent of the author.

The importance of this book is considerably broader. It is the first profound exposition of the scientific principles of monitoring of the state of the environment to appear in our country and abroad and presented from the ecological point of view, from the point of view of optimum interaction between man and nature, assurance of maintenance of a high quality of the biosphere and all its ecological systems. This fact is especially important in connection with the fact that the effect of man's economic activity on the biosphere in general and in individual regions has increased sharply and has acquired a global character. Precisely for this reason the study of interaction between man and the environment has become a problem of fundamental importance.

The book gives a generalization of materials from numerous original investigations of the author himself, scientific personnel working under his direction and the results of Soviet and foreign investigations. It deals with all the principal aspects of the problem of monitoring of the state of the environment carried out on the basis of ecological and geophysical analysis and prediction of anthropogenic changes in the biosphere. The scientific basis of monitoring of the environment is presented and it is shown that it is related to the strategy of regulating the quality of the environment.

In the problem of monitoring the state of the environment the author clearly defines three principal directions taking in the principal aspects of this subject:

1. The problems involved in the admissible load on the biosphere and ecological normalization principles.

2. Scientific substantiation and means to implement monitoring of the environment -- a special information system for observing and analyzing the state of the environment, especially contaminants and the effects caused by them in the biosphere.

3. Regulation of the quality of the environment on the basis of an ecological-economic approach.

What is the distinguishing characteristic of this book, its difference from other publications devoted to environmental monitoring, the ecological aspects of interaction between man and nature? The most important difference is that thorough theoretical investigations and fundamental results are closely intertwined with practical activity and means to implement the proposed decisions are pointed out. It gives a scientific validation of the system for monitoring the state of the environment and proposes means for discriminating anthropogenic changes against a background of natural fluctuations. A scientific approach is given for solving problems involved in preserving the environment on the basis of study of the patterns of functioning and change in ecosystems under the conditions of anthropogenic loads. Methods for optimizing man's relationships with nature are outlined.

Such a formulation of the problem is encountered for the first time in world practice. It is no accident that the author himself assumes that on the basis of studies in recent years a major new direction in science is being formed. He defines it as biospherology or exospherology. It seems that this assertion precisely reflects the present-day status of the science of the biosphere and man's interaction with it.

The book consists of seven chapters. We will examine their content.

The first chapter familiarizes readers with the principles of thorough analysis of the environment. Here there is an evaluation of the role of a thorough analysis of the environment in the optimization of man's interaction with nature, the ecological load is analyzed on a regional scale, analytical methods are described and specific mathematical models are considered. The author shows that a thorough analysis of the environment makes it possible to take into account all the types of effects on different elements of the biosphere.

The second chapter is devoted to a problem which is very complex and important in practical respects: the admissible load on the biosphere and the principles of ecological normalization. Some general approaches to the problem are discussed, a determination of the admissibility of modification is made, the concept of ecological normalization is formulated and a classification of ecosystems is given from the point of view of their resistance to loads. This same chapter examines ecological approaches to the normalization of anthropogenic loads. Particular attention is devoted to the effect of harmful factors on the ecosystem from chemical and biological accumulations of harmful substances as a result of transition

from one medium to another and also the behavior of stable contaminating substances which constitute a special danger as a result of their accumulation in food chains.

The third chapter is devoted to the monitoring of anthropogenic changes in the biosphere. The author here gives a definition of monitoring, its objectives are formulated and a model is given. Also given is a classification of states of the environment, reactions of natural systems, modification sources and factors. This chapter gives the principles for evaluating and predicting anthropogenic changes in the state of the biosphere and deals with the problems involved in ecological losses and the reserves of ecosystems. In our opinion the use of these scientific advances will make possible, on a sound basis, the introduction of corrections into man's economic activity.

An individual section of the chapter is devoted to the probable approach to the evaluation of risk when there is a possible danger for the elements of the biosphere and man. In this section the author introduces the concept of a social evaluation of risk, which is a further development of social investigations initiated by the author as early as 1974.

In the last section of the third chapter the author proposes and substantiates an objective classification of the monitoring of anthropogenic changes in the state of the environment, also giving the principles of the classification and describing monitoring systems already in existence and those which are being developed. This part of the work is original and has no equals in Soviet or foreign publications.

In the fourth chapter the author discusses in detail the problem of ecological monitoring, emphasizing that ecological monitoring is complex environmental monitoring of the biosphere. The principal condition for successful functioning of ecological monitoring is the requirement that the final result will be an evaluation and prediction of the state of ecosystems. This requirement differentiates the ecological monitoring system from other monitoring subsystems. The author emphasizes the need for organizing ecological monitoring, taking into account different levels of modification at global and regional scales.

This same chapter presents ideas concerning background ecological monitoring of continental and oceanic regions and an evaluation of the use of satellite systems in ecological monitoring is given. The author defines the principal tasks of climatic modeling, describes methods for obtaining climatic data and information necessary for an analysis of the variability of climate, and evaluates the role of modeling of climatic processes.

In the author's opinion, the most timely problem is the creation of a system making possible the reliable discrimination of those anthropogenic and other effects which exert the greatest influence on climate and its changes.

The sixth chapter examines problems related to the realization of a global system for monitoring and controlling the state of the environment. The tasks and competence of such a system are defined. Systems for monitoring the environment in the USSR and Great Britain are evaluated. The advantage of a monitoring system in a socialist state is clearly demonstrated.

The book is logically completed with a chapter entitled "Regulation of Environmental Quality" in which the author formulates and solves a number of highly important scientific and socioeconomic problems. It is particularly important to emphasize the rational position of the author, assuming that the task of regulating the quality of the environment must be solved simultaneously with solution of the problem of ensuring man all that he needs in his vital activities. The chapter tells about the social significance of evaluations of the state of the environment. The author emphasizes that a necessary condition for transition to a social optimum is the requirement of a more or less simultaneous attainment of nutritional norms for the population, assurance of housing, norms for a high quality of the environment, etc.

The book is of unquestionable interest for all who are excited by the problem of preservation of the environment. The author in this book has been able to combine a clarity of style and a high scientific level of exposition of the material. In familiarizing himself with this monograph, the reader will obtain a graphic idea concerning those problems which at the present time are facing Soviet and world science in the field of applied ecology.

Among the merits of this book are a logically well-substantiated arrangement of material and excellently designed and unusually graphic illustrative material. The book is written in good language, at a high theoretical level.

It should be noted that the book has special social value. The author's thoughts on the advantages of a socialist economic system over a capitalist system in the field of environmental preservation run through it like a connecting thread.

The monograph seems to us to be a new step forward in the sphere of both the fundamental and applied earth sciences. In a short time it has already become a reference book for specialists in the field of environmental protection and at the same time a bibliographic rarity. In the immediate future it is desirable that the book be published in a second edition and in a large number of copies.

SEVENTIETH BIRTHDAY OF GEORGIY ANISIMOVICH ALEKSEYEV

Moscow METEOROLOGIYA I GIDROLOGIYA in Russian No 4, Apr 81 p 124

[Article by a group of comrades]

[Text] Professor Georgiy Anisimovich Alekseyev, doctor of technical sciences, a leading Soviet professional hydrologist, marked his 70th birthday on 4 February 1981.

G. A. Alekseyev began his scientific and production work in 1930 after graduation from the Leningrad Agricultural Polytechnic School. Already in 1932 he published his first scientific work, devoted to establishing the runoff norms for Leningradskaya Oblast. In 1939, after graduation from the Mathematics-Mechanics Faculty of Leningrad State University, Georgiy Anisimovich arrived at the State Hydrological Institute and since that time his activity has always been associated with the staff of that institute and hydrology.

The scientific interests of G. A. Alekseyev take in many fields of hydrology, but he is devoting much attention to developing a theory of the formation of river runoff and improvement of practical procedures for its computation. He has published more

than 70 scientific studies, among which there were a number of fundamental monographs devoted to objective methods for equalizing and normalizing correlations, methods for evaluating random errors of hydrometeorological information, computations of the high-water runoff of rivers in the USSR, etc.

The distinguishing characteristics of the studies of G. A. Alekseyev are scientific clarity in formulation of the problem, their high theoretical level and the striving to reduce the solutions obtained to specific recommendations suitable for use in practical engineering-hydrological computations in the planning, construction and operation of hydroengineering structures and water management systems.

The method for computing the intensity, duration and frequency of recurrence of precipitation which he developed applicable to the problem of computing rainwater runoff and his method for computing the maximum discharges of spring and rain-induced high waters have gained wide reknown.

G. A. Alekseyev made a particularly significant contribution to science in the field of application of statistical methods for solving many problems in hydrology. The procedure which he developed for the graph-analysis determination and reduction to a long period of the parameters of the distribution curves, and also his investigations of the different problems involved in the use of the curves and surfaces of distribution of probabilities in the analysis of multifactor phenomena have substantially broadened the frameworks of use of the methods of mathematical statistics for solving hydrological problems. The scientific-theoretical research work of Georgiy Anisimovich is combined with great practical engineering activity.

The name of G. A. Alekseyev is well known among the hydrologists of many countries.

Georgiy Anisimovich devotes much attention to the training of young scientists and willingly shares his profound knowledge and experience with scientific workers. He is a member of specialized scientific councils of a number of institutes and a member of the Section on Surface and Ground Water Resources and Water Balance of the Scientific Council "Complex Use and Conservation of Water Resources" of the State Committee on Science and Technology.

Georgiy Anisimovich Alekseyev is a veteran of the Great Fatherland War. For his services to the Motherland G. A. Alekseyev was presented with the Order of the Red Star, a number of medals, the Honorary Diploma of the Presidium of the Supreme Soviet RSFSR, the emblem "Distinguished Worker of the Hydrometeorological Service," honorary diplomas of the Main Administration of the Hydrometeorological Service and the Central Committee of the Trade Union of Aviation Workers.

Georgiy Anisimovich meets his anniversary filled with energy, creative forces and new scientific thought, in the implementation of which all the specialists at the State Hydrological Institute wish him great successes.

AT THE USSR STATE COMMITTEE ON HYDROMETEOROLOGY AND ENVIRONMENTAL MONITORING

Moscow METEOROLOGIYA I GIDROLOGIYA in Russian No 4, Apr 81 p 125

[Article by V. N. Zakharov]

[Text] Sessions of the scientific councils on the results of implementation of the plan for scientific research and experimental design work for 1980 were held in December 1980 - January 1981 at the scientific research institutes of the State Committee on Hydrometeorology and Environmental Monitoring. Since the last year was the last in the Tenth Five-Year Plan, the results of the five-year period were summarized simultaneously with the results of the year.

At a number of institutes, in addition to the plenary sessions, there were sectional sessions. This made possible a more thorough and subject-oriented discussion of the results, the outlining of the positive aspects of the investigations and existing shortcomings. At the individual institutes it was the practice to have a preliminary review of a scientific report by a specially designated reviewer which was presented immediately after the report of the person giving the paper.

On the whole these summary sessions were held at a high scientific level. Participating in their work were representatives of related institutes, administrations of the Hydrometeorological Service, other ministries and departments and the central offices of the State Committee on Hydrometeorology.

CONFERENCES, MEETINGS, SEMINARS

Moscow METEOROLOGIYA I GIDROLOGIYA in Russian No 4, Apr 81 pp 125-127

[Article by O. A. Avaste, L. F. Yermakova and Yu. G. Slatinskiy]

[Text] The Eleventh All-Union Conference on Actinometry and a symposium on phytoactinometry was held by the Institute of Astrophysics and Atmospheric Physics of the Academy of Sciences Estonian SSR and the Radiation Commission of the Section on Meteorology and Atmospheric Physics of the Interdepartmental Geophysical Committee of the Presidium USSR Academy of Sciences at Tallin during the period 8-15 December 1980.

The purpose of the conference and symposium was an exchange of scientific information among different departments, institutes and colleges, discussion of timely problems in actinometry, radiant energy, remote sensing of the earth and atmosphere, actinoclimatology and phytoactinometry.

A plenary session was held and six sections operated. The conference was attended by 332 delegates representing 93 institutes from 41 cities. A total of 233 reports were presented and discussed. A total of 186 persons participated in the sessions.

At the plenary session the following review reports were presented and discussed. T. G. Berlyand -- "Modern Stage in the Development of Climatological Investigations of Solar Radiation," Z. I. Pivovarova -- "Problems in Radiation Climatology in Relation to the Creation of a Climatic Survey of the USSR," Ye. M. Feygel'son -- "Some Problems in Radiation Energy of the Atmosphere," K. Ya. Kondrat'yev -- "Remote Sensing of the Atmosphere and the Earth's Surface," Yu. K. Ross -- "Problems in Phytoactinometry." In these reports there was an analysis of the state of the mentioned branches of science, the achievements were noted and criticism was expressed. Specific measures were proposed for overcoming shortcomings.

The following sections operated:

"Observation Instruments and Methods" (46 reports, section director -- Yu. D. Yanishevskiy).

"Actinoclimatology and Applied Actinometry" (32 reports, section director -- T. G. Berlyand).

"Radiation Energy" (31 reports, section director -- Ye. M. Feygel'son).

"Radiation, Aerosol and Clouds" (38 reports, section director O. A. Avaste).

"Remote Sensing of the Atmosphere and Underlying Surface (36 reports, section director -- Corresponding Member USSR Academy of Sciences K. Ya. Kondrat'yev).

"Phytoactinometry" (43 reports, section director -- Yu. K. Ross).

An increase in the effectiveness of this conference was considerably favored by the circumstance that prior to the beginning of the conference summaries of reports were published in seven volumes. (TEZISY DOKLADOV XI VSESOYUZNOGO SOVESHCHANIYA PO AKTINOMETRII, Tallin, 1980. CHAST' I. PLENARNOYE ZASEDANIYE; CHAST' II. PRIBORY I METODY NABLYUDENIY; CHAST' III. AKTINOKLIMATOLOGIYA I PRIKLADNAYA AKTINOMETRIYA; CHAST' IV. RADIATSIONNAYA ENERGETIKA; CHAST' V. RADIATSIYA, AEROZOL' I OBLAKA; CHAST' VI. DISTANTSIONNOYE ZONDIROVANIYE ATMOSFERY I PODSTILAYUSHCHEY POVERKHNOSTI; CHAST' VII. FITOAKTINOMETRIYA (Summaries of Reports at the Eleventh All-Union Conference on Actinometry), Tallin, 1980. Part I. Plenary Session; Part II. Observation Instruments and Methods; Part III. Actinoclimatology and Applied Actinometry; Part IV. Radiation Energy; Part V. Radiation, Aerosol and Clouds; Part VI; Remote Sensing of the Atmosphere and Underlying Surface; Part VII. Phytoactinometry).

These summaries give a specific review of work in these directions carried out in the USSR. In addition, 15 reports were presented, including the reports "Statistical Model of Aerosol 1980" and "Soviet-American Complex Abastumani Background Experiment in 1979" (G. V. Rozenberg, Institute of Atmospheric Physics USSR Academy of Sciences), as well as a report by G. M. Krekov and R. M. Rakhimov (Institute of Oceanology USSR Academy of Sciences) entitled "Optical-Radar Model of Continental Aerosol."

The attainments in actinometry during the period elapsing since the time of the Tenth All-Union Conference on Actinometry "Use of Actinometric Information in the Weather Service. Preparations for Implementing the First Global Experiment GARP" (Ryl'sk, 1978) were analyzed and summarized in a conference resolution. Here we will cite an excerpt from the resolution:

"Considerable successes have been achieved in the spectroscopic support of algorithms for restoring structural parameters and composition of the atmosphere (investigations of the parameters of the fine structure of absorption spectra, direct computations of molecular absorption, evaluations of the contribution of different components, etc.). Work was successfully continued on the improvement of restoration algorithms. Studies devoted to methods for four-dimensional assimilation of ordinary and radiometric satellite meteorological information are of especially great importance. These are making it possible, to a considerable degree, to increase the effectiveness of the contribution of remote sensing to the results of numerical weather forecasting."

Work is intensively developing on the objective evaluation of the information yield of data from remote sensing and the planning of experiments, including a determination of the makeup of the instrumentation and the conditions for making measurements

(choice of spectral channels, geometry of survey, spatial-temporal scheme for the collection of data). There has been extensive development of investigations for the purpose of solving remote sensing problems, relying on the use of data on the spectral brightness coefficients.

It is necessary to note studies for the parameterization of radiation processes at the surface of the land carried out within the framework of the World Climatological Research Program. The committee on this program proposed that Soviet specialists develop the radiation block in recognition of our successes in this field.

The introduction of algorithms for taking into account radiation effects in models of general circulation of the atmosphere and climate and also in long-range weather forecasting is being productively developed.

Considerable successes have also been achieved in the development of radiation models of clouds and a turbid atmosphere. In particular, important results have been obtained in the field of radiation energy of optically thin crystalline upper-level clouds. Experimental and theoretical investigations facilitated a precise determination of the spectral radiation coefficients for these clouds, and what is especially important, a determination of the coefficients for the window of atmospheric transparency.

In the course of special GARP observation periods major complex experiments were successfully carried out within the program of the Global Aerosol-Radiation Experiment (GAREX). Expeditions operated in 1979 in the Karakum, in the Arctic over SP-22 station and in the region of Kamchatkan volcanoes. As a result, a great volume of data was accumulated on the optical characteristics of the underlying surface and the atmosphere.

Within the framework of the "Intercosmos" program, in cooperation with the academies of sciences of the socialist countries, a whole series of experiments was carried out for investigating different geosystems. A great volume of optical information on natural formations has been accumulated.

Among the successful investigations it is necessary to include the Soviet-American Complex Abastumani Background Experiment carried out in 1978-1979.

The conference noted achievements in the field of aerostat spectroscopic investigations of stratospheric aerosol. At the same time the conference deemed it necessary to carry out more thorough, complex investigations of stratospheric optics with the use of satellite, balloon and surface measurement methods in the interests of climatology and stratospheric physics.

Successes were attained in theoretical studies of the radiation regime of a horizontally inhomogeneous plant cover. The first studies have appeared on the mathematical modeling of the radiation regime of individual plants or the plant cover as a whole by the Monte Carlo method and also by the "returned light" theory.

During the period between the conferences on actinometry a whole series of modern instruments has been developed for measuring spectral brightness in different parts of the spectrum. The designing of systems of network actinometric instruments with black detectors was accomplished, in particular, phytopyranometers, and also with semiconductor thermocouples.

Considerable successes have been achieved in the field of study of the statistical structure of the radiation factors in climate and also in the development of indirect methods for computing the radiation characteristics of water bodies (lakes, seas, oceans). There has been a considerable broadening of the volume of investigations in the field of applied actinometry. For the first time computer archives have been created for the world actinometric network and for data from the actinometric radiosonde network in the USSR.

The considerable successes in the development of actinometry noted above in a number of cases were inadequate for solving new and important problems in the development of Soviet science.

O. A. Avaste

A conference for summarizing the results of the work of the hydrochemical laboratories of the Sea of Azov-Black Sea basin during the Tenth Five-Year Plan was held during the period 18-20 November 1980 at the Sevastopol' Division of the State Oceanographic Institute. The conference was attended by representatives of the State Committee on Hydrometeorology, the State Oceanographic Institute, the Sevastopol' Division of the State Oceanographic Institute, Ukrainian, Northern Caucasus and Georgian Administrations of the Hydrometeorological Service. Reports and communications on the work of hydrochemical laboratories on the collection of information on the state of waters in the basin and the prospects of development of investigations during the Eleventh Five-Year Plan were presented by B. I. Munin (State Committee on Hydrometeorology), Ye. P. Kirillov (State Oceanographic Institute), A. I. Ryabinin, V. B. Belyavskaya, L. F. Yermakova, S. A. Nazarenko and A. D. Bruk (Sevastopol' Division of the State Oceanographic Institute), V. I. Duginov (Administration of the Hydrometeorological Service Ukrainian SSR), L. I. Stepanova and V. A. Garetov (Northern Caucasus Administration of the Hydrometeorological Service), N. G. Davitaya (Batumi Hydrometeorological Observatory).

It was noted that during the years of the Tenth Five-Year Plan the subdivisions of the State Committee on Hydrometeorology carried out much work for preventing the contamination of the Black Sea and Sea of Azov. During these years alone the Sevastopol' Division of the State Oceanographic Institute carried out 54 major expeditions during which about 100,000 hydrochemical determinations were made.

A great volume of information is also annually collected by the hydrochemical laboratories of the marine administrations of the Hydrometeorological Service. In the entire marine network of the Sea of Azov-Black Sea basin during the last five years there have been more than 350,000 hydrochemical observations, including about 160,000 in the mouth regions of the Danube, Dnepr, Don, Kuban and Rioni.

It was noted at the conference that in the course of the past five years the Sevastopol' Division of the State Oceanographic Institute and marine administrations of the Hydrometeorological Service have devoted much attention to research on optimizing the reference network of stations and increasing the quality of the collected information. For this purpose specialists developed some general principles for constructing the observation network, on the basis of which it was possible to ascertain the minimum necessary number of observation stations for each region. For this same purpose in late August 1979 a large-scale experiment was carried out in the Black Sea. The observations were made synchronously by four ships in 16 special

polygons having the configuration of a square with sides having a length of about 10-12 miles. Five abyssal stations, situated at equal distances from one another, were occupied in each polygon. The collected data were used for more precise determination of the network of stations in the open sea and the choice of the most representative observation points.

In order to increase the quality of the collected information the Sevastopol' Division of the State Oceanographic Institute, by way of experimentation, has organized a centralized system for supplying all the hydrochemical laboratories of the basin with standard chemical reagents for some analyses. An arbitration method has been developed for monitoring the quality of all hydrochemical observations in the network. A special system for the internal and external monitoring of adherence to the methods for implementing the most complex and responsible work is being introduced. Each year inspections of laboratories are made and specialists at hydrochemical laboratories receive advance training for the making of new analyses. Conclusions concerning the operation of the network are drawn regularly.

At the same time the conferees emphasized that with respect to a number of problems involved in material-technical support of hydrochemical investigations there must be more active assistance from the local administrations of the Hydrometeorological Service. It was also noted that there has been a delay in solution of the problem of the organization of control determinations of petroleum products by the IR spectrometry method in the hydrochemical laboratories of the hydrometeorological observatories, as is also true of such determinations of organochlorine pesticides by the gas chromatography method, etc. Attention was also given to the need for accelerating the development of remote methods for monitoring the state of the medium, in particular, the broader use of aerial surveys, radar methods, satellite information, etc.

In the adopted resolution the conferees formulated a number of fundamental problems involved in the further development of hydrochemical investigations and monitoring of the state of basin waters.

L. F. Yermakova and Yu. G. Slatinskiy

NOTES FROM ABROAD

Moscow METEOROLOGIYA I GIDROLOGIYA in Russian No 4, Apr 81 pp 127-128

[Article by B. I. Silkin]

[Text] As reported in OCEANUS, Vol 23, No 1, 1980, we will give some results of the implementation of international oceanographic programs.

The purpose of the NORPAX program was a study of the interaction between the ocean and the atmosphere. Applying the methods of modern mathematical analysis, specialists have examined macroscale processes of interaction of these media, likening it to the active interaction of two fluids having a common discontinuity and feedback mechanism. It was taken into account that the enormous thermal and mechanical inertia of the ocean has considerable importance for weather and even climate-forming processes having a scale from 1 month to 1 year.

The expeditions carried out under this program were crowned with the discovery in the northern and equatorial regions of the Pacific Ocean of large "lenses" of water whose temperature differs by 1-1.5°C from the medium surrounding them. Such formations occupy a depth as great as 300 m and extend for a distance as great as 1,500 km. They can exist for a period of 2 1/2 years.

The mathematical model of this phenomenon which was then constructed made it possible to use an electronic computer to predict its appearance, form and intensity for a period up to a season. This is considerably developing the general theory of large-scale long-range meteorological and oceanological forecasting.

Part of this same program was an investigation of the periodically developing El Nino Current near the western shores of South America discovered several years ago. Observations made both on ships and on shore island oceanological stations in the region of the equator indicated that this phenomenon is by no means local, as has been assumed in the past. It was discovered that after the seasonal weakening of the equatorial Trades the mean sea level in the eastern regions of the Pacific Ocean decreases, and in the western regions increases. This makes possible a reliable prediction of the appearance and intensity of the El Nino Current, exerting a great negative influence on fishing in Peru because the anomalous warming associated with it sharply reduces the bioproductivity of the surface waters.

The success of the NORPAX program and the fact that the climatological processes with which it is associated play a major role for the further development of mankind led to a joint resolution of the UN and the International Council of Scientific Unions

to continue its activities into the 1980's.

Until now the most widespread opinion among specialists has been that the world ocean for the most part consists of a great number of calm currents, only locally characterized by a greater intensity, the Gulf Stream, being an example. The international MODE program, representing a possibility for large-scale and thorough areal surveys of the ocean, led to the discovery of eddy movements of large masses of sea water. It has now become clear that the thermal structure of the ocean is determined to a considerable degree by thermal anomalies with a diameter from tens to hundreds of kilometers. The lifetime of such eddylike movements is from several days to several months.

A development of this program and a part of it were expeditions under the POLYMODE program in which Soviet scientists took an especially active part. The fact was established that in a number of regions of the ocean there are not only eddies but also regions characterized by an unusual intensity of change in their physical parameters. Such a phenomenon can take in both regions with a small scale, with a diameter of about 20 km, and large regions, attaining several hundreds of kilometers. The lifetime of such an individual region evidently attains several years.

Participants in the ISOS program carried out a number of expeditions in the high latitudes of the southern hemisphere. Their studies have shown that the cold surface waters near Antarctica form a water mass with an increased density. Plunging, it simultaneously moves toward the middle latitudes, where it replaces intermediate and deep waters. It was also established by observations that the annular circumpolar current washing the shores of Antarctica in its scales is entirely comparable, for example, with the Gulf Stream. In the narrows of Drake Passage, separating South America from Antarctica, it carries about 120 (±20) million cubic meters of water per second. In this current it is possible to discriminate three independent flows, between which there are relatively immobile masses.

In the eastern part of the Antarctic Ocean (in its Indian Ocean sector) the existence of a "lens" of water masses has been discovered. It extends in a meridional direction and within its limits other physical parameters differ sharply from the surrounding waters. In the region 36°W within the limits of the circumpolar current there were annular currents ("rings") whose development could be traced for the first time from their very generation to their disappearance.

Upwelling (the rising of cold deep waters to the surface) was studied in accordance with the CUEA program along the Pacific Ocean coast of the United States (Oregon) and Peru and in the Atlantic -- along the northwestern shores of Africa. It was established that this phenomenon under definite weather (wind) conditions can have a cycle of 3-10 days. Since the upwelling brings a great quantity of nutrients to the surface, this discovery is of interest for the fishing industry.

Geochemical research methods employed in the course of implementation of the GEOSECS program for the first time made it possible to create a map of deep circulation of waters in many regions of the world ocean. Measurements of the content of tritium (a radioactive isotope of hydrogen forming in the course of nuclear reactions in the upper atmosphere under the influence of cosmic rays), carried out along long meridional sections in the Atlantic Ocean, made it possible to trace the course of

penetration of waters forming in the high latitudes into the deep region in the northern parts of this ocean. The data on the content of radon, ^{14}C and CO_2, unique in their completeness, collected in the course of the expeditions, in their comparison are making it possible for the first time with a definite degree of assurance to estimate the quantity of CO_2 entering the ocean as a result of anthropogenic processes and its accumulation in its different layers.

Observations of the distribution of ^{14}C as a tracer element indicated that in the western part of the Atlantic Ocean the rate of water exchange is unexpectedly great; its cycle is only about 300 years. In the Pacific and Indian Oceans this process takes three or four times longer. In the Pacific Ocean deep circulation is associated primarily with bottom waters penetrating from the region lying to the south of New Zealand. Moving northward along the western margin of the ocean, they fill all the depressions situated to the west of the East Pacific Ocean Rise.

In the western region of the Indian Ocean the silicon content, it was found, indicates that the cold bottom water masses, separating from the circumpolar current, move far to the north. A great quantity of this element enters the ocean from the Arabian Sea where processes of precipitation of the skeletons of diatomaceous organisms transpire actively under the influence of upwelling.

5303
CSO: 1864/9

- END -